Characterization of Hydrophobically Modified Starch NanoParticles by Pyrene Fluorescence

by

Damin Kim

A thesis

presented to the University Of Waterloo

in fulfilment of the

thesis requirement for the degree of

Master of Science

in

Chemistry (Nanotechnology)

Waterloo, Ontario, Canada, 2017

AUTHOR'S DECLARATION

I hereby declare that I am the sole author of this thesis. This is a true copy of the thesis, including any required final revisions, as accepted by my examiners.

I understand that my thesis may be made electronically available to the public.

Abstract

Starch nanoparticles (SNPs) were hydrophobically modified with propionic (C3) and hexanoic (C6) anhydride via esterification. Different degrees of substitution (DS) of the hydroxyl groups of the SNPs were achieved by varying the reaction conditions. The relative hydrophobicity of the hydrophobically modified SNPs (HM-SNPs) was examined with pyrene fluorescence. The hydrophobes covalently attached to the SNPs conferred an amphiphilic character to the SNPs whereby hydrophobic microdomains were generated and stabilized by the hydrophilic SNPs in aqueous solution. The hydrophobic microdomains of the HM-SNPs were probed with the hydrophobic dye, pyrene. Several parameters related to the photophysical properties of pyrene, such as the $(I_1/I_3)_o$ ratio, the bimolecular rate constant for quenching k_q, the natural lifetime τ_o, and the equilibrium constant for the binding of pyrene to the HM-SNPs K_B, were found to respond to the expected hydrophobicity of the HM-SNPs, and thus the level of hydrophobic modification. These four parameters, $(I_1/I_3)_o$, k_q, τ_o, and K_B, were examined as a function of the DS and the type of hydrophobic modification (propionic versus hexanoic acid). As the DS of hexanoic acid of the HM-SNPs increased, pyrene experienced a decrease in the polarity of its local environment evident from a decrease in $(I_1/I_3)_o$ while the microviscosity of the hydrophobic aggregates increased as indicated by an increase in τ_o and a decrease in k_q. Moreover, the interactions between SNPs and pyrene became stronger with increasing DS and were dependent on the surface area of the SNPs. All the parameters confirmed that the hydrophobicity of the HM-SNPs increased with increasing DS of hexanoic acid. The parameters also demonstrated that for a same DS, the environment generated by the SNPs modified with hexanoic acid was more hydrophobic than that of the SNPs modified with propionic acid. As it turns out, the photophysical parameters of pyrene retrieved for the SNPs modified with propionic acid were similar to those obtained with the

naked SNPs. A model was proposed to account for the increase in SNP diameter due to aggregation observed at high SNP concentration. Its validity was supported by the good agreement obtained when comparing the average diameter predicted by the model with the hydrodynamic diameter of the SNPs determined by DLS. These studies led to the conclusion that hexanoic anhydride modification of SNPs appears to be more suitable than propionic acid modification to increase the hydrophobicity of SNPs. These measurements carried out with pyrene demonstrate that HM-SNPs can be generated where the level of hydrophobicity can be gauged based on the value of the $(I_1/I_3)_o$, k_q, τ_o, and K_B parameters. Finally, interactions between pyrene and SNPs seem to occur at the SNPs surface which is reduced upon aggregation of the SNPs.

Acknowledgements

My sincere thanks go to Professor Jean Duhamel for giving me the opportunity to realize how much I enjoy research. I would not have enjoyed chemistry as much as I now do without his guidance, inspiration, and encouragement. Every new idea and concerns that he expressed about the observations I made during my research motivated me. This thesis and the last two years of research would not have been possible without his support and concern.

I would like to thank Prof. Mario Gauthier and Prof. Michael Tam for being my committee members and providing thoughtful advice about my research. A special thank goes to Prof. Scott Taylor who accepted to replace Prof. Gauthier as a reader of my thesis.

Many thanks go to Lu Li, a graduate student from Prof. Duhamel's group, for helping and providing many advices on my research, Ryan Amos and Bowen Zhang for their hard work on the modification of starch, and Howard Siu for his many helpful advices.

I would also like to thank all the Duhamel and Gauthier group members for caring, helping, and providing a friendly working environment in the laboratory. It has been wonderful to work with Lu Li, Shiva Farhangi, Solmaz Pirouz, Remi Casier, Kiarash Gholami, Abdullah Basalam, Janine Thoma, Sanjay Patel, Jasmine Zhang, Hunter Little, Ryan Amos, Natun Dasgupta, Joanne Fernandez, Victoria Hisko, Aklilu Worku and many others. Special thanks must be given to EcoSynthetic and the project team members and champions, Drs. Bloembergen, McLennan, Mesnager, and Smeets, for many insightful discussions and advices.

Finally, I would like to express my deepest gratitude to my parents and sisters for their endless support and love.

Dedication

To my family

Table of Contents

List of Figures

List of Tables

List of Schemes

List of Abbreviations

ACS	American Chemical Society
CMC	Critical Micellar concentration
DMAP	4-Dimethylaminopyridine
DMSO	Dimethyl sulfoxide
DLS	Dynamic light scattering
DS	Degree of substitution
^{1}H NMR	Proton nuclear magnetic resonance
HPLC	High performance liquid chromatography
MWCO	MWCO molecular weight cutoff
Py_{bound}	Pyrenes that are bound to SNPs
Py_{free}	Pyrenes that are free in water
RT	Room temperature
TCSPC	Time-correlated single photon counting
THF	Tetrahydrofuran
UV-Vis	Ultraviolet visible spectroscopy

List of Symbols

I	Fluorescence intensity in the presence of quencher
I_o	Fluorescence intensity in the absence of quencher
I_1	First peak of the emission spectrum of pyrene
I_3	Third peak of the emission spectrum of pyrene
f_{bound}	Molar fraction of pyrene bound to SNPs
f_{free}	Molar fraction of pyrene free in water
f_p	Molar fraction of pyrene bound to SNPs and protected from quenching
K_B	Equilibrium constant for binding of pyrene to SNP/HM-SNPs
S_0	Zeroth electronic state
S_1	First electronic state
τ_o	Lifetime of pyrene bound to SNP/HM-SNPs in the absence of quencher
τ_{PySNP}	Lifetime of pyrene bound to SNP/HM-SNP in the presence of quencher
τ_{PyW}	Lifetime of pyrene present in water
$<\tau>$	Number average lifetime of pyrene
C3(x)-SNP	Propionic acid modified SNPs with DS of x
C6(x)-SNP	Hexanoic acid modified SNPs with DS of x
α_{PyW}	Molar fraction of pyrene molecules that are in water
α_{PySNP}	Molar fraction of pyrene molecules that are bound to the SNPs and accessible to the solvent
$\alpha_{PySNP-P}$	Molar fraction of pyrene molecules that are bound to the SNPs but protected from quenching
N_{agg}	Number of SNP/HM-SNPs in an aggregate

V_{agg}	Volume of an SNP/HM-SNP aggregate
D_o	Diameter of the isolated and aggregated SNP/HM-SNPs
D_{agg}	Diameter of aggregated SNP/HM-SNPs
D_h	Hydrodynamic volume
S_{SNP}	Surface of SNP/HM-SNPs
A_{Py}	Absorbance of pyrene at 336 nm
L	Path length used in the absorption measurement
ε_{Py}	Molar extinction coefficient of pyrene.
C_{BP}	Concentration separating the two regimes for the binding of pyrene to isolated and aggregated SNP/HM-SNPs
k_{qW}	Quenching rate constant of pyrene in water
k_{qSNP}	Quenching rate constant of pyrene bound to the SNPs
K_D	Stern Volmer Constant
p	Probability
m	Slope
b	Intercept

.

Chapter 1
Introduction

1.1 Background

As increasing numbers of insoluble drugs have shown promising activity in vitro, many strategies have been introduced to overcome the poor aqueous solubility of these drugs.[1] One of the strategies that has been most extensively studied and developed is the encapsulation of a hydrophobic drug in carriers made of an apolar core and a water-soluble shell. In this regard, amphiphilic polymers consisting of hydrophobic and hydrophilic moieties can self-assemble in aqueous solution into well-organized structures referred to as polymeric micelles consisting of a hydrophilic shell and a hydrophobic core.[2] The hydrophobic core which is shielded from water by the hydrophilic shell represents an ideal site for hydrophobic drugs to partition into.

Micellar encapsulation offers many advantages for carrying a drug. The encapsulation of a hydrophobic drug into polymeric micelles increases the solubility of the hydrophobic drug in water and its bioavailability while extending its circulation period in the blood stream. The size of polymeric micelles can typically be adjusted between 10 and 100 nm. This range of size is small enough to ensure cell uptake but too large to be cleared from the blood stream through the kidneys. As a result, longer circulation times are obtained that enhance the probability of the encapsulated drug to reach its intended target. Moreover, drugs encapsulated in micelles are often protected from attacks by the body's immune system.[3,4] Despite possessing excellent drug encapsulation qualities, the possible toxicity of using polymeric micelles prepared with synthetic polymers[5,6] has shifted the attention of the scientific community to natural polymers such as polysaccharides.[7]

Starch is constituted of two types of polysaccharides namely, amylopectin and amylose. Amylopectin is a highly branched macromolecule consisting of many short oligosaccharide side chains connected via α–1,6 glycosidic bonds to long linear polysaccharide chains. As for

amylose, the short side chain oligosaccharides and long polysaccharides found in amylopectin are linear chains made of anhydrogluocose units linked by α–1,4 glycosidic bonds. The chemical structures of amylose and amylopectin are shown in Figure 1.1.

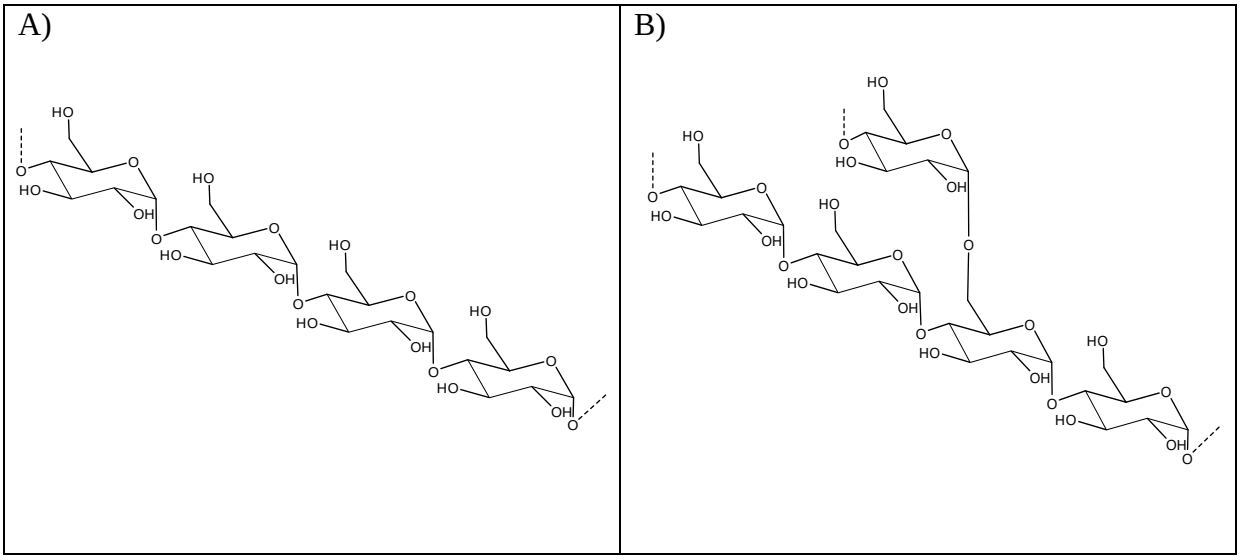

Figure 1.1 Chemical structures of A) amylose and B) amylopectin

The main characteristics of starch are that it is a water-soluble, biodegradable, biocompatible, inexpensive, and non-toxic polymer bearing numerous hydroxyl groups that can be targeted relatively easily for chemical modifications. These advantages explain why modified starch is employed in numerous industrial applications as a thickener in food,[8] a disintegrating component in pharmaceutical,[9] or a binder in paper coating.[10] However, starch in its natural form is viscous, not readily soluble in water, and large in size, all aspects that limit its usage in industrial applications.[10]

These limitations can be overcome by breaking starch down into nano-sized particles via enzymatic hydrolysis or microfludization.[11] Nano-sized starch particles or starch nanoparticles (SNPs) can also be modified with hydrophobic groups. The self-aggregation of hydrophobes present in the hydrophobically modified SNPs (HM-SNPs) into stable aggregates generates hydrophobic domains where hydrophobic molecules in an aqueous

solution can partition into. There have been several studies already where HM-SNPs have been used as potential hydrophobic carriers of drugs and flavours.[12-15] The possible application of HM-SNPs as carriers has been examined by characterizing their ability to form hydrophobic microdomains and encapsulate, protect, and release an apolar cargo to a desired target.[13-15]

1.2 Structure, Properties, and Hydrophobic Modification of SNPs

This thesis focuses on the SNPs provided by EcoSynthetix via a reactive extrusion process at high temperature.[16] The extrusion process reduces micro-sized granules of waxy starch composed mainly of amylopectin into SNPs having diameters between 10 and 50 nm depending on the extrusion conditions.[10] Thus, many problems associated with the large size of amylopectin such as the high viscosity of its dispersion or its poor solubility in water can be circumvented by working with SNPs instead of amylose or amylopectin.[10] SNPs have been already widely used in paper coating applications as a replacement for primary paper coating materials such as styrene butadiene and styrene acrylate latex which are relatively expensive and environmentally unfriendly.

The hydrophobic modification of SNPs is expected to expand their range of industrial applications possibly including their use as carriers of a hydrophobic cargo. To this end, SNPs can be hydrophobically modified via esterification with an alkanoic anhydride as shown in Scheme 1.

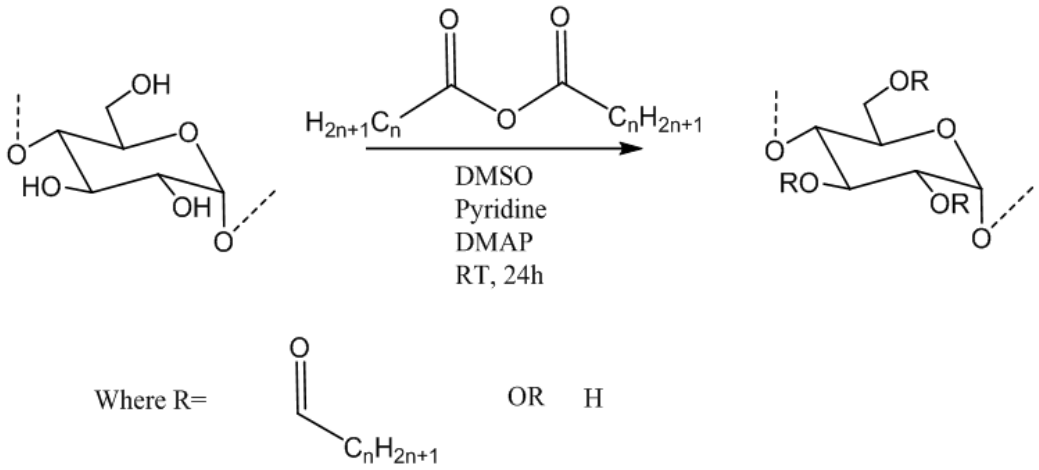

Scheme 1.1. Hydrophobic modification of SNPs with hexanoic (n=5) and propionic (n=2) anhydride.

The level of interactions between the hydrophobic pendants grafted onto the SNPs will depend on the degree of substitution (DS) of the SNPs and the nature of the alkyl chains. The effect of the alkyl chain length on the self aggregation of polymeric micelles has been studied.[17] For instance, the hydrophobicity of the alkyl group can be adjusted by changing its chain length. Longer alkyl chains tend to form more hydrophobic microdomains that have a lower water content compared to those generated by shorter alkyl chains.[18-19] Since more hydrophobic microdomains can hold on more tightly to apolar compounds, the relative hydrophobicity of these microdomains becomes an important parameter for their characterization. Fluorescence was selected to characterize the relative hydrophobicity of the modified SNPs and these experiments were conducted with the dye pyrene. As a result, the following sections provide some basic information about the fluorescence of pyrene in general and more specific aspects of pyrene fluorescence that was taken advantage of to characterize the modified SNPs.

1.3 Pyrene Fluorescence

Fluorescence has been highly successful at characterizing the hydrophobic microdomains of

self-assembled amphiphilic macromolecules in aqueous solution such as those generated by drug delivery agents.[20-22] Fluorescence is the emission of light occurring when an excited electron in a singlet state relaxes back to the ground state. The absorption and emission of light by molecules can be described by the Jablonski diagram shown in Figure 1.2.

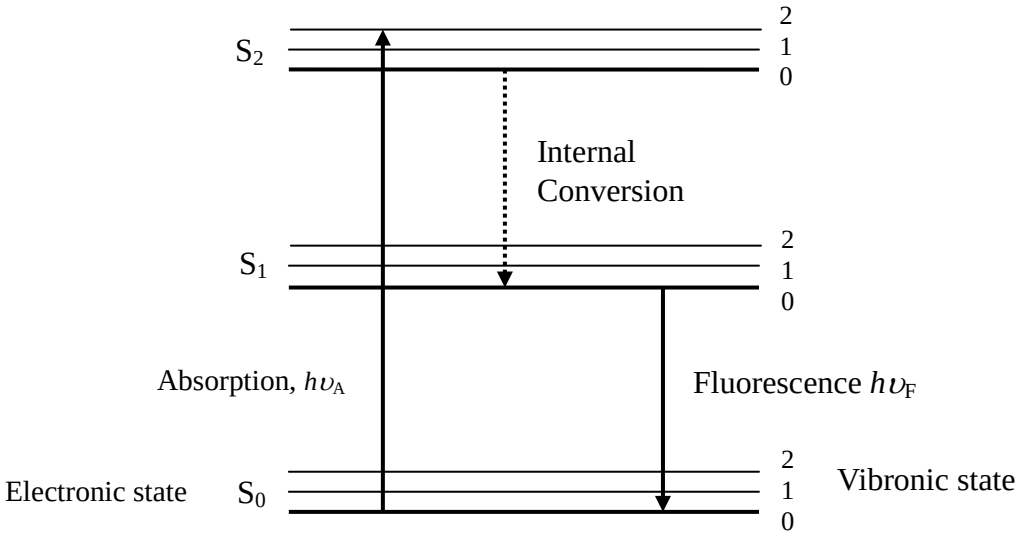

Figure 1.2. Simplified Jablonski Diagram[23]

When a fluorophore is excited at a wavelength λ_{ex} to a higher electronic state, it absorbs a photon of energy $h\nu_A$. Following absorption, the fluorophore relaxes rapidly to the lowest vibrational level of the electronic state S_1, a process described as internal conversion in Figure 1.2. The energy loss undergone during the internal conversion results in a Stokes shift of the emission to higher wavelengths compared to the absorption wavelength. Most aromatic molecules fluoresce and, among them, pyrene has been referred to as an ideal fluorophore to study macromolecules due to its exceptional photophysical properties that have been presented in numerous reviews.[24-26] Its chemical structure is shown in Figure 1.3.

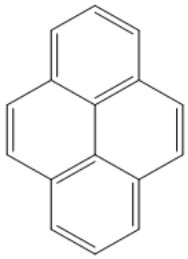

Figure 1.3 Chemical structure of pyrene

Among the most prominent features of pyrene as a fluorophore, the following properties come to the fore. First, it has a relatively high quantum yield (ϕ =0.32 in cyclohexane)[27] and molar extinction coefficient ($\varepsilon_{Py\ 336nm}$= 45000 $M^{-1}cm^{-1}$ in THF), thereby enabling efficient absorption and emission of light. These features result in a strong fluorescence signal that can be detected even at extremely low (< 10^{-6} M) pyrene concentration thus avoiding the inner filter effect, a classic artifact encountered with concentrated dye solutions.[23] Second, pyrene has a relatively long lifetime which can reach up to 400 ns in unaerated organic solvents such as cyclohexane.[28] The long lifetime of pyrene provides an extended time window to observe its dynamics either as a free molecule in solution or covalently bound to a macromolecule. Third, pyrene can form an excimer which is a fluorescent complex formed by two pyrenes. Finally, the individual fluorescence of monomeric pyrene responds to the polarity of its local environment according to the I_1/I_3 ratio obtained from the intensity of the first (I_1) and third (I_3) band of its emission spectrum.[29]

1.3.1 Lifetime of Pyrene

The lifetime (τ_o) of a fluorophore is the average time that an excited fluorophore remains in the excited state prior to relaxing back to the ground-state. The lifetime of a fluorophore can be reduced if quenchers are present. There are two types of quenching: static and dynamic quenching. Static quenching occurs when pyrene forms a non fluorescent complex with a

quencher. When the complex absorbs a photon of light, the complex immediately relaxes to the ground-state without emitting light. Static quenching decreases the number of fluorophores that contribute to the fluorescence which results in a decrease in the fluorescence intensity. However, the observed lifetime is not affected by static quenching as the non-complexed fluorophore fluoresces as if no quencher was present.

Dynamic (collisional) quenching is the second type of quenching and it occurs when an excited fluorophore collides with a quencher which then relaxes to its ground-state without emitting light. This type of quenching results in a decrease in fluorescence intensity and lifetime of the fluorophore. The effect that dynamic quenching has on the fluorescence intensity and lifetime can be quantified by using Equation 1.1.[23]

$$\frac{I_0}{I} = \frac{\tau_0}{\tau} = k_q \tau_0 [Q] + 1 = K_D [Q] + 1 \qquad (1.1)$$

In Equation 1.1, I, I_o and τ, τ_o represent the fluorescence intensities and lifetimes of pyrene where the presence or absence of quencher in the solution is indicated without or with a subscript "o". k_q is the bimolecular quenching rate constant. Equation 1.1 predicts that a plot of I_o/I or τ_o/τ as a function of quencher concentration should yield a straight line of intercept unity and slope $k_q\tau_o$ equal to K_D. Such a plot is referred to as a Stern Volmer plot and the slope K_D is called the Stern Volmer constant. A high quencher concentration results in more encounters between fluorophores and quenchers thereby leading to a shorter lifetime (τ). The efficiency of quenching is reflected by the value of k_q whose expression is given in Equation 1.2.[23]

$$k_q = 4\pi N_A (R_F + R_Q)(D_F + D_Q) p \qquad (1.2)$$

In Equation 1.2, R_F and R_Q are the radii of the fluorophore and quencher and D_F and D_Q are

their respective diffusion coefficients. The parameter p is the probability of observing quenching when an excited fluorophore encounters a quencher. Equation 1.2 predicts that k_q will change greatly whether the fluorophore is free in solution or bound to a larger macromolecule. Assuming that the quencher is a small water-soluble molecule of size comparable to that of pyrene, k_q will be much larger in the former case where $D_F \approx D_Q$ than in the latter case where $D_F << D_Q$. These considerations were taken advantage of in this thesis to estimate the binding constant of pyrene to SNPs in aqueous solution. Pyrene bound to SNPs was much less sensitive to quenching by oxygen than free pyrene in water, thus resulting in very different lifetimes. The difference in lifetime was probed by time-resolved fluorescence and was employed to characterize the relative hydrophobicity of the HM-SNPs since a more hydrophobic SNP would shield pyrene more from the aqueous solution thus reducing the probability p in Equation 1.2 and consequently, k_q.

1.3.2 Equilibrium Constant K_B

Pyrene is so hydrophobic that it will bind to any substance dissolved in water. It is thus not surprising that pyrene would bind to SNPs or HM-SNPs dispersed in water. The equilibrium between pyrene free in solution (Py_{free}) and pyrene bound to SNPs (Py_{bound}) can be described by Equation 1.3

$$Py_{free} + SNP \underset{}{\overset{K_B}{\rightleftharpoons}} Py_{bound} \qquad (1.3)$$

Since binding of pyrene to SNPs greatly decreases oxygen quenching (see Equation 1.2), the lifetime of free pyrene in water (τ_{PyW}) was found to be substantially shorter than the lifetime of pyrene bound to SNPs (τ_o). As a result, the lifetimes τ_{PyW} and τ_o could be easily assigned from the analysis of the fluorescence decays acquired with pyrene in aqueous dispersions of SNPs. In turn, the pre-exponential factors associated with the lifetimes τ_{PyW} and τ_o were

directly related to the ratio f_{bound}/f_{free} of the molar fractions representing Py_{bound} and Py_{free}. The ratio f_{bound}/f_{free} was then employed to determine K_B quantitatively. Since pyrene would bind more strongly to more hydrophobic HM-SNPs, the magnitude of K_B was used to assess the relative hydrophobicity of the different HM-SNPs investigated in this thesis.

1.3.3 Sensitivity of Pyrene to the Polarity of its Local Environment

Pyrene presents a fine emission spectrum with distinguishable vibronic bands in Figure 1.4. The intensity of each vibronic band in the fluorescence spectrum reflects the probability that a transition from the lowest vibrational level of the electronic level S_1 to one of the vibrational levels of the ground-state is allowed. The first peak to the left of the fluorescence spectrum represents the transition from the zeroth vibronic level of S_1 to the zeroth vibronic level of S_0 and is referred to as the 0-0 transition. This transition is symmetry forbidden. The third peak in the fluorescence spectrum represents the transition from the zeroth vibronic level of S_1 to the second vibronic level of S_0, namely the 0-2 transition. Whereas the 0-2 transition is allowed and is relatively independent of solvent polarity, the 0-0 transition is not allowed in apolar solvents but is partially recovered in more polar solvents. The polarity of the solvent can be inferred by comparing the intensity of the first peak (I_1) to the intensity of the third peak (I_3) with the I_1/I_3 ratio. The I_1/I_3 ratio of pyrene equals 1.8 in water and 0.6 in cyclohexane (Figure 1.4). The change in polarity of the local environment of pyrene reflected in the changes of the I_1/I_3 ratio has been applied to probe the interactions of pyrene with different macromolecular objects in water as for the determination of the critical micellar concentration (CMC) of surfactants.[20-22,29]

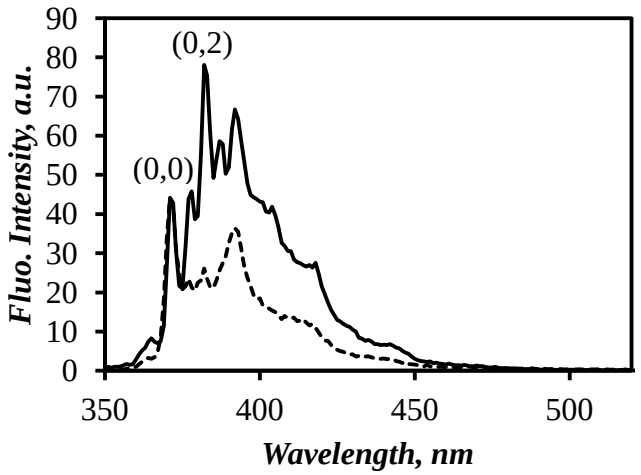

Figure 1.4 Fluorescence spectrum of pyrene in (---) water and (—) cyclohexane. λ_{ex}=336 nm.

1.4 Thesis Outline

This thesis aimed to evaluate the strength of the interactions between HM-SNPs and the hydrophobic dye pyrene and use this information to quantitatively rank their relative hydrophobicity. The research conducted to achieve this goal is presented in the following manner. The introduction provided some basic information on well-characterized amphiphilic drug carriers, starch and SNPs, and the fluorescence of pyrene. The experimental procedures and instruments employed in this study are introduced in Chapter 2. Chapter 3 describes how the loading capacity of pyrene in HM-SNPs was determined along with the binding constant, K_B. Chapter 4 discusses the level of protection afforded by HM-SNPs for the quenching of pyrene by nitromethane, a known water-soluble quencher of pyrene. Chapter 5 summarizes the key findings from the previous chapters and suggests future work.

Chapter 2

Experimental Section

2.1 Instrumental

UV-Vis Absorption: A Cary 100 bio-UV-Vis spectrophotometer was used to acquire the absorption spectra.

Steady-State Fluorescence: The emission spectra were acquired with a Photon Technology International LS-100 fluorometer. The fluorescence spectra of pyrene were obtained by exciting the pyrene solution at 338 nm and monitoring the fluorescence intensity from 348 nm to 600 nm.

Time-Resolved Fluorescence (Time-Correlated Single Photon Counting (TCSPC)): An IBH Ltd. fluorometer equipped with an IBH 340 nm NanoLED was used to acquire the time-resolved fluorescence decays. Dispersions of SNPs and HM-SNPs exhibited a shorter lived fluorescence which appeared as a spike at the beginning of the fluorescence decay of pyrene. The magnitude of the spike depended on the concentration of the SNP/HM-SNPs used to prepare the dispersions. SNP/HM-SNPs dispersions were excited at 338 nm and the fluorescence decays of pyrene were acquired at 375 nm. More than 10,000 counts were collected at the decay channel where the spike in the decay due to the SNP fluorescence tailed off to ensure that the part of the fluorescence decay corresponding to the emission of the long-lived pyrene would be represented with a good signal-to-noise ratio. The fluorescence decays were fitted with a sum of exponentials as described in Equation 2.1

$$[Py^*]_t = [Py^*_{diff}]_{t=0} \times \left(\alpha_{PyW} \exp\left[-t\left(k_{qW}[Q] + \frac{1}{\tau_{PyW}} \right) \right] + \alpha_{PySNP} f_{PySNP}(t) + \alpha_{PySNP-P} \exp\left[-\frac{t}{\tau_0} \right] \right) + \alpha_{SNP} f_{SNP}(t) \tag{2.1}$$

In Equation 2.1, τ_{PyW} and τ_o are the lifetimes and k_{qW} and k_{qSNP} are the quenching rate

constants of pyrene in water and bound to the SNPs, respectively. The molar fractions $\alpha_{PyW,}$ α_{PySNP}, and $\alpha_{PySNP\text{-}P}$ represent the pyrene molecules that are in water (Py_W*), bound to the SNPs and accessible to the solvent (Py_{SNP}*), and bound to the SNPs but protected from quenching ($Py_{SNP\text{-}P}$*), respectively. The molar fraction α_{SNP} corresponds to the contribution of the short-lived SNP fluorescence to the fluorescence decays. The species $Py_{SNP\text{-}P}$* decayed with a long lifetime ($\tau_o \geq 200$ns). The pyrene molecules that were bound to the SNPs and were accessible to quencher could be represented by one or two exponentials and this function was described by $f_{PySNP}(t)$.

The fluorescence decay analysis needed to account for the fluorescence decays of the SNP or HM-SNP dispersions which needed to be fitted with a sum of exponentials (see Figure 2.1A). This fluorescence contribution was represented by the function $f_{SNP}(t)$ in Equation 2.1 and it was handled as follows. In fluorescence experiments that did not involve pyrene quenching ([Q]=0 M), the decay times associated to pyrene in water (τ_{PyW} = 130 ns) and pyrene bound to the SNPs ($\tau_o \geq 200$ ns) were much larger than those representing $f_{SNP}(t)$ which tailed off within 30 ns. Under such conditions, the species Py_{SNP}* and $Py_{SNP\text{-}P}$* were equivalent and the analysis program could easily distinguish between the two remaining components of Equation 2.1. Consequently, the fluorescence decay analysis of pyrene in aqueous dispersions of SNPs was handled by starting the analysis 5 – 10 channels away from the decay maximum so that $f_{SNP}(t)$ representing the long tail of the SNP decays could be approximated by one or two exponentials with short (10 – 30 ns) decay times. In this case, the fluorescence decays were fitted with a sum of three (or four) exponentials where one (or two) exponential had a short decay time that was optimized to handle $f_{SNP}(t)$, another had an intermediate decay time that was fixed to equal 130 ns, the lifetime of pyrene in water, and

the last exponential had a long floating decay time for the Py_{SNP}* species.

While efficient in the absence of quencher, this procedure could not be applied for the fluorescence quenching experiments since quenching pyrene resulted in decreased decay times that approached those used in $f_{SNP}(t)$. These decay times could not be resolved by the decay analysis program that now dealt with a sum of four distinct components since the species Py_{SNP}* and $Py_{SNP\text{-}P}$* were no longer equivalent. In this case, the decay of the SNP aqueous dispersion was fitted to a sum of three exponentials and the normalized pre-exponential factors and decay times were used to fix the expression of $f_{SNP}(t)$ in the decay analysis based on Equation 2.1. Fits of the fluorescence decays were deemed satisfactory when χ^2 was smaller than 1.2 and the residuals and auto-correlation function of the residuals were randomly distributed around zero. An example of such fits is shown in Figure 2.1.

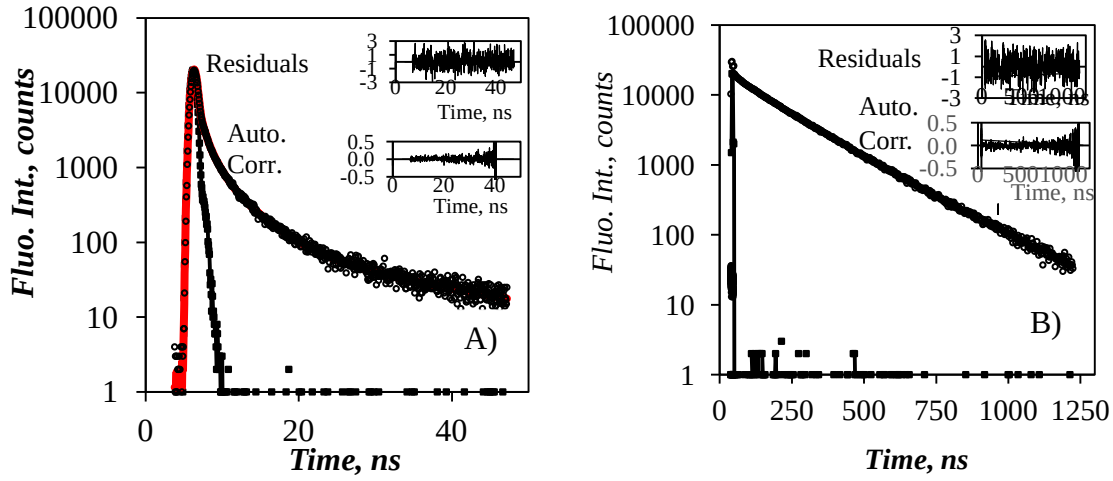

Figure 2.1. Fluorescence decays of A) 2.1 wt% aqueous SNP(A) dispersion and B) the same dispersion with $0.5x10^{-6}$ M pyrene. The fit of A) with a sum of exponentials yielded the function $f_{SNP}(t)$ which was used to fit B) with Equation 2.1

Proton Nuclear Magnetic Resonance (^{1}H NMR) Spectroscopy: ^{1}H NMR spectra of SNPs before and after dialysis against Milli-Q water were acquired with a Bruker 300 MHz high

resolution NMR spectrometer. Deuterated DMSO (99.9 atom% D, Sigma-Aldrich) was used as the solvent with addition of a few drops of trifluoroacetic acid to shift the hydroxyl protons of starch down field. The ^{1}H NMR spectra of SNPs were acquired with an SNP concentration higher than 10 g/L to ensure a sufficient signal-to-noise ratio. (See Figure A.1-9)

Dynamic Light Scattering (DLS): The distribution of hydrodynamic volumes of HM-SNPs was determined with a Malvern Zetasizer Nano-ZS using HM-SNPs aqueous dispersions with a concentration ranging from 0.2 to 2 g/L. The measurements were done at 25 ^{o}C.

Lyophilization: The dialyzed SNPs were lyophilized with a Freezone 6, Labconco freeze-dryer.

Centrifugation: Centrifugation was carried out with an Avanti J-30I centrifuge at 20 ^{o}C and at a rotation rate of 5000 rpm for 3 min.

2.2 Materials: Pyrene (98 %) and organic solvents including dimethyl sulfoxide (DMSO, ACS reagent, ≥ 99.9 %), deuterated DMSO (99.9 % atom), ethanol (HPLC grade), acetone (HPLC, ≥ 99.9 %), and trifluoroacetic acid (Reagent plus, 99 %) were purchased from Sigma Aldrich. Tetrahydrofuran (distilled in glass) was purchased from Caledon. EcoSynthetix supplied a series of six experimental grade samples named SNP(A-F) with diameters ranging between 12 and 47 nm (see particle characterization in Table 2.1). Experimental grade SNPs modified with hexanoic acid and propionic acid were prepared by Ryan Amos from Prof. Mario Gauthier's research group. After modification, all SNPs were dialyzed against water. Doubly distilled Milli-Q water was obtained from a Millipore Milli-RO 10 Plus or Milli-Q UFPlus, Bedford, MA system. A dialysis membrane bag with a 1 kDa MWCO was purchased from Spectrum Laboratories Inc. All chemicals beside pyrene and the modified and

unmodified SNPs were used as received.

Table 2.1. Hydrodynamic diameters and intrinsic viscosity results obtained by Lu Li for the experimental grade SNPs provided by EcoSynthetix.

	SNP(A)	SNP(B)	SNP(C)	SNP(D)	SNP(E)	SNP(F)
D_h (nm)	47 ± 2	23 ± 1	17 ± 0.5	15 ± 20.5	12 ± 0.5	12 ± 0.5
[η] ($mL.g^{-1}$)	57 ± 2	38 ± 2	21 ± 2	20 ± 2	25 ± 2	23 ± 2

2.3 Recrystallization of Pyrene: The fluorescence decay of the 98 % pure pyrene purchased from Aldrich in deoxygenated THF could be fitted with a sum of two exponentials and the fit yielded a long decay time of 363 ns with a pre-exponential contribution of 96 %. This result implied that pyrene from Aldrich was 96 % pure. Pyrene was recrystallized in ethanol at least four times until the pre-exponential contribution of the long lifetime reached a minimum contribution of 99 %. Recrystallized pyrene was used in all experiments.

2.4 Purification of SNPs: Dispersions of 5 wt% SNP in DMSO were prepared by stirring the dispersion at 60 ^{o}C overnight. Visual inspection of the clear dark brown color of the SNP dispersions demonstrated their homogeneity. The homogenous SNP dispersions were removed from the hot plate, cooled down to room temperature, and precipitated in acetone. The precipitate was collected through suction filtration, rinsed with a large amount of acetone to wash away any DMSO, and finally air dried. After the weight of the precipitate remained constant over time, the dried sample was then kept in a clear jar.

2.5 Preparation of Aqueous SNP Dispersions: A 2.1 wt% aqueous dispersion of SNP was prepared by placing the desired amount of dry SNP in Milli-Q water and stirring the mixture at 60 ^{o}C in a shaker overnight. In the morning, the homogenous dispersion was removed from

the shaker and cooled down to room temperature before use. The 2.1 wt% aqueous dispersions were then diluted to the desired concentration with Milli-Q water.

2.6 Dialysis of SNPs/HM-SNPs: The 2.1 wt% aqueous experimental grade SNP/HM-SNP dispersions were added to a dialysis bag with a 1 kDa MWCO. The membranes were immersed in Milli-Q water and dialysis was conducted for 5 days with stirring. The Milli-Q water was replaced every day. After 5 days of dialysis, the SNP dispersion remaining in the membrane was transferred to a vial and lyophilized for 3 days. White puffy powders were obtained and stored in clear vials.

2.7 Binding Constant Experiments

These experiments consisted in monitoring the fluorescence decays of aqueous dispersions prepared with different HM-SNP concentrations ranging from 0 to 20 g/L and a same 0.5 μM pyrene concentration. The upper HM-SNP concentration depended on the dispersability of the HM-SNP in water. To this end, a 2.2 μM pyrene solution in THF (3.4 g) was placed in a vial which was covered with aluminum foil. THF was evaporated and Milli-Q water (15 g) was added into the vial after complete evaporation of THF. Dissolution of pyrene in Milli-Q water was ensured by gentle stirring of the vial in a shaker overnight at room temperature. The gentle stirring prevented the pyrene aqueous solution from touching the plastic lid of the vial where hydrophobic pyrene would stick. The final concentration of pyrene was 0.5 μM. A similar procedure was applied to prepare aqueous SNP dispersions with 0.5 μM of pyrene by replacing water by the SNP dispersion.

The fluorescence experiments consisted in placing 2 g of a concentrated aqueous HM-SNP dispersion containing 0.5 μM of pyrene in a 1 cm x 1 cm quartz fluorescence cell. Known amounts of a 0.5 μM pyrene solution in water were added to the HM-SNP aqueous

dispersion containing 0.5 μM pyrene. This procedure enabled the dilution of the concentrated HM-SNPs dispersion while ensuring that the concentration of pyrene would remain constant at 0.5 μM. After addition of the aqueous 0.5 μM pyrene solution, the diluted SNP dispersion was gently shaken by hand to ensure homogeneous mixing of the SNP dispersion with the pyrene solution in water. Steady-state and time-resolved fluorescence experiments were then carried out on the dilute HM-SNP aqueous dispersions containing 0.5 μM pyrene.

2.8 Loading of Pyrene in SNP Dispersions: Excess amounts of pyrene crystals were added to aqueous HM-SNP dispersions. All vials containing pyrene were covered with aluminum foil to minimize pyrene exposure to light. The HM-SNP dispersions were gently stirred in the shaker overnight at 25 ^{o}C. The pyrene crystals remaining in the vials were removed from the HM-SNP dispersions by centrifugation. The supernatant of the SNP dispersions was transferred to a UV-Vis cuvette. A cuvette with a 1 cm path length was used for the measurements of all of the C6(*x*)-SNP(A) samples. A cuvette with a 10 cm path length was used only for the experiments conducted with C6(0.15)-SNP(A) to determine the molar absorption coefficient of pyrene in the dispersions. The absorbance spectra were acquired. They needed to be corrected by subtracting the absorbance spectra obtained with the SNP dispersions containing no pyrene. After the measurements were complete, the SNP dispersions were re-transferred into a vial and an excess amount of pyrene crystals was added. The cycle of shaking, isolating the SNP dispersions, and acquiring the absorbance and fluorescence spectra was repeated once a day until the absorption of pyrene in the SNP dispersions remained constant.

2.9 Quenching Experiments

2.9.1 Preparation of Quencher Solution: Nitromethane (500 mg, 8.2 mmol) was dissolved in 10 g of Milli-Q water to obtain a concentration of 0.082 M.

2.9.2 Preparation of Pyrene in SNP Dispersions: A concentrated HM-SNP aqueous dispersion was prepared with 0.65 μM pyrene as described in section 2.8.1 and its volume was split in two. To one half, a set amount of Milli-Q water was added while the other half was mixed with a same amount of 0.082 M nitromethane in water to yield two HM-SNP aqueous dispersions containing 0.5 μM pyrene, one without and the other with 20.5 mM nitromethane.

The fluorescence quenching experiments were conducted with either 0.2 wt% or 1.3-1.6 wt% HM-SNP aqueous dispersions (depending on the dispersability of the HM-SNPs) containing 0.5 μM pyrene. For a given HM-SNP, the HM-SNP dispersion without nitromethane (2 g) was placed in a 1 cm x 1 cm quartz fluorescence cell. Aliquots of the HM-SNP dispersions containing 20.5 mM nitromethane were added. This procedure ensured that, in these experiments, only the concentration of nitromethane was varied while the concentrations of pyrene and HM-SNPs remained the same. The emission spectra and fluorescence decays of pyrene in the HM-SNP dispersions were acquired 5 minutes after the two dispersions were mixed to ensure their homogeneity.

Chapter 3

Loading Capacity of SNPs/HM-SNPs

The hydrophobic pendants that were grafted onto the HM-SNPs were expected to associate in aqueous solution and generate hydrophobic microdomains where pyrene would partition into. Although pyrene has a low solubility in water, some pyrene remained in water and was in equilibrium with pyrene bound to HM-SNPs. This chapter was designed to determine the equilibrium constant, size, and the loading capacity of pyrene in SNP/HM-SNPs by conducting a series of fluorescence experiments which are described hereafter.

3.1 Determination of the Equilibrium Constant K_B for the Binding of Pyrene to Unmodified SNP(A)

The binding constant K_B was determined from the analysis of the fluorescence decays of pyrene in HM-SNP dispersions without quencher. In this analysis, Equation 2.1 could be simplified into Equation 3.1 by omitting the quenching rate constant k_{qW} and k_{qSNP}.

$$[Py^*]_t = [Py^*_{diff}]_{t=0} \times \left(\alpha_{PyW} \exp\left[-t\left(\frac{1}{\tau_{PyW}} \right) \right] + \left(\alpha_{PySNP-P} + \alpha_{PySNP} \right) \exp\left[-\frac{t}{\tau_0} \right] \right) + \alpha_{SNP} f_{SNP}(t) \qquad (3.1)$$

As illustrated in Figure 2.1A and B and described by Equation 3.1, two long decay times (τ_{PyW} and τ_0) and a much shorter contribution ($f_{SNP}(t)$) were detected in the 0.5 μM pyrene aqueous dispersions of SNP(A). The short (< 30 ns) decay was a result of the intrinsic fluorescence of SNP(A). Changes in the concentration of SNP(A) affected the contribution (α_{SNP}) of $f_{SNP}(t)$ to the fluorescence decay. At low SNP(A) concentration, α_{SNP} in Equation 3.1 and light scattering caused by the particles on the emission spectrum were reduced in Figure 3.1.

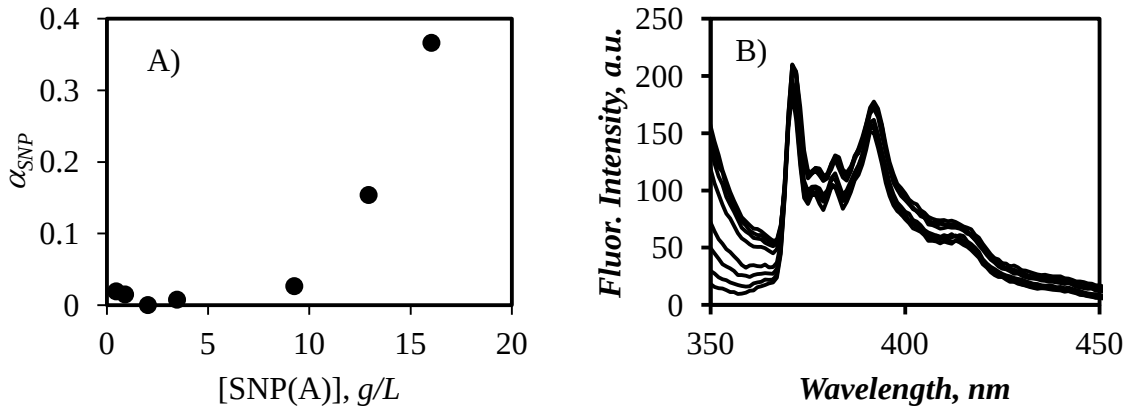

Figure 3.1. A) Plot of α_{SNP} as a function of SNP(A) and B) fluorescence spectra of 0.5 μM pyrene in the concentrated SNP(A) dispersion from bottom to top: [SNP(A)] ranges from 16 g/L to 0.5 g/L. λ_{ex}= 346 nm.

The two long decay times retrieved from the fluorescence decay analysis with Equation 3.1 were due to pyrene. One decay time equal to 130 ns corresponded to the lifetime of pyrene in aerated water (τ_{pyw}= 130 ns)[30] and it was fixed in Equation 3.1. The other long decay time retrieved from the decay analysis was found to equal 206 ± 5 ns regardless of SNP concentration (Figure 3.2).

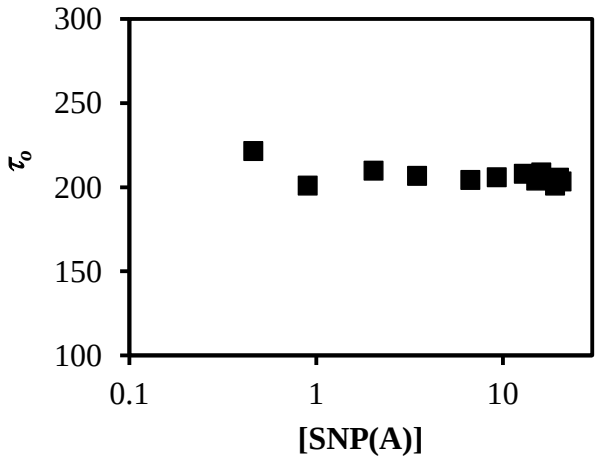

Figure 3.2. Plot of τ_o as a function of SNP(A) concentration

This 206 ns decay time was attributed to pyrene molecules that were bound to the SNPs and it was referred to as τ_o in Equation 3.1. That τ_o was larger than τ_{PyW} reflected the slower mobility of pyrene bound to SNPs which reduced quenching by oxygen dissolved in water (see Equation 1.2). At low SNP concentration, little pyrene was bound to the SNPs and the long fluorescence decay could no longer be detected. In this case, the exponential term for τ_o in Equation 3.1 was omitted.

The pre-exponential factors in Equation 3.1 associated with the different lifetimes of pyrene were used to determine the molar fraction of pyrene free in water (f_{free}) and bound to SNP (f_{bound}) and the equilibrium constant, K_B, for the binding of pyrene to the SNPs by applying Equation 3.2.

$$K_B = \frac{f_{bound}}{[HM-SNP] f_{free}} \tag{3.2}$$

The expressions for f_{bound} and f_{free} were given in Equation 3.3 using the pre-exponential factors α_{pyW}, α_{pySNP}, and $\alpha_{pySNP\text{-}P}$ obtained from the decay analysis with Equation 3.1.

$$f_{bound} = \frac{\alpha_{PySNP} + \alpha_{PySNP-P}}{\alpha_{PyW} + \alpha_{PySNP} + \alpha_{PySNP-P}} \quad \text{or} \quad f_{free} = \frac{\alpha_{PyW}}{\alpha_{PyW} + \alpha_{PySNP} + \alpha_{PySNP-P}} = 1 - f_{bound} \tag{3.3}$$

As the SNP(A) concentration increased from 0 to 21 g/L, f_{bound} increased and f_{free} decreased in Figure 3.3B. The f_{bound}/f_{free} ratio was plotted as a function of SNP(A) concentration in Figure 3.3B. The linear relationship observed between the ratio f_{bound}/f_{free} and the SNP(A) concentration was expected from Equation 3.2. However, f_{bound}/f_{free} did not pass through the origin and indicated that 4 (±2) % of pyrene with a long lifetime were still detected in water from the fluorescence decay analysis. The small contribution was attributed to the analysis program having difficulty distinguishing between background noise and a small contribution

of a long-lived species. To overcome this problem, the f_{bound}/f_{free} ratio obtained by extrapolating the plot to zero SNP concentration was subtracted from the ratios obtained at all SNP concentrations as shown in Figure 3.3C. The binding constant (K_B) was determined from the slope of the plot in Figure 3.3C and found to equal 5.0 (± 0.1) × 10^{-2} L/g.

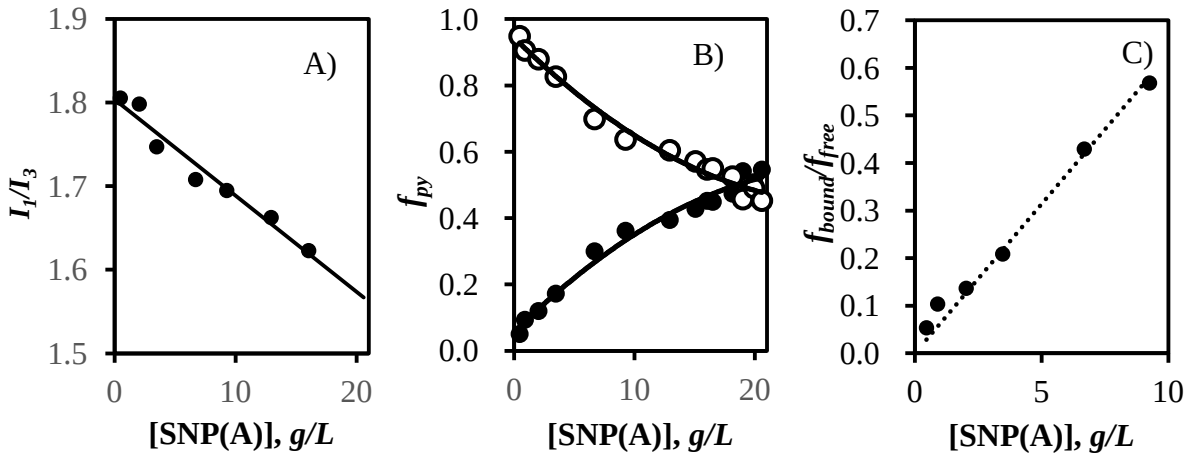

Figure 3.3 Plots of A) the I_1/I_3 ratio, B) the molar fractions of pyrene (●) bound to SNP (f_{bound}) and (○) free in water (f_{free}), and C) the ratio f_{bound}/f_{free} as a function of SNP(A) concentration.

As the concentration of SNP(A) and f_{bound} increased in Figure 3.3B, the I_1/I_3 ratio, which reflects the average polarity of the different environments experienced by pyrene, decreased in Figure 3.3A. In Figure 3.3B, f_{PyW} decreased from 1 to 0.4 as the concentration of SNP(A) increased from 0 to 21 g/L. If all pyrene molecules were bound to SNP(A) (f_{bound} = 1 and f_{free}= 0), the I_1/I_3 ratio would reflect the polarity of the environment experienced by pyrene to SNP(A). The I_1/I_3 ratio was plotted as a function of f_{free}/f_{bound} in Figure 3.4. The y-intercept of the plot of the I_1/I_3 ratio versus the concentration of SNP(A) was obtained by extrapolating the trend to a zero f_{free}/f_{bound} ratio to yield the $(I_1/I_3)_o$ ratio corresponding to

pyrene bound to SNP(A). The $(I_1/I_3)_o$ ratio obtained equaled 1.7 (± 0.0) in Figure 3.4, slightly lower than the I_1/I_3 ratio of 1.8 obtained for pyrene in water, thus indicating that pyrene bound to SNP(A) must be fairly exposed to water.

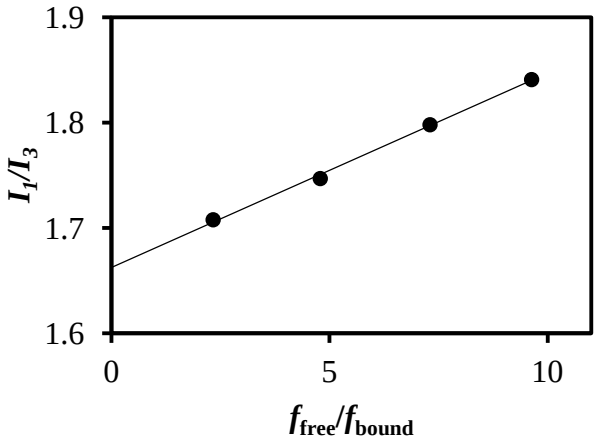

Figure 3.4. Plot of I_1/I_3 as a function of the f_{free}/f_{bound} ratio for SNP(A).

3.2 Determination of the Binding Constant K_B for Hydrophobically Modified SNP(A)

SNP(A) was modified with hexanoic acid to yield C6(*x*)-SNP(A) where *x* represented the DS of hexanoic acid which was varied from 0 to 0.15. Pyrene (0.5 μM) was dissolved in aqueous dispersions of different C6(*x*)-SNP(A) particles and its photophysical properties were examined by steady-state and time-resolved fluorescence. A significant amount of pyrene free in water emitting with the lifetime τ_{PyW} of 130 ns was detected from the analysis of the fluorescence decays with Equation 3.1. Pyrene did not bind to C6(*x*)-SNP(A) at low concentration of C6(*x*)-SNP(A) and the long lifetime of pyrene bound to SNP ($\tau_{PySNP} \sim 300$ ns) could not be detected. At low concentrations of C6(*x*)-SNP(A), the fluorescence decays were analyzed with Equation 3.1 where the second term was omitted ($\alpha_{PySNP\text{-}P} + \alpha_{PySNP} = 0$). At higher C6(*x*)-SNP(A) concentrations where pyrene bound to C6(*x*)-SNP(A) could be detected and f_{bound} could be determined, the f_{bound}/f_{free} ratio was calculated and plotted as a function of SNP(A) concentration in Figure 3.5A. As for SNP(A), the f_{bound}/f_{free} ratio increased linearly

with increasing C6(x)-SNP(A) concentration, as expected from Equation 3.3. The slope of these straight lines yielded K_B which was plotted as a function of the DS of hexanoic acid in Figure 3.5B.

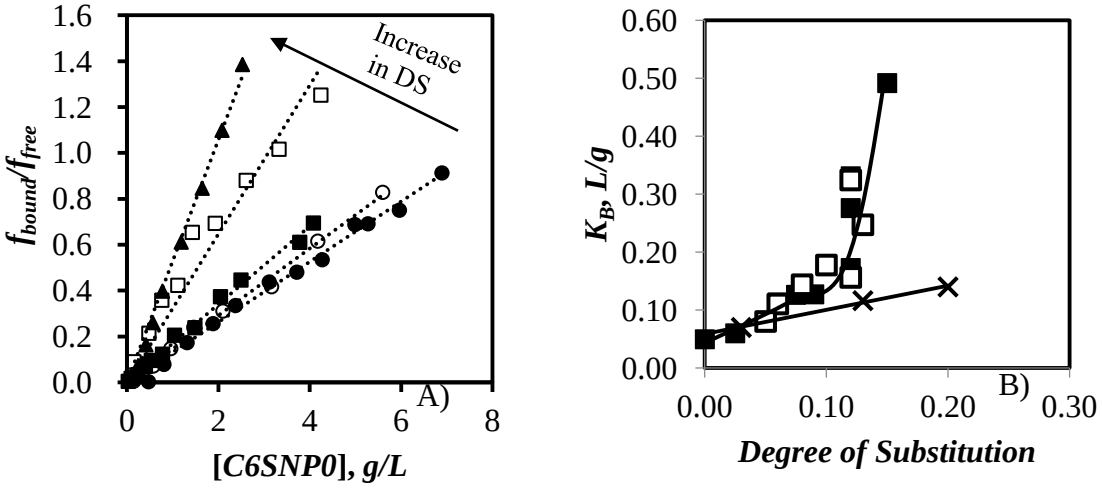

Figure 3.5. Plots of A) the ratio f_{bound}/f_{free} as a function of C6(x)-SNP(A) concentration with x equal to (●) 0.08, (○) 0.09, (■) 0.11, (□) 0.12, and (▲) 0.15 and B) K_B versus DS for (■) C6-SNP(A), (□) C6-SNP(F), and (x) C3-SNP(F).

Binding of pyrene to the C6(x)-SNP(A) particles was enhanced with increasing DS of hexanoic acid, resulting in a less polar environment for pyrene. The $(I_1/I_3)_o$ ratio of each C6(x)-SNP(A) sample was obtained by extrapolating a plot of the I_1/I_3 ratio measured at different C6(x)-SNP(A) concentrations as a function of the f_{free}/f_{bound} ratio and extrapolating the trend to a zero f_{free}/f_{bound} ratio as shown in Figure 3.6A. A plot of $(I_1/I_3)_o$ ratio versus DS is shown in Figure 3.6B. Considering the change in K_B values when DS increased from 0.05 to 0.15, $(I_1/I_3)_o$ ratio showed little change over the same range of DS. This observation indicates that the environment provided by the microdomains generated by the hexanoic acid groups did not change much when DS was increased from 0.05 to 0.15.

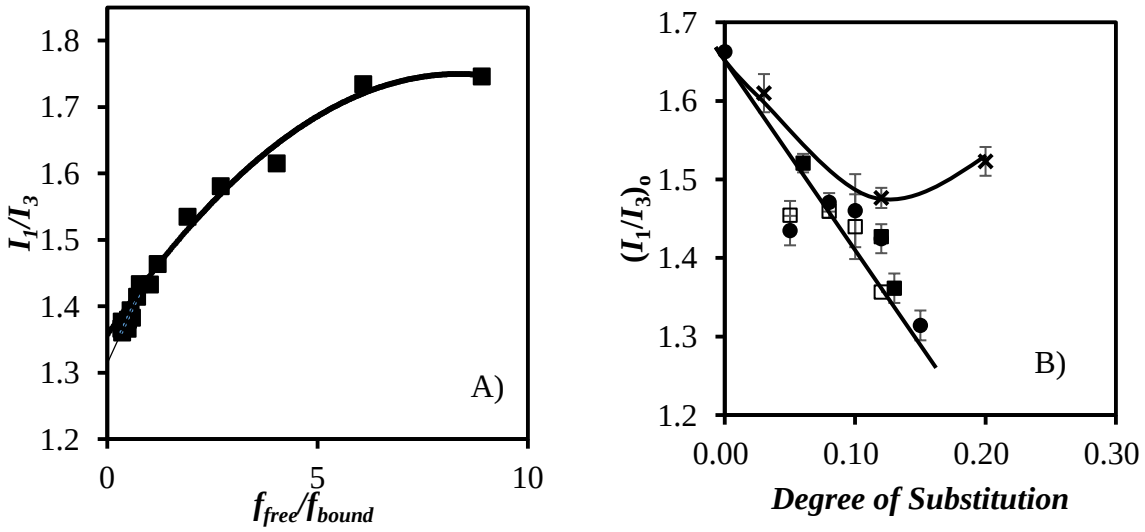

Figure 3.6. Plots of A) the I_1/I_3 ratio of C6(0.12)-SNP(A) as a function of the ratio f_{free}/f_{bound} and B) the $(I_1/I_3)_0$ ratio of pyrene bound to (■) C6(*x*)-SNP(A), (□) dialyzed C6(*x*)-SNP(F), and (x) dialyzed C3(*x*)-SNP(F) as a function of DS.

Beside SNP(A), SNP(F) was also modified with hexanoic acid to yield a series of C6(*x*)-SNP(F) samples having a much smaller size (see Table 2.1) and thus, a larger surface area. The fluorescence spectra and decays of 0.5 μM pyrene in aqueous dispersions of dialyzed C6(*x*)-SNP(F) were acquired and analyzed to yield their I_1/I_3 ratios and the molar fractions f_{free} and f_{bound}. The ratio f_{bound}/f_{free} were plotted as a function of C6(*x*)-SNP(F) concentration to yield K_B which was added to Figure 3.5B. The I_1/I_3 ratios plotted as a function of f_{bound}/f_{free} were extrapolated to zero to yield the $(I_1/I_3)_o$ ratio reflecting the intrinsic polarity of the C6(*x*)-SNP(F) samples. Their $(I_1/I_3)_o$ ratio was plotted as a function of DS in Figure 3.6. The behavior of the C6(*x*)-SNP(F) samples was found to be identical to that of the C6(*x*)-SNP(A) samples, both from the trend obtained with K_B in Figure 3.5B and the $(I_1/I_3)_o$ ratio in Figure 3.6B. Consequently, the substrate onto which the hydrophobic modification had been applied did not seem to affect the microdomains generated by the hydrophobic

pendants.

The effect of the alkyl chain length of the hydrophobes was examined by comparing the behavior of the SNP(F) particles that were modified with propionic acid (C3(*x*)-SNP(F)) and hexanoic acid (C6(*x*)-SNP(F)). The same experiments were carried out and K_B and the $(I_1/I_3)_o$ ratio were determined for the C3(*x*)-SNP(F) samples. K_B in Figure 3.5B was found to increase with increasing DS of propionic acid, but C3(*x*)-SNP(F) had smaller K_B values compared to C6(*x*)-SNP(F) at DS greater than 0.1. Similarly, $(I_1/I_3)_o$ for the C3(*x*)-SNP(F) was larger than for the C6(*x*)-SNP(F) particles having a DS larger than 0.1. Consequently, the microdomains formed by the hexanoic ester groups appeared to be more hydrophobic than those formed with the propionic ester pendants at a same DS which resulted in stronger pyrene binding and a more apolar environment for pyrene bound to the C6(*x*)-SNP.

3.3 Aggregation of HM-SNPs

As it turned out, plots of f_{bound}/f_{free} as a function of SNP/HM-SNP concentration obeyed a linear relationship only up to a certain concentration of SNP/HM-SNP. At high SNP concentration, a break point was observed above which f_{bound}/f_{free} was found to increase linearly with increasing SNP/HM-SNP concentration but with a smaller slope than at SNP concentration below the break point as shown in Figure 3.7. The two linear regions of the plots reflected two regimes for the binding of pyrene to SNP/HM-SNP. A decrease in the slope of the plot past the break point indicated a weaker binding of pyrene to the SNPs. The SNP concentration at the break point separating the two regimes was determined from the intercept of the two lines representing the f_{bound}/f_{free} trends in Figure 3.7. The SNP concentration at the break points (C_{BP}) was plotted as a function of DS of hexanoic acid in Figure 3.8.

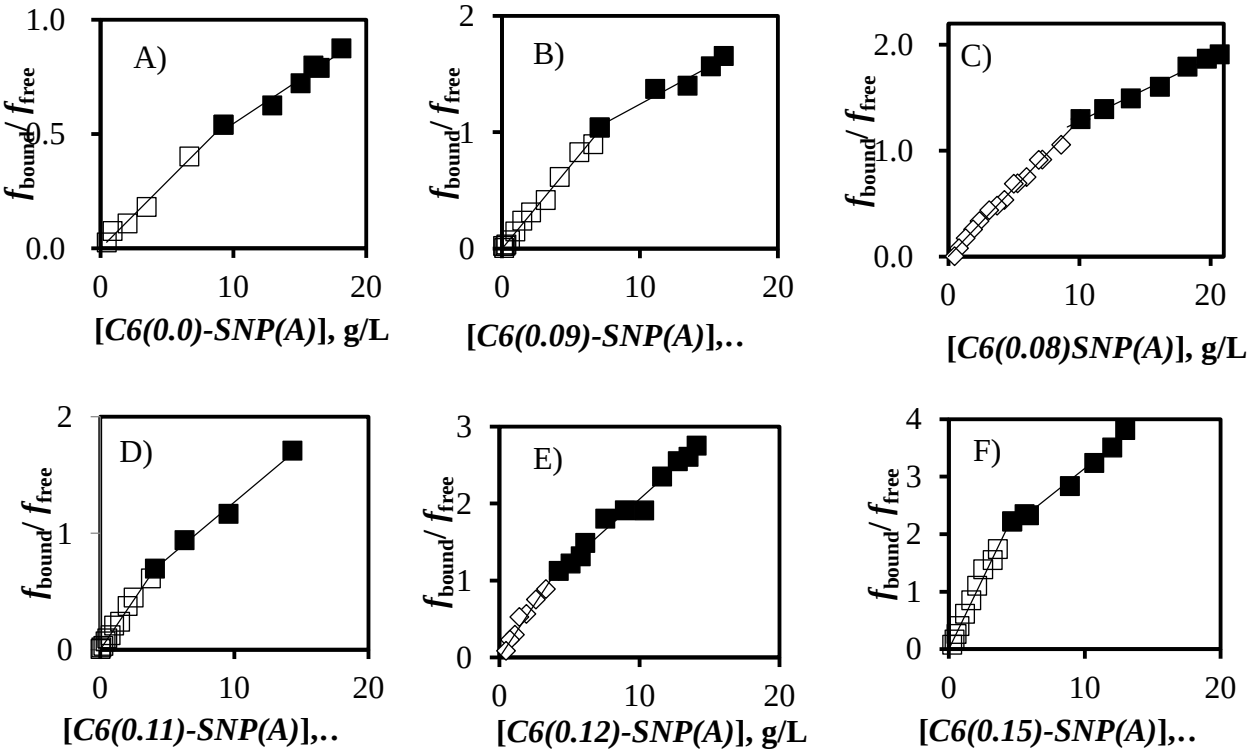

Figure 3.7. Plots of the f_{bound}/f_{free} ratio as a function of C6(x)-SNP(A) concentration where x equals A) 0.0, B) 0.09, C) 0.08, D) 0.11, E) 0.12, and F) 0.15.

In Figure 3.8, C_{BP} was found to be between 3 and 8 g/L without much evidence of a trend. Assuming that binding of pyrene occurred mostly at the surface of the SNPs, the break point would then reflect a decrease in the surface area of the SNPs due to their aggregation (Scheme 3.1). The self-aggregation might be induced by the interactions between oligosaccharides dangling at the surfaces of the particles and enhanced by the hydrophobes present on the surface of the HM-SNPs.

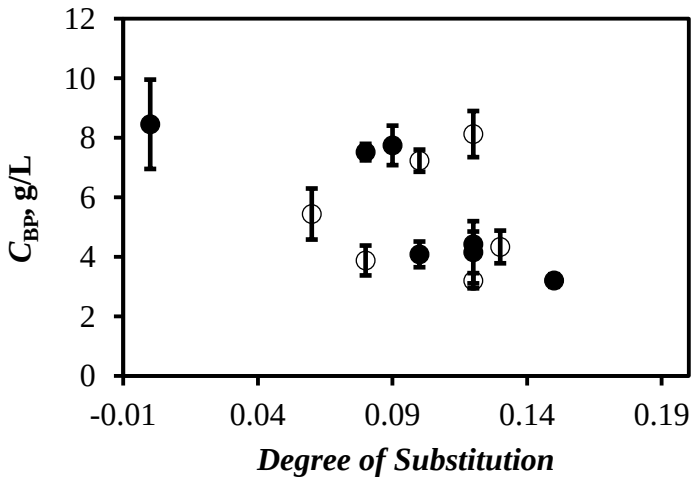

Figure 3.8. Plot of C_{BP} as a function of DS of hexanoic acid for (●) C6(*x*)-SNP(A) and (○) dialyzed C6(*x*)-SNP(F).

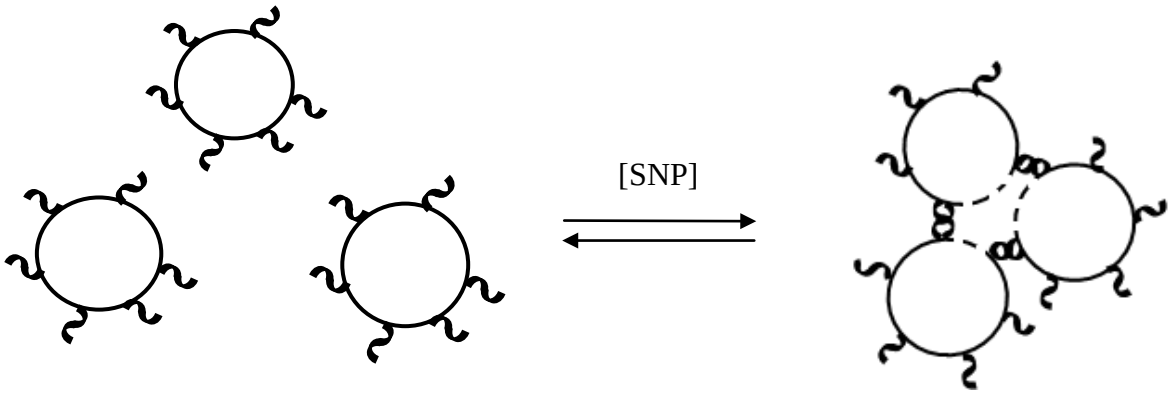

Scheme 3.1. Change in the surface area of SNP/HM-SNP that is (—) accessible and (---) inaccessible to pyrene

The break point shown in Figure 3.7 is proposed to be a consequence of pyrene binding to the surface of the SNPs and of the aggregation of the SNPs which reduces their surface and thus binding of pyrene. Before the break point, the surface area generated by the SNPs increases proportionally to the SNP concentration. Past the break point, aggregation of the particles reduces the SNP surface that is accessible to pyrene. Consequently, the f_{bound}/f_{free} ratio is not exactly equal to $K_B[SNP]$ as suggested in Equation 3.2 but rather to the product

K_{BS} x S_{SNP} where S_{SNP} represents the total surface area generated by the SNPs. At SNP concentrations lower than C_{BP}, S_{SNP} is proportional to the SNP concentration and a linear relationship is observed between the f_{bound}/f_{free} ratio and the SNP concentration as predicted by Equation 3.2. But above the break point where SNP aggregates are being formed, S_{SNP} is no longer proportional to the SNP concentration and f_{bound}/f_{free} now reflects the binding of pyrene to the surface of SNP aggregates.

To investigate the validity of the proposed rational to explain the break point observed in the plots shown in Figure 3.7, a model was implemented that was based on the following assumptions. 1) SNP aggregates were constituted of a number N_{agg} of individual SNPs. 2) As for surfactants, the concentration of isolated SNPs in the dispersions at SNP concentrations greater than C_{BP} remained constant and equal to C_{BP}, the SNP concentration at the break point. 3) At SNP concentrations greater than C_{BP}, the aqueous dispersions contained solely isolated SNPs at a concentration C_{BP} and aggregated SNPs made of a number (N_{agg}) of individual SNPs.

Based on these assumptions, the volume of a SNP aggregate (V_{agg}) would be equal to the molar volume of an individual SNP (V_0) times N_{agg} as shown in Equation 3.4,

$$V_{agg} = N_{agg} \frac{\pi D_o^{\,3}}{6} = \frac{\pi D_{agg}^{\,3}}{6} \qquad (3.4)$$

where D_o and D_{agg} are the diameter of the isolated and aggregated SNPs, respectively. This equation could be rearranged into Equation 3.5 that yielded N_{agg} as a function of D_o and D_{agg}.

$$N_{agg} = \left(\frac{D_{agg}}{D_o} \right)^3 \qquad (3.5)$$

Since the hydrophobic diameter of an individual particle (D_o) can be determined by dynamic light scattering (DLS), Equation 3.5 implies that a second equation is required to determine either D_{agg} or N_{agg}. This second equation is obtained by considering that the f_{bound}/f_{free} ratio is proportional to S_{SNP} as shown in Equation 3.6 where K_{BS} is the equilibrium constant for the binding of pyrene to the surface of the SNPs. Since the f_{bound}/f_{free} ratio can be approximated by a straight line of slope m and intercept b in Figure 3.7, S_{SNP} can be approximated as $B \times (m[SNP]+ b)$ where B is a proportionality constant to be determined.

$$\frac{f_{bound}}{f_{free}} = K_{BS} \times S_{SNP} = K_{BS}B\,(m[SNP]+b) \tag{3.6}$$

Past the break point, S_{SNP} could be described by Equation 3.7 which is obtained by considering the surface area of the isolated and aggregated SNPs.

$$S_{SNP} = [SNP]_o 4\pi D_o^2 + \frac{[SNP]-[SNP]_o}{N_{agg}} 4\pi D_{agg}^2 = B(m[SNP]+b) \tag{3.7}$$

The proportionality constant B in Equation 3.7 was obtained by noting that at the break point, the SNP concentration equals $[SNP]_o$, thus yielding the expression of B given by Equation 3.8. In this discussion, $[SNP]_o$ and C_{BP} have been used interchangeably.

$$B = \frac{[SNP]_0 4\pi D_0^2}{m[SNP]_0 + b} \tag{3.8}$$

Substituting the expression of B in Equation 3.8 into Equation 3.7 provided an expression for N_{agg} and D_{agg}/D_o in Equations 3.9 and 3.10, respectively.

$$N_{agg} = \left(\frac{D_{agg}}{D_0}\right)^2 \frac{m[SNP]_0 + b}{m[SNP]_0} \tag{3.9}$$

$$\frac{D_{agg}}{D_0} = \frac{m[SNP]_0 + b}{m[SNP]_0} \tag{3.10}$$

These expressions could then be used to establish the number average diameter <*D*> of a dispersion made of $[SNP]_o$ isolated particles and a concentration ($[SNP]$-$[SNP]_o$)/N_{agg} of SNP aggregates as shown in Equation 3.11.

$$< D >= \frac{[SNP]_o D_o + \left(\frac{[SNP] - [SNP]_o}{N_{agg}} \right) D_{agg}}{[SNP]_o + \left(\frac{[SNP] - [SNP]_o}{N_{agg}} \right)} \tag{3.11}$$

Using the parameters *m*, *p*, D_o, and $[SNP]_o$ determined experimentally, <*D*> could be compared to the number average hydrodynamic radius obtained from DLS experiments conducted on aqueous dispersions of SNPs at different concentrations of particles. The diameter of the SNP aggregates (D_{agg}) was determined by introducing the parameters *m*, *p*, $[SNP]_o$, and D_o into Equation 3.10. In turn, N_{agg} was obtained by using Equation 3.9. All the parameters were listed in Table 3.1

Table 3.1. Parameters D_0, C_{BP}, *m*, *b*, D_{agg} and N_{agg} obtained for the C6(*x*)-SNP(A) series with different DS.

DS	D_0, nm	C_{BP}, g/L	Slope, *m*	Intercept, *b*	D_{agg} nm	N_{agg}
0.00	46.2 (±2.6)	8.5 (± 3.3)	0.06 (±0.00)	0.2 (± 0.0)	61	2
0.05	43.6 (±0.2)	7.6 (± 0.6)	0.04 (± 0.01)	0.6 (± 0.1)	140	11
0.08	38.7 (±2.0)	7.5 (± 0.3)	0.07(± 0.00)	0.6 (± 0.0)	86	5
0.09	42.8 (±1.8)	7.7 (± 0.7)	0.06 (± 0.01)	0.6 (± 0.1)	93	5
0.11	36.2 (±1.9)	4.1 (± 0.4)	0.1 (± 0.01)	0.3 (± 0.1)	63	3
0.12	33.5 (±1.5)	4.4 (± 0.4)	0.1 (± 0.01)	0.8 (± 0.1)	85	7
0.15	36.7 (±0.8)	3.2 (± 0.2)	0.2 (± 0.02)	1.2 (± 0.1)	101	8

To further validate this model, the hydrodynamic diameters of aqueous dispersions of C6(0.15)-SNP(A) were determined by DLS at concentrations ranging from 0.2 to 20.5 g/L.

These concentrations were selected by considering the homogeneity and turbidity of the C6(0.15)-SNP(A) dispersions. At higher concentrations of C6(0.15)-SNP(A), the turbidity of the dispersion was so high that it induced multiple scattering that was not accounted for by the analysis software of the DLS instrument. At C6(0.15)-SNP(A) concentrations lower than 0.2 g/L, the dilute dispersions generated a noisy auto correlation function which could not be easily analyzed by the instrument. In the range of C6(0.15)-SNP(A) concentrations considered, the PDI obtained from the DLS measurements was always smaller than 0.25. The $\langle D \rangle$ values determined by applying Equation 3.11 were then compared to the D_h values retrieved by DLS in Figure 3.9. The good agreement observed between $\langle D \rangle$ and D_h in Figure 3.9 suggested that the assumptions made to determine $\langle D \rangle$ were justified, and more importantly, that pyrene fluorescence measurements might provide a measure of the total surface area generated by SNPs in aqueous dispersions.

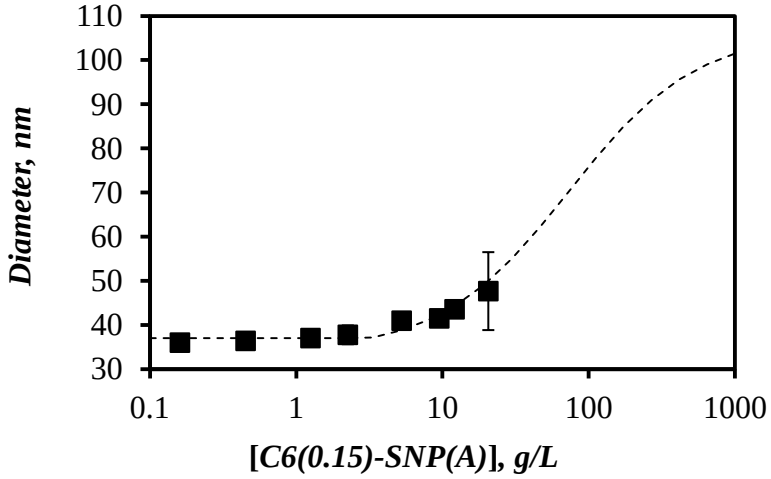

Figure 3.9. Plot of (---) $\langle D \rangle$ predicted from Equation 3.11 and (■) D_h determined from DLS measurements as a function of C6(0.15)-SNP(A) concentration.

3.4 Determination of the Loading Capacity of Pyrene in HM-SNPs

The loading capacity of pyrene in the C6(x)-SNP(A) particles was determined by measuring the absorbance of a C6(x)-SNP(A) dispersion saturated with pyrene crystals. The absorbance

was measured with a UV-Vis spectrophotometer at different times until the absorbance remained constant over time in Figure 3.10. The constant absorbance of pyrene observed over longer times indicated that the C6(*x*)-SNP(A) particles were fully loaded with pyrene and it was used to calculate the maximum loading capacity of pyrene in the HM-SNPs by applying Beer Lambert's Law in Equation 3.12.

$$A_{Py} = l\varepsilon_{Py}[Py] \tag{3.12}$$

In Equation 3.12, A_{Py} is the absorbance of pyrene at 336 nm, l is the path length of the absorption cuvette, and ε_{Py} is the molar extinction coefficient of pyrene.

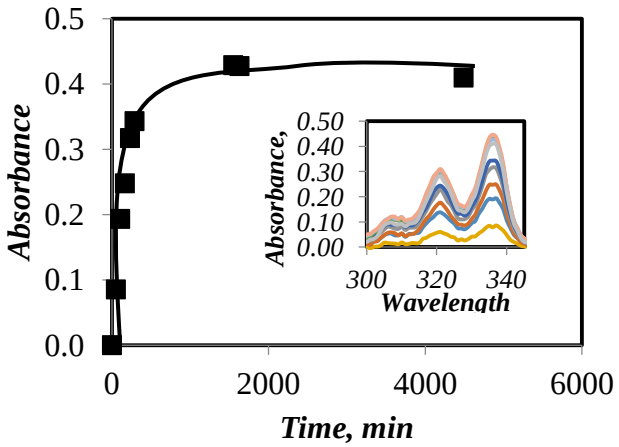

Figure 3.10. Plot of the absorbance of pyrene at 336 nm as a function of time. Insert: Absorbance spectra of pyrene in a 2 g/L aqueous dispersion of C6(0.15)-SNP(A) acquired at the pyrene concentrations used to build the plot.

The determination of the loading capacity of pyrene to the C6(*x*)-SNP(A) particles required the knowledge of ε_{PySNP} which was determined with dispersions of C6(*x*)-SNP(A) that showed the largest K_B in Figure 3.5B (i.e. C6(0.15)-SNP(A)).

The absorbance of 0.5 μM of pyrene in water equaled 0.16 OD obtained with a cell

having a 10 cm path length. Equation 3.12 was applied to determine the molar absorption coefficient of pyrene in water (ε_{PyW}) which equaled 32500 $M^{-1}cm^{-1}$. The molar absorption coefficient of pyrene in C6(0.15)-SNP(A) (ε_{PySNP}) was determined by measuring the absorbance of a known concentration of pyrene in a dispersion of a given C5(0.15)-SNP(A) concentration. The concentration of pyrene free in water $[Py]_{free}$ was calculated from Equation 3.13. ε_{PySNP} was determined by applying Equation 3.14 and found to equal 29600 (± 3800) $M^{-1}cm^{-1}$.

$$[Py]_{free} = \frac{A_{Py}}{\varepsilon_{PyW}(1 + K_B[SNP])} \tag{3.13}$$

$$\varepsilon_{PySNP} = \frac{A_{Py} - \varepsilon_{PyW}[Py]_{free}}{[Py]_{bound}} \tag{3.14}$$

The absorbance of pyrene present in the dispersion (A_{Py}) included pyrene free in water. The maximum absorbance of pyrene in water (A_{PyW}) was determined with a 10 cm path length and equaled 0.18 (±0.01) representing a pyrene concentration of 0.55 μM, close to the expected concentration of 0.7 μM reported for a saturated pyrene aqueous solution.[31] The concentration of pyrene bound to C6(*x*)-SNP(A) was calculated as described in Equation 3.15. It was then divided by the concentration of C6(*x*)-SNP(A) to determine the loading capacity of pyrene per gram of SNP.

$$[Py]_{bound} = \frac{A_{Py} - A_{PyW}}{\varepsilon_{PySNP}} = \frac{A_{PySNP}}{\varepsilon_{PySNP}} \tag{3.15}$$

In Equation 3.15, A_{PySNP} is the absorbance of pyrene bound to SNPs. The loading capacity of

pyrene in C6(*x*)-SNP(A) was calculated and plotted as a function of DS in Figure 3.11A. The loading capacity of C6(*x*)-SNP(A) increased with DS of hexanoic acid.

The concentrations of pyrene in water and bound to SNPs determined for different SNP concentrations yielded K_B. The K_B values determined by absorption measurements and decay analysis in Section 3.2 were compared in Figure 3.11B. Similar K_B values were obtained that increased with increasing DS of hexanoic acid. One of the difficulties encountered during the measure of the loading capacities of pyrene in HM-SNPs was their rather low value. As a result, pyrene dissolved in C6(*x*)-SNP(A) dispersions gave a weak absorbance signal resulting in large standard deviations for the K_B values obtained from the absorption measurements compared to the K_B values obtained from the fluorescence decay analysis. Nevertheless, a good agreement was observed for the K_B values obtained by fluorescence and absorption measurements.

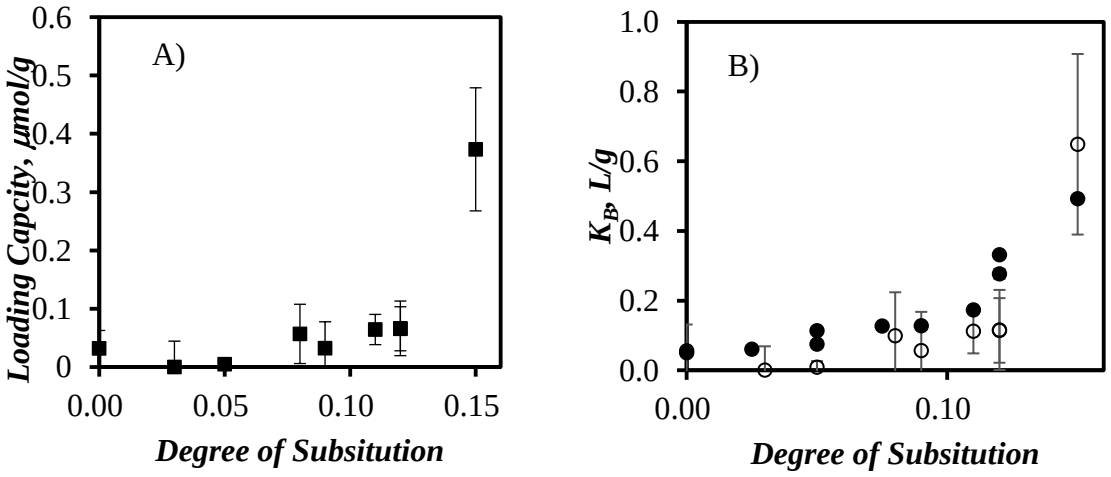

Figure 3.11. Plots of A) the loading capacity of pyrene and B) K_B of pyrene binding to SNPs determined from the analysis of (●) fluorescence decays and (○) absorption spectra.

3.5 Conclusions

The equilibrium constant, K_B, for the binding of pyrene to hydrophobically modified SNPs was determined from the analysis of fluorescence decays acquired with aqueous dispersions of HM-SNPs containing 0.5 μM pyrene. The $(I_1/I_3)_o$ ratio provided a measure of the polarity of the local environment probed by pyrene and it was determined for the HM-SNPs. The $(I_1/I_3)_o$ ratio decreased and K_B increased with increasing DS for SNPs modified with propionic and hexanoic acid reflecting the increased hydrophobicity of the particles. At a same DS, the C6(*x*)-SNP(F) samples were found to be more hydrophobic than the C3(*x*)-SNP(F) samples as reflected by their lower $(I_1/I_3)_o$ and higher K_B values. All particles were found to aggregate at high SNP concentration from the break point observed in all plots of f_{bound}/f_{free} as a function of SNP concentration. The break point in the plots observed at an SNP concentration C_{BP} defined a boundary between two regimes. At SNP concentrations lower than C_{BP}, individual particles existed but at concentrations larger than C_{BP}, a mixture of individual particles and particle aggregates coexisted in the aqueous dispersions. Pyrene most likely bound to the surface of the SNPs resulting from the many interfaces generated during extrusion by shearing the large starch granules into the much smaller SNPs. The ability of pyrene molecules to bind to the particles reflected the accessibility of the particles surface to pyrene. Particle aggregation reduced the accessible surface and thus, the binding of pyrene to the particles. A model was introduced to predict the average diameter, $<D>$, of the particles and their aggregates in the dispersion. Comparison of $<D>$ predicted by the model and the hydrodynamic diameter D_h of aqueous dispersions of SNPs determined at different SNP concentrations showed sufficiently good agreement to support the validity of the proposed model.

The loading capacity of pyrene in aqueous dispersions of HM-SNP(A) was

determined by UV-Vis spectroscopy. C6(0.15)-SNP(A) had the highest loading capacity. As longer alkyl chains and higher DS increased the binding and loading capacity of pyrene, modification of SNPs with alkyl chains that are longer than hexanoic acid is expected to yield HM-SNPs that could uptake larger quantities of a hydrophobic cargo and as such, might be good candidates for drug delivery applications.

Chapter 4

The Protection Afforded by SNP/HM-SNPs

One of the most important properties that a carrier of hydrophobic molecules must display is its ability to protect its cargo from the solvent. Chapter 3 demonstrated that hydrophobic microdomains can be generated onto SNPs where pyrene could partition into. The level of protection afforded by these HM-SNPs is characterized in this chapter by conducting quenching studies of pyrene with nitromethane, a water-soluble quencher. The most interesting result of these studies was the detection of a long-lived unquenched pyrene species at high nitromethane concentration indicating that some pyrene molecules were inaccessible to nitromethane and protected from quenching. The molar fraction of pyrene protected from quenching reflected the level of protection provided by HM-SNPs to pyrene and were determined from the fluorescence analysis of the fluorescence decays of 0.5 μM pyrene in aqueous dispersion of HM-SNPs in the presence of nitromethane.

4.1 Quenching of Pyrene in Water

The accessibility of water to pyrene bound to SNPs was characterized by conducting fluorescence quenching experiments with nitromethane. However, the binding studies described earlier have established that a significant fraction of pyrene remained in water in the aqueous SNP dispersions. Consequently, the quenching of pyrene in water needed to be characterized. To this end, fluorescence experiments were conducted to determine the rate constant characterizing the quenching of pyrene by nitromethane in water. The fluorescence spectra and decays of pyrene in water were acquired at different nitromethane concentrations. Due to the strong scattering of the solutions at the low pyrene concentration (0.5 μM) used, decays in Figure 4.1 B showed a short component. The decays were analyzed with a sum of two exponentials where the long contribution was attributed to pyrene in water as described by Equation 4.1.

$$[Py^*]_t = [Py^*_{diff}]_{t=0} \times \exp\left[-t\left(k_{qW}[Q] + \frac{1}{\tau_{PyW}}\right)\right] \quad (4.1)$$

The quantity $(k_{qW}[Q] + 1/\tau_{PyW})^{-1}$ in Equation 4.1 was referred to as τ for the lifetime of pyrene in water in the presence of nitromethane. The quenching of pyrene in water by nitromethane was characterized by the quenching rate constant k_{qW} and resulted in a decrease in the fluorescence intensity and shortening of the fluorescence decay of pyrene as illustrated in Figure 4.1.

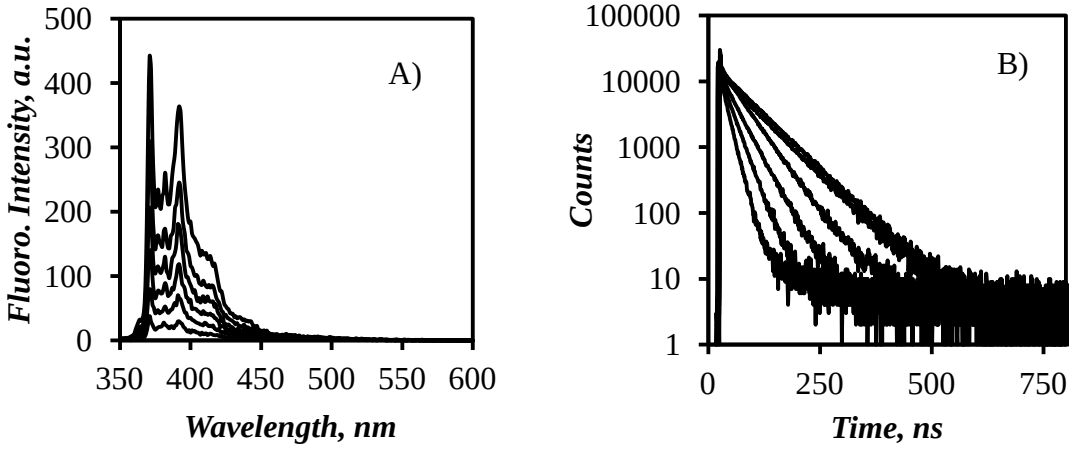

Figure 4.1. A) Fluorescence spectra and B) fluorescence decays of pyrene in water with different nitromethane concentrations. From top to bottom: [$MeNO_2$] increases from 0 to 0.082 M, λ_{ex}=338 nm.

The bimolecular rate constant k_{qW} for the quenching of pyrene by nitromethane in water was determined by fitting a plot of I_o/I and τ_{PyW}/τ according to Equation 1.1. As expected from Equation 1.1, a linear relationship was obtained in Figure 4.2 by plotting the ratios I_o/I and τ_{PyW}/τ as a function of nitromethane concentration. τ_{PyW} was determined to equal 130 ns in agreement with reported literature value.[25] The slope K_D of the τ_{PyW}/τ ratio versus nitromethane concentration in Figure 4.2 was determined and found to equal 873 (±7)

M^{-1}. Theoretically the data points obtained for the ratios of I_o/I and τ_{PyW}/τ in Figure 4.2 should overlap, but residual static quenching between pyrene and nitromethane resulted in I_o/I ratios being slightly larger than the τ_{PyW}/τ ratios. Since the τ_{PyW}/τ ratios describe dynamic quenching only, the rate constant k_{qW} in Equation 1.1 was determined from the ratio K_D/τ_{PyW} and equaled 6.5 (± 0.05) x 10^9 $M^{-1}s^{-1}$, close to reported values.[30]

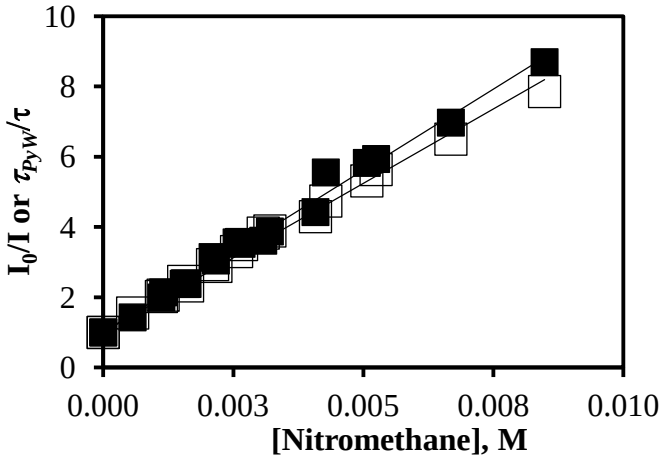

Figure 4.2. Plot of of I_o/I and τ_{PyW}/τ as a function of nitromethane concentration for 0.5 μM pyrene in water.

4.2 Quenching of Pyrene in Aqueous Dispersions of SNPs

The SNPs exhibited some intrinsic fluorescence that overlapped the pyrene fluorescence and whose intensity increased with the extent of shearing applied during extrusion resulting in smaller hydrodynamic radii in Table 2.1. The SNP fluorescence distorted the fluorescence spectra of pyrene and appeared as a sharp peak at the early times of the fluorescence decays (Figure 4.3). The fluorescence of the SNPs was found to decay within 30 ns (Figure 4.3D).

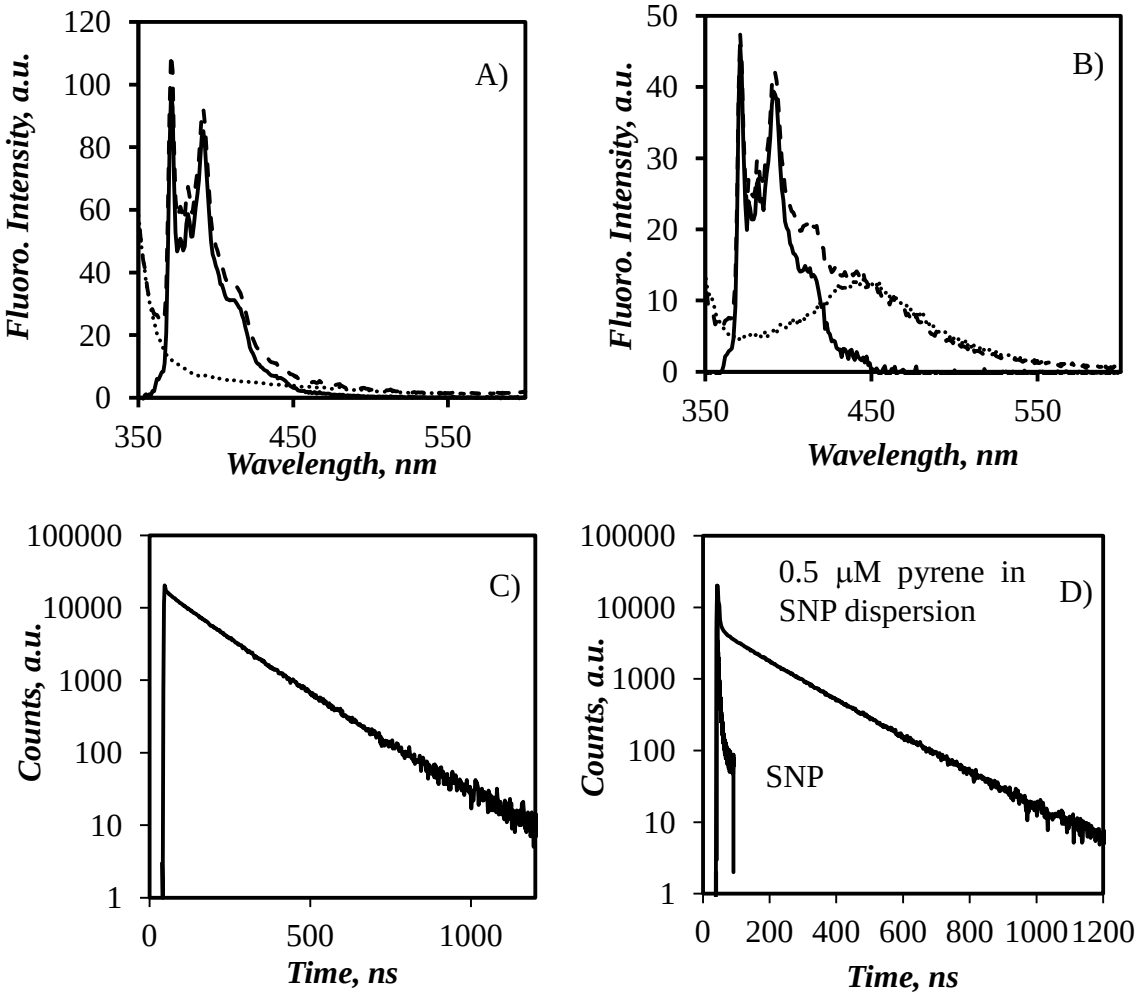

Figure 4.3. Fluorescence spectra of A) (---) 0.5 μM pyrene in 16 g/L SNP(A) dispersion, (…) 16 g/L SNP(A) dispersion, and (—) 0.5 μM pyrene after correction, B) (---) 0.5 μM of pyrene in 16 g/L SNP(F) dispersion, (…) 16 g/L SNP(F) dispersion, and (—) 0.5 μM pyrene after correction. Fluorescence decay of 0.5 μM of pyrene in C) 16 g/L SNP(A) dispersion and D) 16 g/L SNP(F) dispersion. The short decay in D) represents the function $f_{SNP}(t)$ in Equation 2.1 of the SNP(F) dispersion.

The fluorescence spectra of pyrene were obtained after subtracting the emission spectrum of the SNP dispersions normalized between 350 nm and 360 nm where pyrene does not emit. The fluorescence decays were fitted with Equation 2.1 where the parameters τ_{pyW} (= 130 ns),

k_{qW}[=6.5 (± 0.05) x 10^9 $M^{-1}s^{-1}$], and τ_o were fixed in the fluorescence decay analysis. As for pyrene in water, addition of nitromethane to aqueous dispersions of SNPs containing 0.5 μM pyrene resulted in a decrease of the fluorescence intensity and a reduction in the fluorescence lifetime as described in Figure 4.4A and 4.4B, respectively.

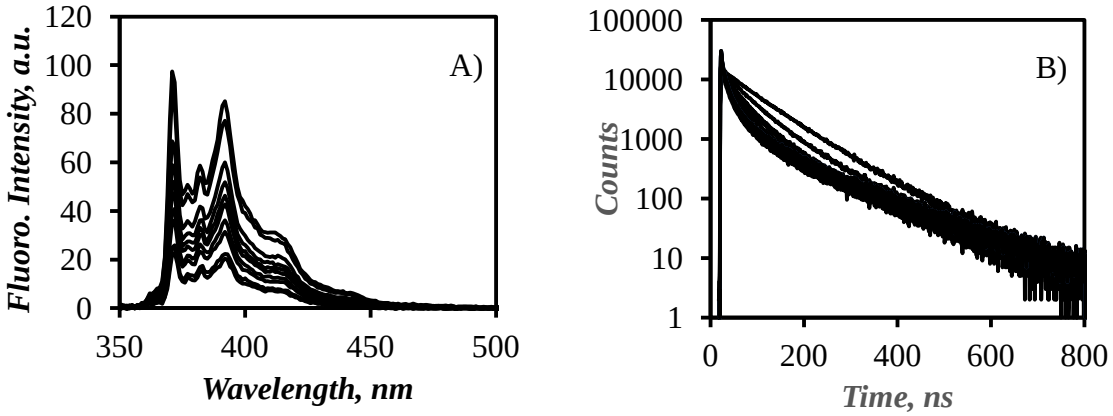

Figure 4.4 A) Fluorescence spectra and B) fluorescence decays of pyrene in a 16 g/L SNP(A) dispersion with different nitromethane concentrations. Top to bottom: [$MeNO_2$] ranges from 0 to 0.09 M. [Py] = 0.5 x 10^{-6} mol/L.

Three pyrene species are expected to be present in the SNP dispersions. They are the pyrene molecules that are in water (Py_W), bound to the SNPs but accessible to the quencher (Py_{SNP}), and bound to the SNPs and protected from quenching ($Py_{SNP\text{-}P}$) and they are represented in Equation 2.1 by their molar fraction α_{PyW}, α_{PySNP}, and $\alpha_{PySNP\text{-}P}$, respectively. The natural lifetimes of pyrene in water and pyrene bound to the SNPs were τ_{PyW} (= 130 ns) and τ_o, respectively. τ_o was determined by fitting the fluorescence decays of pyrene in aqueous SNP dispersions without nitromethane and setting α_{PySNP} in Equation 2.1 equal to zero. τ_o was then fixed in Equation 2.1 to fit the fluorescence decays of pyrene in SNP dispersions with quencher. The average decay time associated with the function $f_{PySNP}(t)$ in Equation 2.1 for the species Py_{SNP} was referred to as τ_{PySNP} and equaled $(k_{qSNP}[Q]+1/\tau_o)^{-1}$.

Since k_{qW} (= 6.5 x 10^9 $M^{-1}s^{-1}$) and τ_{PyW} (= 130 ns) were known, the decay time representing the quenching of pyrene in water Py_W by nitromethane in Equation 2.1 could be determined independently for a given nitromethane concentration and was fixed during the decay analysis. The lifetime τ_o for pyrene bound to the SNPs remained constant regardless of the size of the particles as shown in Table 4.1 and equal to 192 (±11) ns. τ_o was 50 % longer than τ_{PyW} and similar to the lifetime of 195 ns for pyrene bound to the hydrocarbon core of the SDS micelles as reported in the literature.[32] At low quencher concentration, the analysis program could not distinguish between the contributions α_{PySNP} and $\alpha_{PySNP\text{-}P}$ in Equation 2.1 of the exponentials associated with τ_{PySNP} and τ_0 since both lifetimes were too close from each other. However, α_{PySNP} and $\alpha_{PySNP\text{-}P}$ could be determined with better accuracy at high quencher concentration where τ_{PySNP} and τ_o were sufficiently different. Indeed, the ratio $\alpha_{PySNP\text{-}P}/\alpha_{PySNP}$ reached a constant value at high quencher concentrations in Figure 4.5. The ratios $\alpha_{PySNP\text{-}P}/\alpha_{PySNP}$ that yielded a constant value were averaged and the average ratio was then fixed in the decay analysis with Equation 2.1.

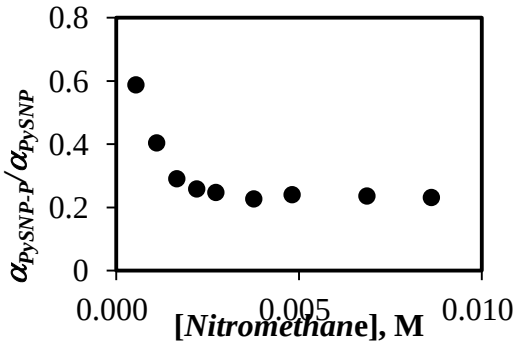

Figure 4.5. Plot of $a_{PySNP\text{-}P}/a_{PySNP}$ of pyrene loaded in SNP(A) dispersion as a function of nitromethane concentration. [SNP(A)]= 16 g/L.

Under these conditions, the decay fits yielded the decay time τ_{PySNP} and the ratio $<\tau_o>/<\tau>$ could be determined. The average lifetime of pyrene $<\tau>$ was calculated according to Equation 4.2.

$$<\tau>=\frac{\alpha_{PyW}\tau_{PyW}+\alpha_{PySNP}\tau_{PySNP}+\alpha_{PySNP-P}\tau_o}{\alpha_{PyW}+\alpha_{PySNP}+\alpha_{PySNP-P}} \quad (4.2)$$

The ratios I_o/I and $<\tau_o>/<\tau>$ obtained from, respectively, the analysis of the fluorescence spectra in Figure 4.4A and fluorescence decays in Figure 4.4B overlapped in Figure 4.6 indicating that both measurements reflected the diffusional quenching of pyrene by nitromethane and that little static quenching took place. Plots of the I_o/I and $<\tau_o>/<\tau>$ ratios as a function of nitromethane concentration did not yield a linear Stern Volmer plot as would have been expected from Equation 1.1. Instead, the plots showed a downward curvature indicative of protective quenching. Protective quenching is observed when some of the pyrenes are inaccessible to the quencher.[23,32-33] SNPs appeared to provide distinct environments for pyrene dyes that experienced different accessibilities to nitromethane with some pyrene molecules being either protected from or exposed to nitromethane in water. The pyrenes that could not be quenched by nitromethane retained the same fluorescence intensity regardless of nitromethane concentration. The downward trend in the plot in Figure 4.6 and the long-lived pyrene species observed in the fluorescence decays shown in Figure 4.4B found at high quenching concentration were clear evidence that some pyrenes were protected from quenching in the SNP dispersions.

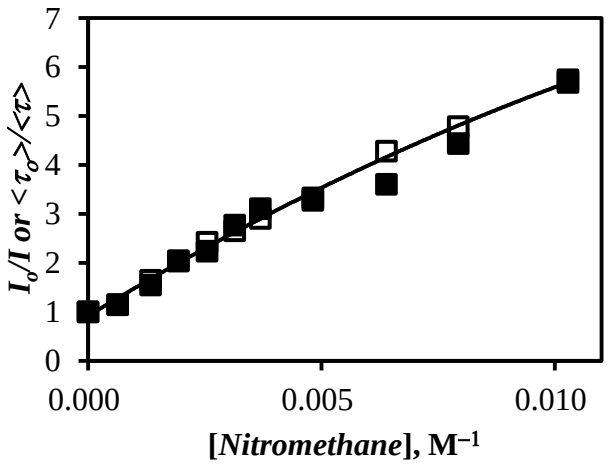

Figure 4.6. Plot of (■) I_o/I and (□) $<\tau_o>/<\tau>$ as a function of nitromethane concentration based on the analysis of the data shown in Figures 4.4A and B.

While the steady-state fluorescence spectra in Figure 4.4A illustrated the decrease in fluorescence intensity resulting from the addition of nitromethane, the heterogeneity of the aqueous SNP dispersions, where no less than three different pyrene species were identified prevented a complete spectrum analysis. By contrast, the fluorescence decays were much more straightforward to analyze as a specific lifetime retrieved from the fluorescence decay analysis could be attributed to each pyrene species in the SNP dispersions.

The decay analysis with Equation 2.1 also yielded the ratio τ_o/τ_{PySNP} which, according to Equation 1.1, was expected to increase linearly with increasing nitromethane concentration. This was indeed found to be the case in Figure 4.7 for all experimental grade SNP(*x*) samples.

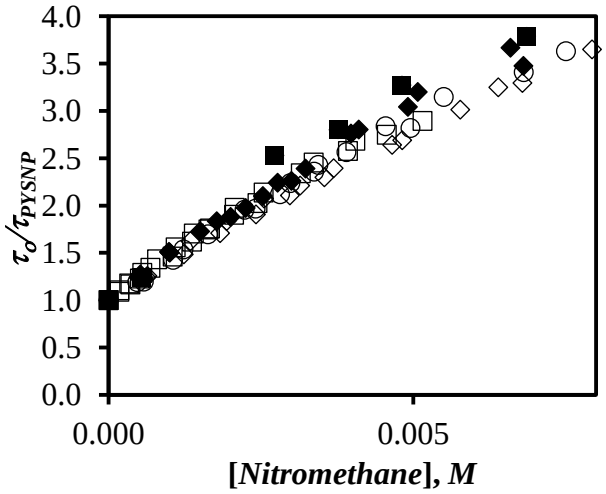

Figure 4.7. Plots of τ_o/τ_{PySNP} for (■) SNP(A), (□) SNP(B), (◆) SNP(C), (◇) SNP(D), (●) SNP(E), and (○) SNP(F) as a function of nitromethane concentration.

All τ_o/τ_{PySNP} plots yielded straight lines in Figure 4.7 whose slope yielded K_D. Dividing K_D by τ_o yielded the k_{qSNP} values which were listed in Table 4.1. The ratio $\alpha_{PySNP\text{-}P}/\alpha_{PySNP}$ that was fixed in the fluorescence decay analysis could be rearranged to yield the molar fraction f_p $(= 1+ 1/(\alpha_{PySNP\text{-}P}/\alpha_{PySNP}))^{-1}$ of pyrene molecules that were protected from quenching. The highest f_p value was obtained for the largest SNPs. f_p for the smaller SNPs was small and averaged 0.028 (±0.004) indicating that most of the pyrene molecules bound to the SNPs were accessible to quencher. k_{qSNP} remained constant in Table 4.1 and equaled 1.8 (±0.1) x $10^9\ M^{-1}s^{-1}$ regardless of the size of the SNPs. k_{qSNP} (= 1.8 x $10^9\ M^{-1}s^{-1}$) was 3.8 ± 1.0 smaller than k_{qW} (6.5 x $10^8\ M^{-1}s^{-1}$) as predicted by Equation 1.2 since pyrene bound to the SNPs was in effect immobile on the time scale of the pyrene fluorescence and thus less likely to be quenched as predicted by Equation 1.2. k_{qSNP} was also 1.7 ± 0.5 times smaller than the rate

constant k_q of pyrene present in the hydrocarbon core of SDS micelles and quenched by nitromethane.[30] Pyrene seemed to experience a more rigid environment when bound to the unmodified SNPs resulting in a smaller k_q and a non zero f_p value contrary to the large k_q and zero f_p value found for pyrene in SDS micelles.

Table 4.1. Parameters D_h, τ_0, K_D, k_{qSNP}, and f_p obtained from the quenching study of pyrene in aqueous dispersions of SNP(x) samples.

	D_h (nm)	τ_0, ns	K_D, x 10^3 M^{-1}	k_{qSNP}, x 10^{-9} $M^{-1}s^{-1}$	f_p
SNP(A)	47	218	2.8	1.7 ±0.01	0.24 ±0.01
SNP(B)	23	200	2.6	1.9 ±0.01	0.02 ±0.02
SNP(C)	17	197	1.9	1.7 ±0.01	0.03 ±0.01
SNP(D)	15	191	2.0	1.6 ±0.01	0.03 ±0.01
SNP(E)	12	191	2.0	1.8 ±0.00	0.04 ±0.00
SNP(F)	12	188	2.3	2.0 ±0.01	0.03 ±0.01

4.3 Quenching of Pyrene Bound to C6(x)-SNP(A) Particles

SNP(A) was hydrophobically modified with different DS of hexanoic acid to yield C6(x)-SNP(A). When Equation 2.1 was applied to fit the fluorescence decays of 0.5 μM pyrene in aqueous dispersions of C6(x)-SNP(A) without quencher ($\alpha_{PySNP} = \alpha_{PySNP\text{-}P} = 0$, $\tau_{PyW} = 130$ ns), τ_o plotted in Figure 4.8A as a function of DS was found to increase from 200 to 308 ns when DS increased from 0 to 0.15. These changes in lifetime were attributed to differences in oxygen quenching experienced by pyrene when bound to the different C6(x)-SNP(A). The increase in lifetime observed with increasing DS in Figure 4.8A was strong evidence that increasing DS reduced oxygen quenching of pyrene bound to the particles. This reduction in quenching was most likely a consequence of an increase of the microviscosity experienced by

the pyrene molecules bound to the hydrophobic microdomains generated by the hexanoic acid moieties. A 300 ns pyrene lifetime has already been reported for pyrene bound to highly viscous hydrophobic microdomains generated by polysoaps in water.[22,34-35]

Equation 2.1 was also applied to fit the fluorescence decays acquired with 0.5 μM pyrene in aqueous C6(*x*)-SNP(A) dispersions in the presence of quencher. The ratio $<\tau_o>/<\tau>$ where $<\tau>$ calculated according to Equation 4.2 was plotted as a function of quencher concentration in Figure 4.8B where it was compared to the I_o/I ratio. Comparison of the two trends indicates that the ratio I_o/I was larger than the ratio $<\tau_o>/<\tau>$ suggesting some static quenching of pyrene by nitromethane (i.e. pyrene and nitromethane formed a complex in the ground-state). Static quenching which occurs instantaneously can only be observed in the analysis of the fluorescence spectra. Consequently, only the lifetime measurements were considered hereafter to describe the dynamic quenching of pyrene by nitromethane.

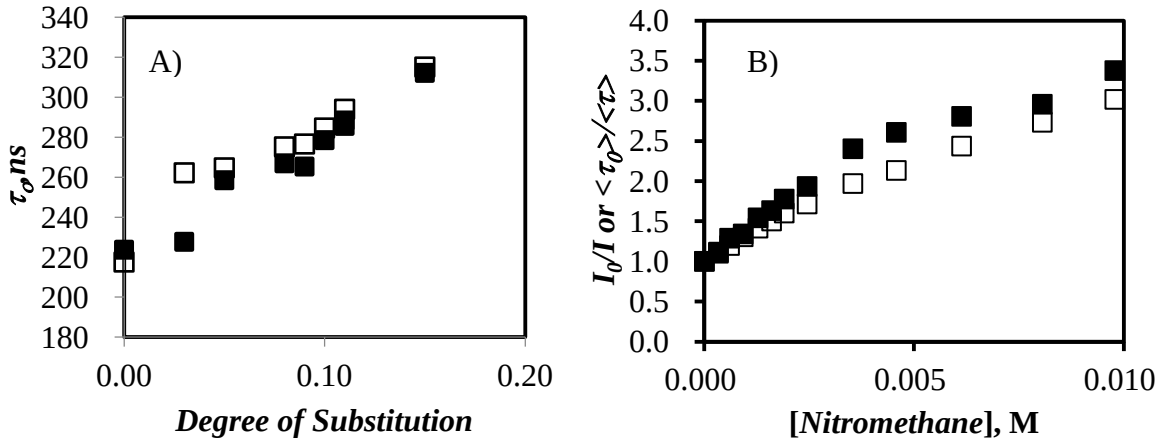

Figure 4.8. Plots of A) τ_o as a function of DS for C6-SNP(A) at (■) 2g/L and (□) 13-16 g/L and B) (■) I_0/I and (□) $<\tau_o>/<\tau>$ as a function of nitromethane concentration for a 2.2 g/L C6(0.15)-SNP(A) dispersion. [*Py*]= $0.5\text{x}10^{-6}$ M.

Equation 2.1 was applied to fit the fluorescence decays of 0.5 μM pyrene in aqueous dispersions of the C6(*x*)-SNP(A) samples. The same protocol as that used for pyrene in aqueous dispersions of unmodified SNPs was employed and the lifetime τ_{PySNP} of pyrene bound to C6(*x*)-SNP(A) that was accessible to quencher was determined. The ratio τ_o/τ_{PySNP} was plotted as a function of quencher concentration in Figure 4.9A. Straight lines were obtained, implying that Equation 1.1 could be applied to yield the rate constant k_{qSNP}. It was plotted as a function of DS for the C6-SNP(A) particles in Figure 4.9B.

k_{qSNP} decreased with increasing DS in Figure 4.9B. The reason for this trend was similar to the one used to rationalize the trend shown for τ_o in Figure 4.8A. Increasing DS generates more viscous hydrophobic microdomains in the C6(*x*)-SNP(A) particles which decrease the mobility of pyrene bound to the particles. Pyrene in the hydrophobic microdomains diffused more slowly to the interface with water where quenching by water-soluble nitromethane could occur, thus reducing the probability *p* of quenching in Equation 1.2 and resulting in lower k_{qSNP} values. As for the unmodified SNPs, the level of protection of pyrene in C6(*x*)-SNP(A) was determined from the molar fraction of protected pyrene, f_p, which was obtained from the analysis of the fluorescence decays. No distinct trend could be determined for f_p with respect to DS in Figure 4.9C. Within experimental error, the level of protection of pyrene loaded in the hydrophobic microdomains of the C6(*x*)-SNP(A) samples remained constant, regardless of DS of hexanoic acid. On average, the f_p values equaled 0.034 (±0.003), a value similar within experimental error to that of 0.028 (±0.004) obtained with the unmodified SNPs.

It was shown in Chapter 3 that the binding of pyrene to HM-SNPs depends on the total surface area generated by the particles. Past a certain concentration of HM-SNPs, pyrene

was found to bind less efficiently to HM-SNPs (see Figure 3.7). This observation led to the proposal that pyrene was likely to bind to the surface of the HM-SNPs and that aggregation of HM-SNPs reduced their overall surface area, thus reducing pyrene binding. Fluorescence experiments were conducted to investigate the effect that HM-SNP aggregation might have on the solvent accessibility and the level of protection of pyrene bound to HM-SNPs. Since all HM-SNPs showed a break point at C_{BP} indicative of aggregation between 3 g/L and 8 g/L (see Figure 3.7), the quenching experiments conducted at a HM-SNP concentration of 2 g/L below C_{BP} were repeated at a concentration above C_{BP} between 13 and 16 g/L. The concentrations of 2 and 13-16 g/L were below and above the break point and corresponded to conditions where the HM-SNPs were isolated and aggregated, respectively.

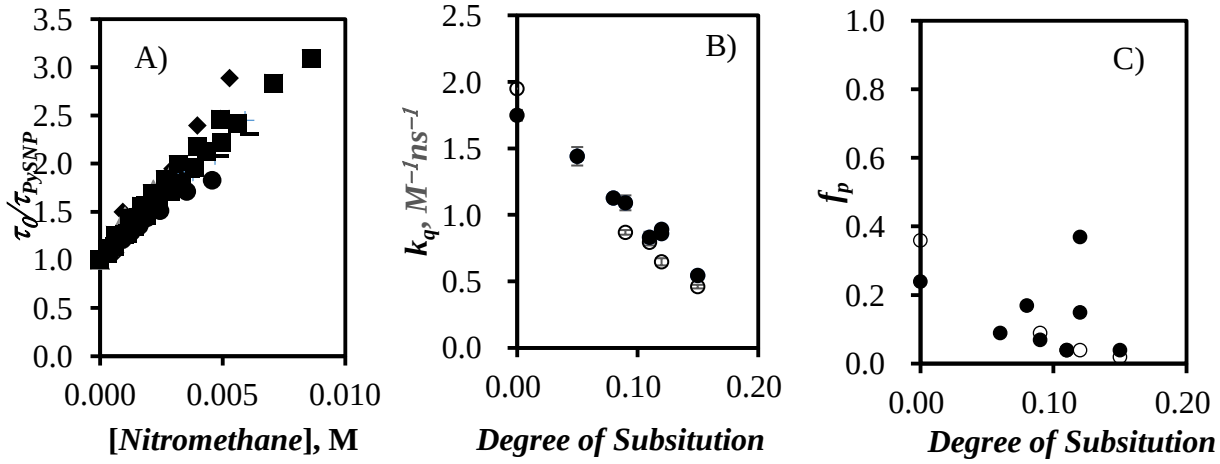

Figure 4.9. Plot of A) τ_o/τ_{PySNP} versus nitromethane concentration for C(x)-SNP(A) samples where x varies from 0 to 0.15 and plots of B) k_{qSNP} and C) f_p as a function of DS of hexanoic acid for C6-SNP(A) concentrations of (●) 2 g/L and (○) 13-16 g/L before and after the break point, respectively.

First the efficiency of quenching of pyrene by oxygen dissolved in water was compared in Figure 4.8A at HM-SNP concentrations before and after C_{BP} by determining τ_o at

both concentrations. As shown in Figure 4.8A, τ_o values obtained at HM-SNP concentrations lower and higher than C_{BP} showed the same increasing trend with increasing DS. Similar τ_o values were observed at both HM-SNP concentrations but the τ_o values obtained at HM-SNP concentrations above C_{BP} were systematically larger than those obtained at a HM-SNP concentration below C_{BP}. Since a higher τ_o value reflects a less efficient quenching of pyrene by oxygen, the systematic decrease in τ_o obtained in Figure 4.8A at lower HM-SNP concentration suggested that pyrene access to oxygen was being more hindered at high HM-SNP concentration. Since HM-SNP aggregates would most likely occur via interaction between the hydrophobic microdomains that are generated at the surface of the HM-SNPs where pyrene binds, hydrophobic interactions between different HM-SNPs would likely decrease the mobility of pyrene in the hydrophobic microdomains resulting in the observed increase in τ_o.

The decrease in mobility experienced by pyrene bound to aggregated HM-SNPs was further confirmed by conducting fluorescence quenching experiments with water-soluble nitromethane. A similar effect was observed in Figure 4.9B where k_{qSNP} was plotted as a function of DS. k_{qSNP} obtained at a HM-SNP concentration above C_{BP} was consistently smaller than that measured at a HM-SNP concentration above C_{BP} reflecting reduced pyrene mobility. f_p was also determined and appeared to be unaffected by HM-SNP concentration as shown in Figure 4.9C.

4.4 SNP(A) and SNP(F) Hydrophobically Modified with Hexanoic Acid

HM-SNP(F) were prepared by reacting hexanoic anhydride with SNP(F). Quenching studies were conducted for the C6(x)-SNP(F) samples where x was varied between 0 and 0.13. Protective quenching of pyrene was observed. The parameters τ_o and k_{qSNP} were determined

by acquiring the fluorescence decays of 0.5 μM pyrene in C6(*x*)-SNP(F) dispersions and fitting them with Equation 2.1 and they were plotted in Figures 4.10A and 4.10B, respectively.

Interestingly, the trends obtained for τ_0 and k_{qSNP} for the C6(*x*)-SNP(F) particles overlapped the trends obtained for the C6(*x*)-SNP(A) particles as shown in Figure 4.10. This observation led to the conclusion that the hydrophobic microdomains generated by hexanoyl pendants covalently attached onto SNPs generated similar hydrophobic microdomains for a given DS, regardless of whether the modification was conducted on SNP(A), or SNP(F) particles.

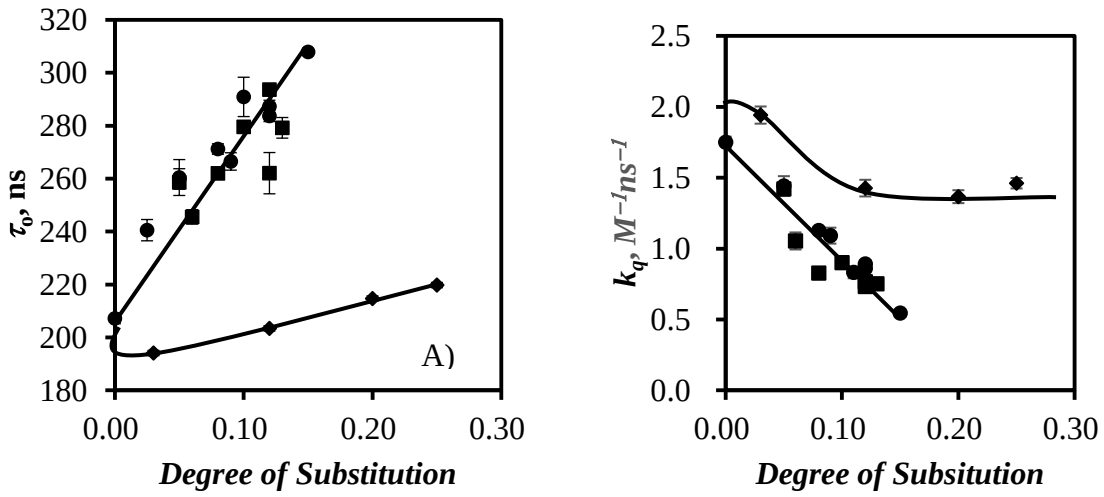

Figure 4.10. Plots of A) τ_o and B) k_{qSNP} as a function of DS for 2 g/L aqueous dispersions of (●) C6-SNP0, (■) C6-SNP(F) and (◆) C3-SNP(F) dialyzed after modification with propionic anhydride.

4.5 The Effect of Hydrophobe Length on Hydrophobically Modified SNPs

SNP(F) particles were hydrophobically modified with propionic anhydride to yield C3(*x*)-SNP(F) particles. Their hydrophobicity was assessed relative to that of the C6(*x*)-SNP(A) and C6(*x*)-SNP(F) particles by determining the τ_o and k_{qSNP} values. To this end, the fluorescence decays acquired for pyrene in aqueous C3(*x*)-SNP(F) dispersions in the absence of

nitromethane were fitted with Equation 2.1 to determine the natural lifetime τ_0 of pyrene bound to the C3(*x*)-SNP(F) particles. τ_0 increased by about 7% when the DS of propionic acid increased from 0 to 0.25. Even with a DS 70% larger than that used for the C6-modified SNPs, the 7% increase in τ_o observed for the C3(0.25)-SNP(F) particles was much smaller than the 49% increase in τ_o observed for the C6(0.15)-SNP(A) particles. This result indicated that dynamic quenching of pyrene by oxygen was much more efficient for the C3(*x*)-SNP(F) particles than for the C6(*x*)-SNP(A) and C6(*x*)-SNP(F) samples.

Quenching experiments conducted with nitromethane on 0.5 μM pyrene in aqueous dispersion of the C3(*x*)-SNP(F) particles yielded k_{qSNP} from the analysis of the fluorescence decays with Equation 2.1. The k_{qSNP} values were plotted in Figure 4.10A as a function of the DS of propionic acid. As DS of propionic acid increased, k_{qSNP} decreased in Figure 4.10.

The decrease in k_{qSNP} observed with increasing DS of propionic acid indicated that the hydrophobicity of the C3(*x*)-SNP(F) particles increased with increasing DS of propionic acid as was observed for the C6(*x*)-SNP particles. However, the decrease in k_{qSNP} for C3(*x*)-SNP(F) was much weaker than that observed for the C6(*x*)-SNP samples. Since pyrene molecules bound to SNPs were effectively immobile over the time scale (~1 μs) of pyrene fluorescence, differences in fluorescence behavior reflected differences in the environment generated by the C3 and C6 pendants. Consequently, these results indicated that for a same DS, C6 pendants generated apolar microdomains that were much more hydrophobic and based on the trends obtained for k_{qSNP}, afforded more protection from the aqueous phase than those generated by the C3 pendants.

4.6 Conclusions

The microviscosity of the environments generated by unmodified SNPs and SNPs hydrophobically modified with hexanoic and propionic acid were examined by conducting quenching experiments with pyrene and nitromethane. Since some pyrene molecules did not bind to the particles, quenching of pyrene by nitromethane in water needed to be accounted for to assess quantitatively the quenching of pyrene bound to SNPs and HM-SNPs. To this end, k_{qW} was determined to equal 6.5 (± 0.05) x 10^9 $M^{-1}s^{-1}$ and it was used to predict the lifetime of pyrene in water at any nitromethane concentration. The analysis of the fluorescence data needed to account for the intrinsic fluorescence of the SNPs and HM-SNPs which interfered with the pyrene fluorescence. Furthermore, some pyrene molecules bound to SNPs and HM-SNPs were inaccessible to the water-soluble quencher and protected from quenching resulting in a non-linear Stern Volmer plot (see Figures 4.5 and 4.8B). The fluorescence decay analysis program was implemented to account for these different fluorescence species and yielded τ_o, k_{qSNP}, and f_p. The size of the SNPs was found to have little effect on τ_o and k_{qSNP}.

Upon binding to the SNPs, pyrene became much less mobile than pyrene in water. These less mobile pyrene molecules were quenched less efficiently by oxygen and nitromethane dissolved in water. Indeed, this reduced efficiency of quenching was reflected in the values of τ_o (197 (±11) ns) and k_{qSNP} (1.8 (±0.4) x 10^9 $M^{-1}s^{-1}$) which were 1.5 ±0.1 times larger and 3.8 ±1.0 times smaller than τ_{PyW} and k_{qW}, respectively. Dialyzed C6(*x*)-SNP(F) particles generated similar hydrophobic microdomains in terms of hydrophobicity and microviscosity as the C6(*x*)-SNP(A) particles. For a same DS of hexanoic acid, the

hydrophobicity of the HM-SNPs was the same regardless of the type of SNPs used for the hydrophobic modification, but the hydrophobicity of the HM-SNPs increased with increasing DS. The more viscous and apolar environment generated at high DS of hexanoic acid resulted in longer τ_o and smaller k_{qSNP} values. SNP aggregation observed at higher particle concentration was found to reduce slightly quenching of pyrene by oxygen and nitromethane thus resulting in slightly longer τ_o and smaller k_{qSNP} values in Figure 4.8A and 4.9B, respectively. The effect of a different alkyl length on the hydrophobic microdomains was examined by modifying the SNPs with propionic and hexanoic acid. Even a DS of propionic acid as high as 0.25 did not provide a hydrophobic environment for the modified SNPs that was as viscous and as apolar as that afforded by the SNPs modified with a DS of 0.15 of hexanoic acid. Hexanoic acid-modified SNPs were more hydrophobic than the propionic acid-modified SNPs, and therefore provided better protection from the solvent to pyrene.

Chapter 5
Conclusions and Future Work

5.1 Conclusions

The goal of this research was to characterize the hydrophobicity of HM-SNPs by applying pyrene fluorescence. The hydrophobicity of SNPs modified with either hexanoic or propionic acid was examined as a function of DS and the length of the alkyl chain used for the modification and the type of SNPs employed as substrate for the modification. The HM-SNPs were expected to form hydrophobic microdomains where pyrene would partition into. Since changes in the polarity and viscosity of the local environment of pyrene affect its fluorescence, different aspect of the fluorescence of pyrene were investigated to characterize the relative hydrophobicity of the HM-SNPs. A quick summary of the main conclusions drawn from these studies is presented hereafter.

Five indicators of hydrophobicity were selected that could all be obtained by monitoring the interactions of pyrene with the HM-SNPs. These were the binding constant of pyrene to the HM-SNPs (K_B), the $(I_1/I_3)_o$ ratio, the rate constant (k_q) for the quenching of pyrene by nitromethane, the lifetime of pyrene (τ_o) bound to the HM-SNPs, and the loading capacity of the HM-SNPs. All these parameters responded to an increase in the HM-SNPs hydrophobicity that correlated nicely with an increase of DS of the hexanoyl or propionyl pendants. As would be expected, the hexanoyl pendants were found to generate HM-SNPs that were more hydrophobic than those prepared with propionyl pendants. These trends were found to be independent on the size of the SNPs used as substrate for the hydrophobic modification. While such conclusions might have been forgone, the real contribution of this thesis was the ability to obtain quantitative information about the relative hydrophobicity of each of the HM-SNPs based on the parameters K_B, $(I_1/I_3)_o$, k_q, and τ_o. This certainly sets this work apart from many others.

For instance, the trends obtained with the four parameters led to the conclusion that

the hydrophobic modification of SNPs with propionyl pendants resulted in HM-SNPs that were less hydrophobic than the SNPs modified with half the amount of hexanoyl pendants even though it would represent identical modifications in terms of number of carbon atoms per anhyroglucose unit. In other words, longer and more hydrophobic pendants generated HM-SNPs that were more hydrophobic than HM-SNPs modified with shorter pendants for a modification involving a same number of carbon atoms. Another example was the observation that two clear regimes could be detected in the binding of pyrene to the HM-SNPs depending on the particle concentration. This behavior was traced back to the onset of SNP association in solution and it led to the development of a model predicting the size of SNP aggregates. Together these findings enrich our knowledge of SNPs and their hydrophobically modified equivalent.

References

1. Khadka, P.; Ro, J.; Kim, H.; Kim, I.; Kim, J. T.; Kim, H.; Cho, J. M.; Yun, G.; Lee, J. Pharmaceutical Particle Technologies: An Approach to Improve Drug Solubility, Dissolution and Bioavailability. *Asian J. Pharmacol.* **2014**, *9*, 304-316.
2. Duncan, Ruth. The Dawning Era of Polymer Therapeutics. *Nat. Rev. Drug Discov*. **2003**, *2*, 347-360.
3. Jones, M. C.; Leroux, J. C. Polymeric Micelles - a New Generation of Colloidal Drug Carriers. *Eur. J. Pharm. Biopharm.* **1999**, *48*, 101-111.
4. Torchilin, V. Structure and Design of Polymeric Surfactant-Based Drug Delivery Systems. *J. Control. Release* **2001**, *73*, 137–172.
5. Yokohama, M. Polymeric Micelles as Drug Carriers: Their Lights and Shadows. *J. Drug Target*. **2014**, *22*, 576–583.
6. Knop, K.; Hoogenboom, R.; Fischer, D.; Schubert, U. S. Poly(Ethylene Glycol) in Drug Delivery: Pros and Cons as Well as Potential Alternatives. *Angew. Chem. Int. Ed*. **2010**, *49*, 6288 – 6308.
7. Builders, P. F.; Arhewoh, M. I. Pharmaceutical Applications of Native Starch in Conventional Drug Delivery. *Starch/Stärke **2016**, 68*, 864-873.
8. Bhosale, R.; Singhal, R. Process Optimization for the Synthesis of Octenyl Succinyl Derivative of Waxy Corn and Amaranth Starches. *Carbohydr. Polym.* **2006**, *66*, 521–527.
9. Visavarungroj, N.; Remon, J. P. Crosslinked Starch as a Disintegrating Agent. *Int. J. Pharm.***1990,** 62, 125-131.
10. Bloembergen, S.; McLennan, I.; Lee, D. I.; Leeuwen, J. V. Paper Binder Performance with Biobased Nanoparticles. Papercon, TappI, **2008**.

11. Corre, D.; Coussy, H. A. Preparation and Application of Starch Nanoparticles for Nanocompoites: a Review. *React. Funct. Polym*. **2014**, *85*, 97–120.
12. Yu, H.; Huang, Q. Enhanced in Vitro Anti-cancer Activity of Curcumin Encapsulated in Hydrophobically Modified Starch. *Food Chem.* **2010**, *119*, 669–674.
13. Ortega, M. J. S.; Stauner, T.; Loretz, B.; Vinuesa, J. T. L.; González, D. B.; Wenz. G.; Schaefer, U. F.; Lehr, C. M. Nanoparticles Made from Novel Starch Derivatives for Transdermal Drug Delivery. *J. Control. Release* **2014**, *141*, 85-92.
14. Tuovinen, L.; Peltonen, S.; Jarvinen, K. Drug Release from Starch-Acetate Films. *J. Control. Release* **2003**, *91*, 345–354
15. Ju, B.; Yan, D.; Zhang, S. Micelles Self-Assembled from Thermoresponsive 2-Hydroxy-3-Butoxypropyl Starches for Drug Delivery. *Carbohydr. Polym*. **2012**, *87*, 1404–1409.
16. Bloembergen, S.; McLennan, I.; Lee, D. I.; Leeuwen, J. V. Specialty Biobased Monomers and Emulsion Polymer Derived from Starch. PTS Advanced Coating Fund. Symp., Munich, Oct. 11-14, **2010**.
17. Chung, J. E.; Yokoyama, M.; Suzuki, K.; Aoyagi, T.; Sakuai, Y.; Okano, T. Reversibly Thermoresponsive Alkyl Terminated Poly(*N*-isopropylacrylamide) Core-Shell Micellar Structure. *Colloids Surf. B* **1997**, *9*, 37-48.
18. Becerra, N.; Toro, C.; Zanocco, A. L.; Lemp, E.; Günther, G. Characterization of Micelles Formed by Sucrose 6-O-monoesters. *Colloids Surf. A* **2008**, *327*, 134-139.
19. Blecker, C.; Piccicuto, S.; Lognay, G.; Deroanne, C.; Marlier, M.; Paquot, M. Enzymatically Prepared n-Alkyl Esters of Glucuronic Acid: The Effect of Hydrophobic Chain Length on Surface Properties. *J. Colloid Interface Sci*. **2002**, *247*, 424-428.
20. Piñeiro, L.; Freire, S.; Bordello, J.; Novo, M.; Soufi, W. A. Dye Exchange in Micellar Solutions. Quantitative Analysis of Bulk and Single Molecule Fluorescence Titrations. *Soft Matter* **2013**, *9*, 10779–10790.

21. Piñeiro, L.; Novo, M.; Soufi, W. A. Fluorescence Emission of Pyrene in Surfactant Solutions. *Adv. Colloid Interface Sci*. (in press).
22. Anthony, O.; Zana, R. Fluorescence Investigation of the Binding of Pyrene to Hydrophobic Microdomains in Aqueous Solution of Polysoaps. *Macromolecule*s **1994**, *27*, 3885-3891.
23. Lakowicz, R. J. *Principles of Fluorescence Spectroscopy*. 3rd ed. Baltimore: Springer, **2006**.
24. Duhamel, J. Internal Dynamics of Dendritic Molecules Probed by Pyrene Excimer Formation. *Polymers* **2012**, *4*, 211-239.
25. Duhamel, J. New Insights in the Study of Pyrene Excimer Fluorescence to Characterize Macromolecules and their Supramolecular Assemblies in Solution. *Langmuir* **2012**, *28*, 6527-6538.
26. Winnik, F. M. Photophysics of Preassociated Pyrenes in Aqueous Polymer Solutions and in Other Organized Media. *Chem. Rev.* **1993**, *93*, 587-614.
27. Berlman, I. B. *Handbook of Fluorescence Spectra of Aromatic Molecules*. 2nd ed. N.Y: Academic Press, **1971**.
28. Birks, J. B.; Dyson, D. J.; Munro, I. H. 'Excimer' Fluorescence II. Lifetime Studies of Pyrene Solutions. *Proc. R. Soc. A.* **1963**, *275*, 575-588.
29. Kalyanasundaram, K.; Thomas, J. K. Environmental Effects on Vibronic Band Intensities in Pyrene Monomer Fluorescence and their Application in Studies of Micellar Systems. *J. Am. Chem. Soc.* **1977**, *99*, 2039–2044
30. Barros, T. C.; Adronov, A.; Winnik, F. M.; Bohne, C. Quenching Studies of Hydrophobically Modified Poly(N-isopropylacrylamides). *Langmuir* **1997**, *13*, 6089-6094.
31. Baig, C. K.; Duhamel, J.; Fung, S. Y.; Bezaire, J.; Chen, P. Self-Assembling Peptide as a

Potential Carrier of Hydrophobic Compounds. *J. AM. CHEM. SOC.* **2004**, *126*, 7522-7532.

32. Claracq. J.; Santos, S. F. C. R.; Duhamel, J.; Dumousseaux, C.; Corpart, J. M. Rigid Interior of Styrene-Maleic Anhydride Copolymer Aggregates Probed by Fluorescence Spectroscopy. *Langmuir* **2002**, *18*, 3829-3835.
33. Zhao, C.; Wu, D.; Lian, X.; Zhang, Y.; Song, X.; Zhao, H. Amphiphilic Asymmetric Comb Copolymer with Pendant Pyrene Groups and PNIPAM Side Chains: Synthesis, Photophysical Properties, and Self-Assembly. *J. Phys. Chem. B* **2010**, *114*, 6300–6308.
34. Chu, D.Y.; Thomas, J. K. Photophysical and Photochemical Studies on a Polymeric Intramolecular Micellar System, PA-18K2. *Macromolecules* **1987**, *20*, 2133-2138.
35. Binana-Limbele, W.; Zana, R. Fluorescence Probing of Microdomains in Aqueous Solutions of Polysoaps. 1. Use of Pyrene to Study the Conformational State of Polysoaps and Their Comicellization with Cationic Surfactants. *Macromolecules* **1987**, *20*, 1331-1335.

Appendices

A.^{1}H-NMR (300MHz, DMSO^{d})

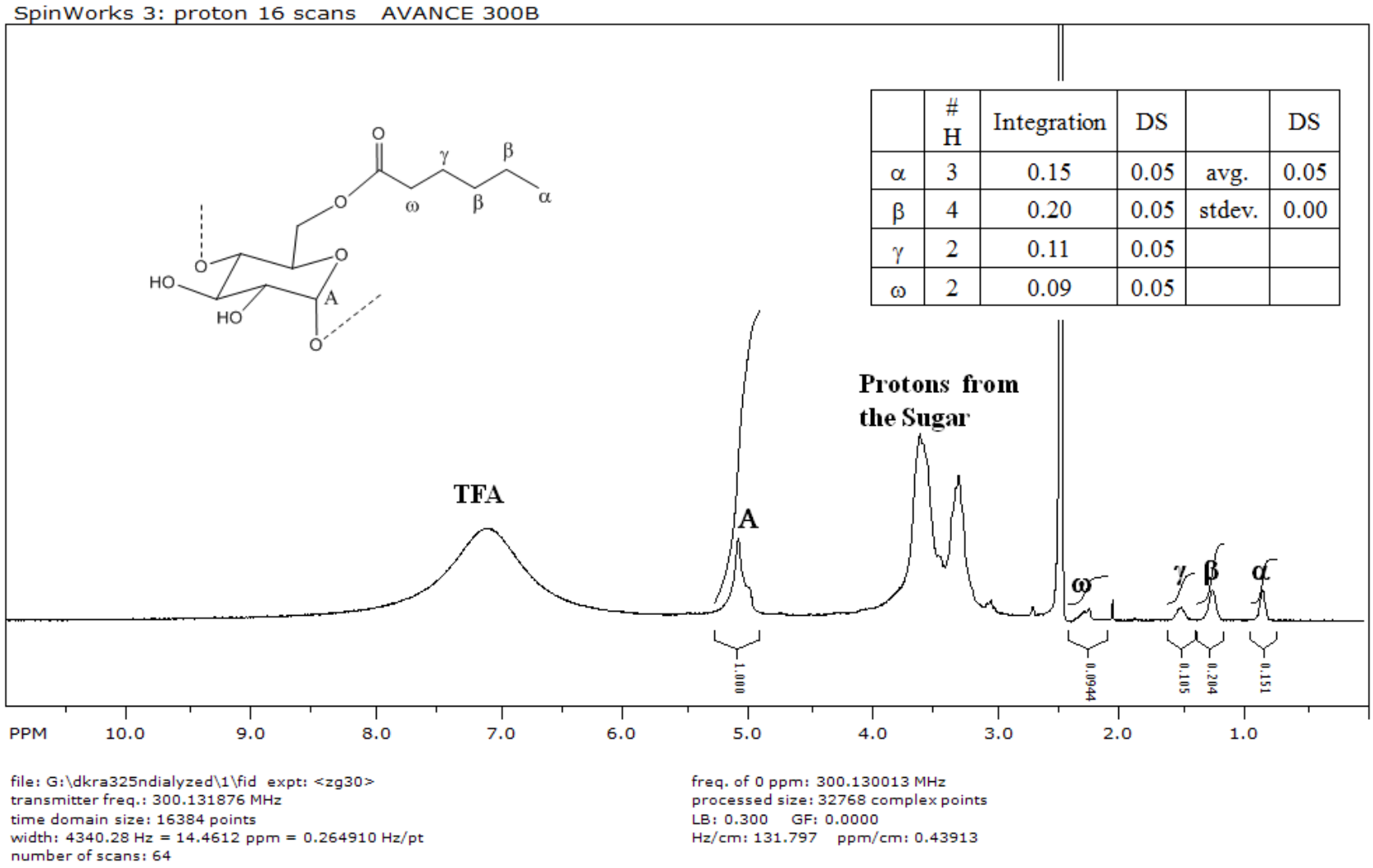

	# H	Integration	DS		DS
α	3	0.15	0.05	avg.	0.05
β	4	0.20	0.05	stdev.	0.00
γ	2	0.11	0.05		
ω	2	0.09	0.05		

Figure A.1.1. ^{1}H-NMR (300MHz, DMSO^{d}) of undialyzed C6(0.06)-SNP(0) in the presence of a trace amount of TFA

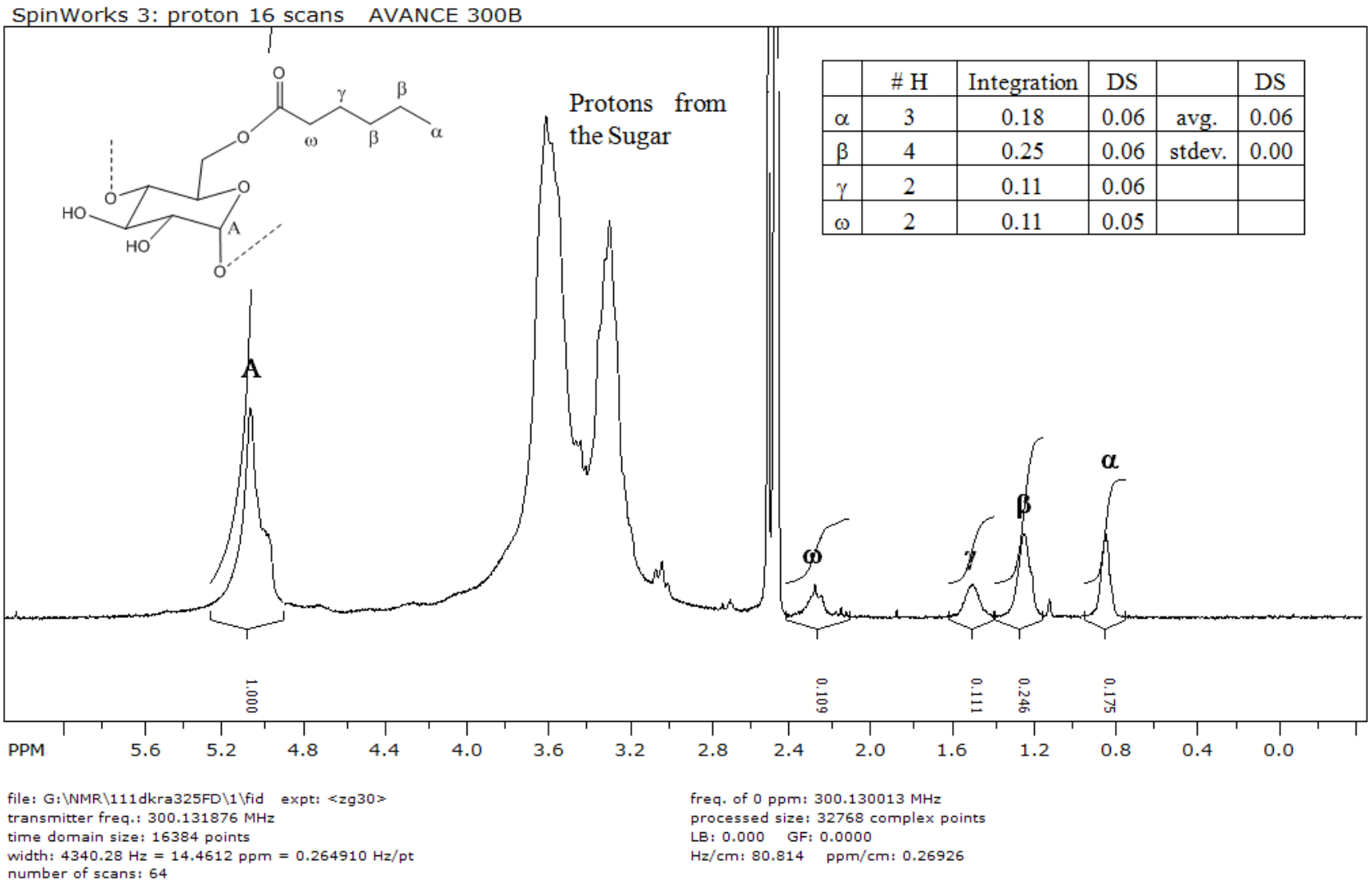

	# H	Integration	DS		DS
α	3	0.18	0.06	avg.	0.06
β	4	0.25	0.06	stdev.	0.00
γ	2	0.11	0.06		
ω	2	0.11	0.05		

Figure A.1.2. ^{1}H-NMR (300MHz, DMSO^{d}) of dialyzed C6(0.06)-SNP(0) in the presence of a trace amount of TFA

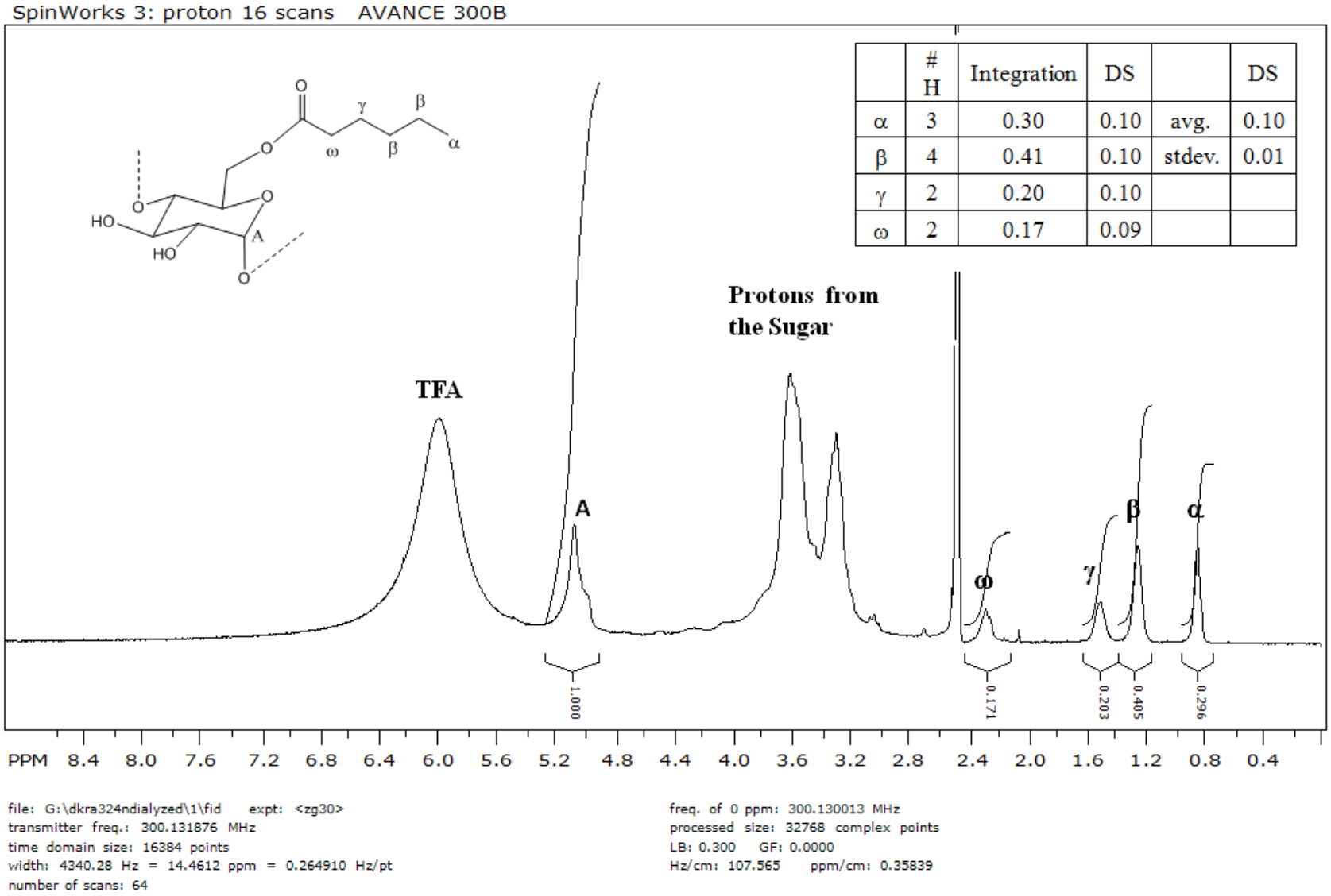

	# H	Integration	DS		DS
α	3	0.30	0.10	avg.	0.10
β	4	0.41	0.10	stdev.	0.01
γ	2	0.20	0.10		
ω	2	0.17	0.09		

Figure A.2.1. ^{1}H-NMR (300MHz, DMSO^{d}) of undialyzed C6(0.11)-SNP(0) in the presence of a trace amount of TFA

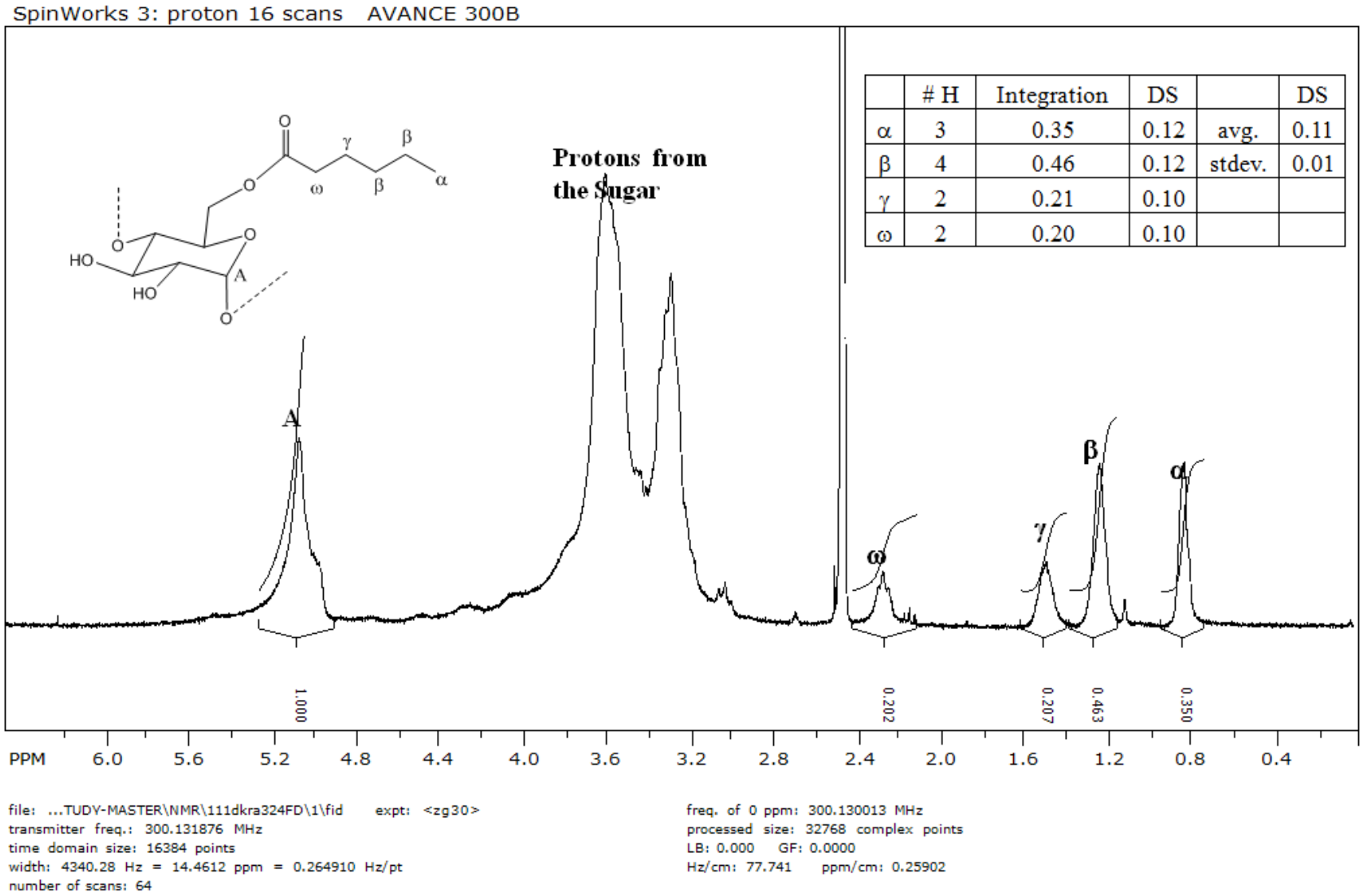

	# H	Integration	DS		DS
α	3	0.35	0.12	avg.	0.11
β	4	0.46	0.12	stdev.	0.01
γ	2	0.21	0.10		
ω	2	0.20	0.10		

Figure A.2.2. ^{1}H-NMR (300MHz, DMSO^{d}) of dialyzed C6(0.11)-SNP(0) in the presence of a trace amount of TFA

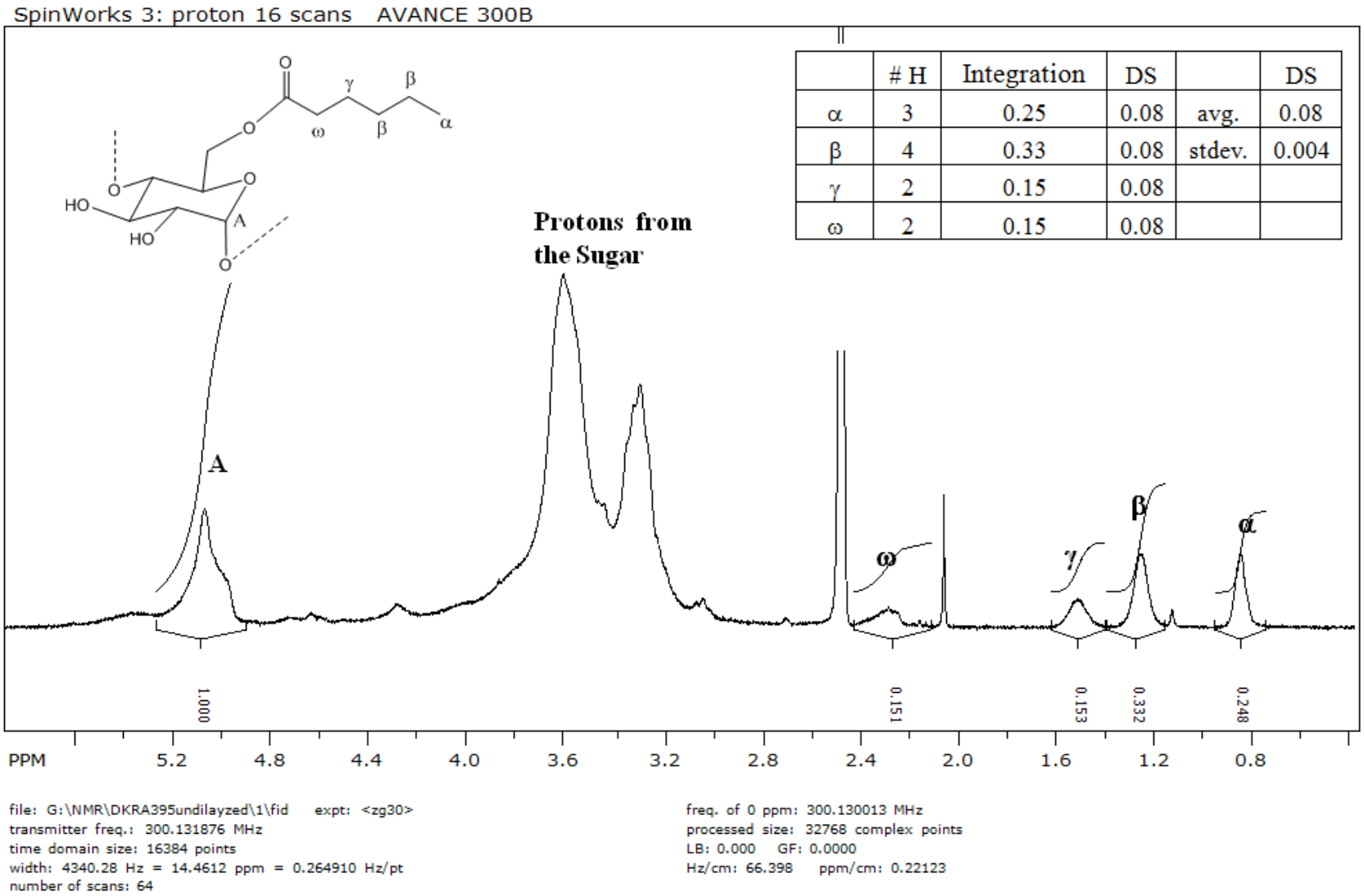

	# H	Integration	DS		DS
α	3	0.25	0.08	avg.	0.08
β	4	0.33	0.08	stdev.	0.004
γ	2	0.15	0.08		
ω	2	0.15	0.08		

Figure A.3.1. ^{1}H-NMR (300MHz, DMSO^{d}) of undialyzed C6(0.06)-SNP(5) in the presence of a trace amount of TFA

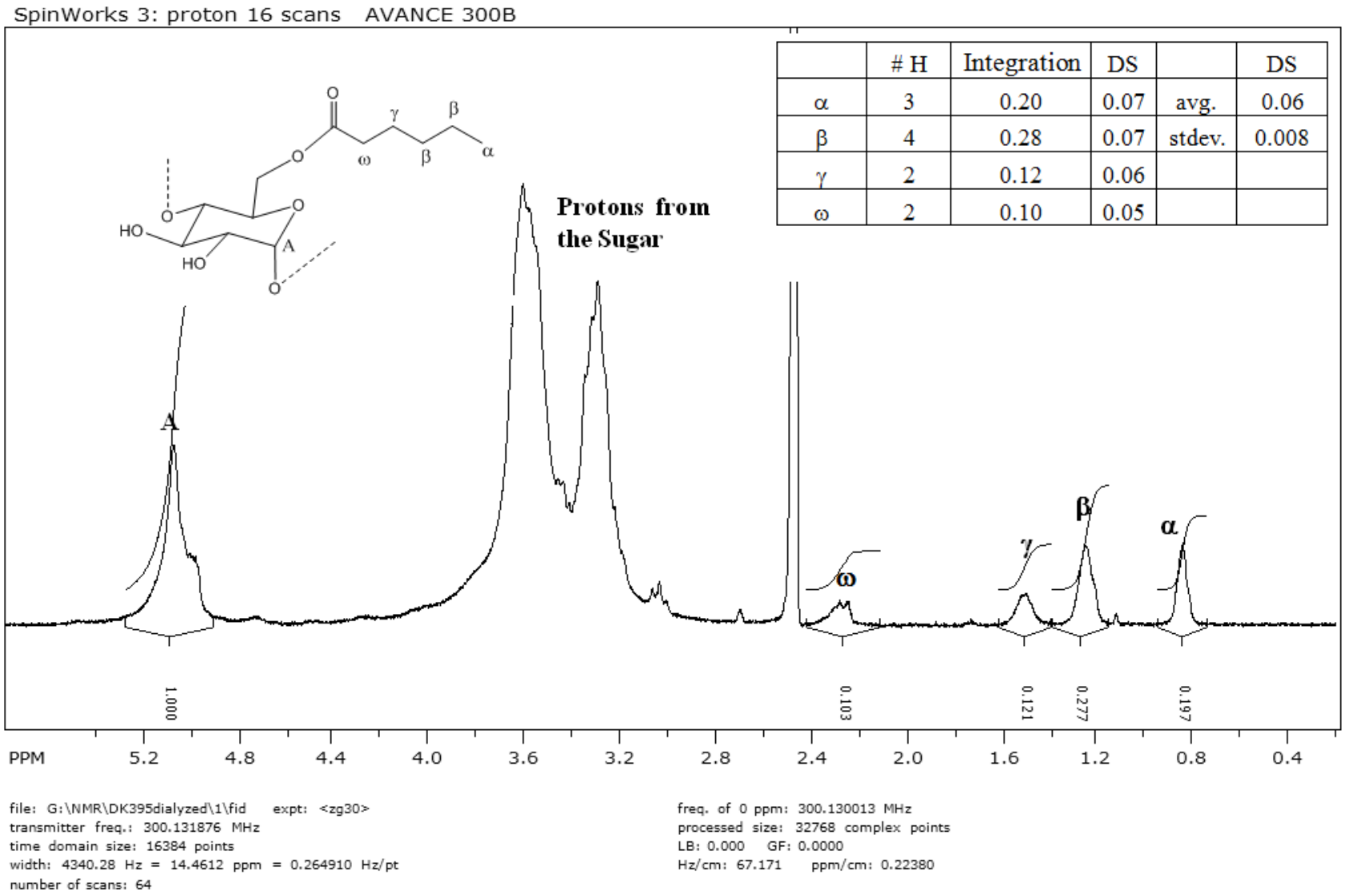

	# H	Integration	DS		DS
α	3	0.20	0.07	avg.	0.06
β	4	0.28	0.07	stdev.	0.008
γ	2	0.12	0.06		
ω	2	0.10	0.05		

Figure A.3.2. ^{1}H-NMR (300MHz, DMSO^{d}) of dialyzed C6(0.06)-SNP(5) in the presence of a trace amount of TFA

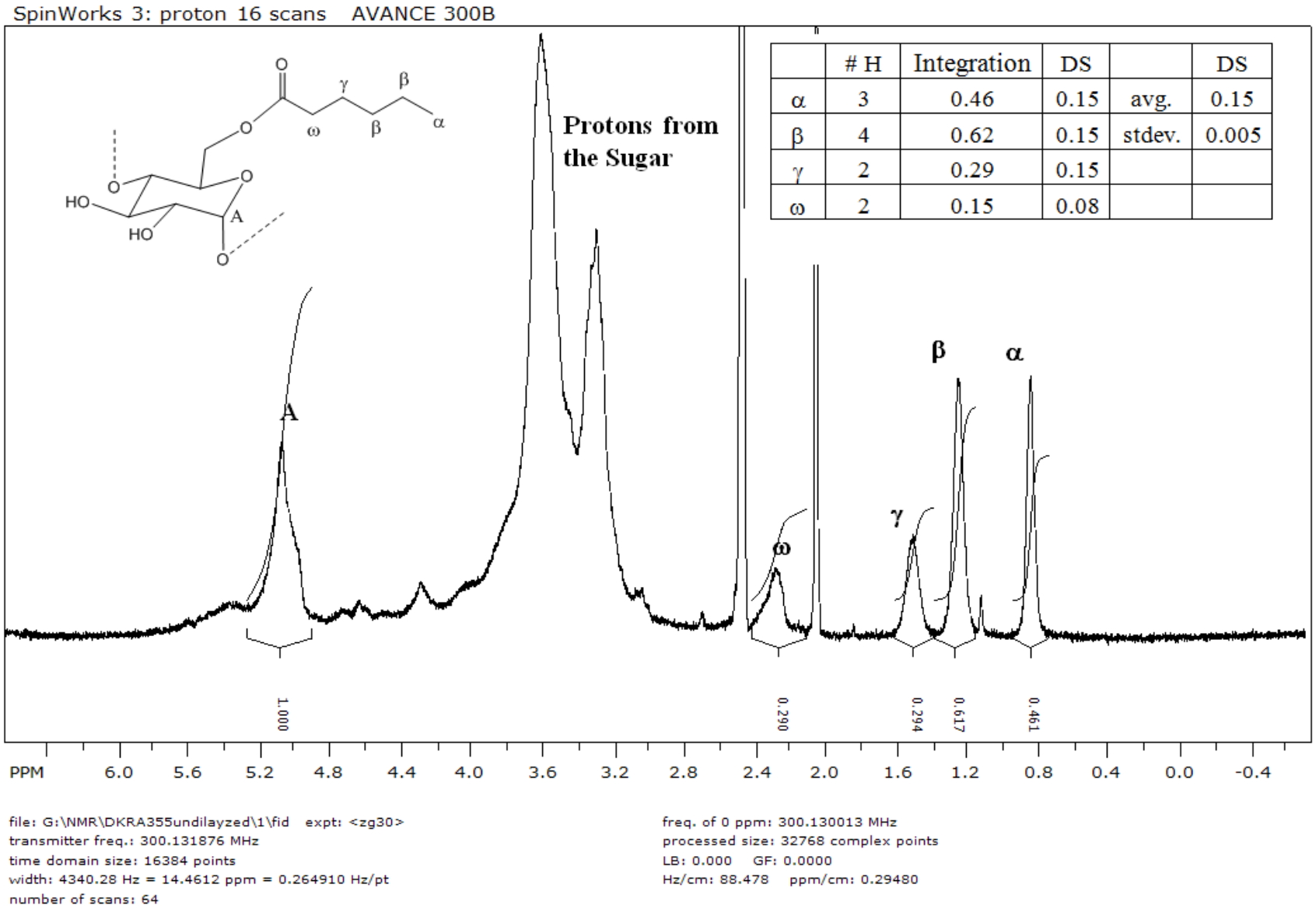

	# H	Integration	DS		DS
α	3	0.46	0.15	avg.	0.15
β	4	0.62	0.15	stdev.	0.005
γ	2	0.29	0.15		
ω	2	0.15	0.08		

Figure A.4.1. ^{1}H-NMR (300MHz, DMSO^{d}) of undialyzed C6(0.12)-SNP(5) in the presence of a trace amount of TFA

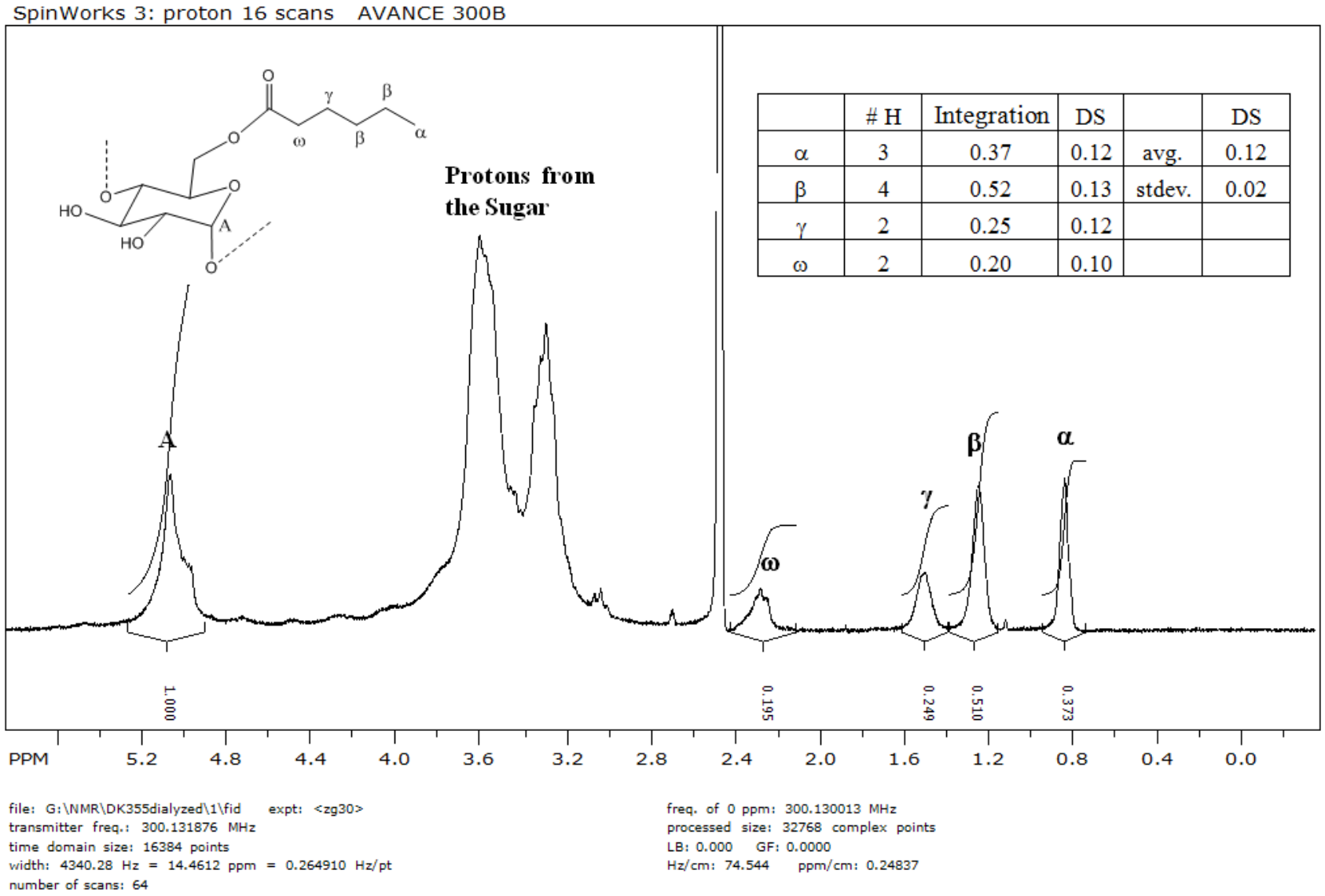

	# H	Integration	DS		DS
α	3	0.37	0.12	avg.	0.12
β	4	0.52	0.13	stdev.	0.02
γ	2	0.25	0.12		
ω	2	0.20	0.10		

Figure A.4.2. ^{1}H-NMR (300MHz, DMSO^{d}) of dialyzed C6(0.12)-SNP(5) in the presence of a trace amount of TFA

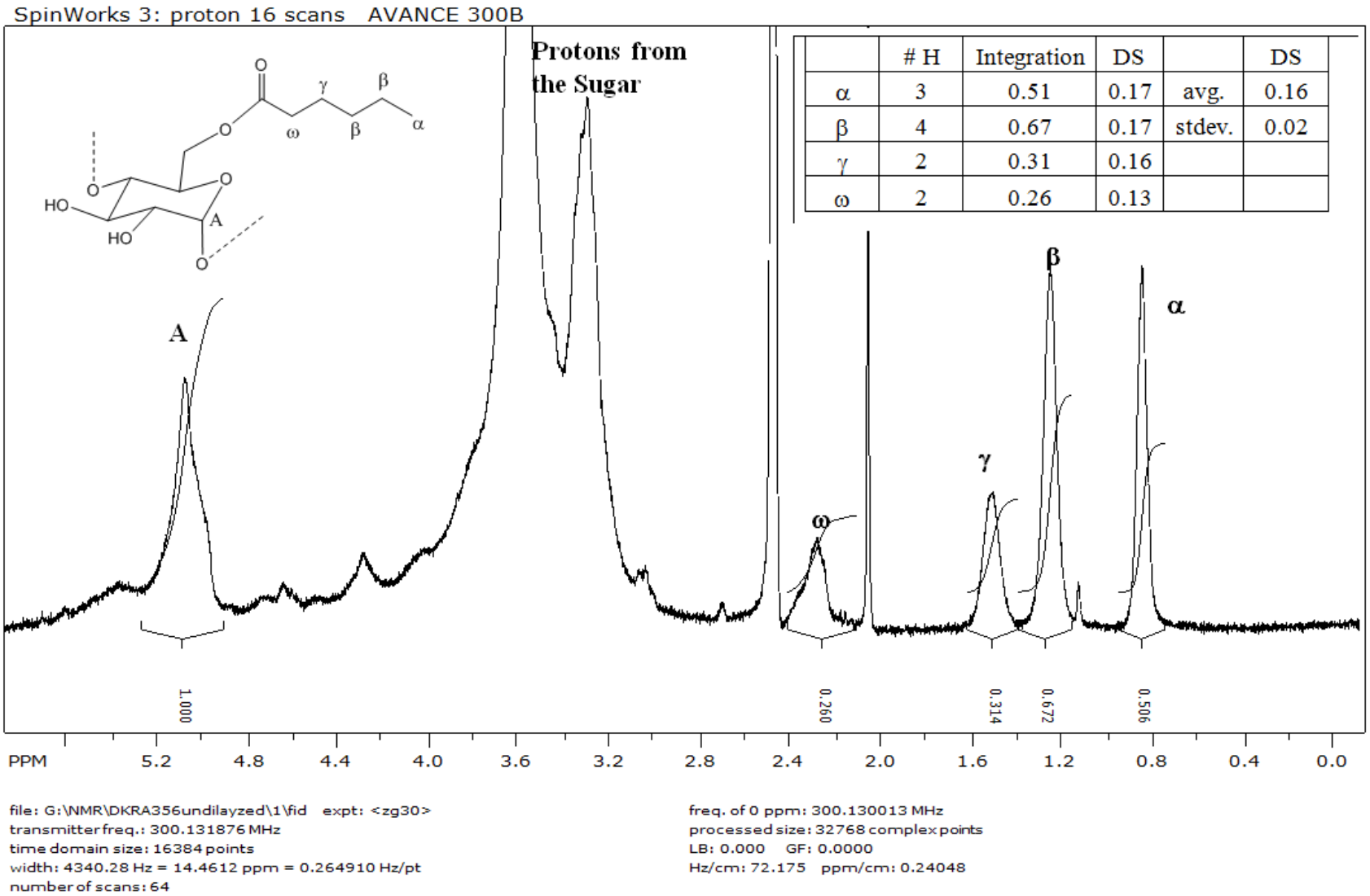

	# H	Integration	DS		DS
α	3	0.51	0.17	avg.	0.16
β	4	0.67	0.17	stdev.	0.02
γ	2	0.31	0.16		
ω	2	0.26	0.13		

Figure A.5.1. ^{1}H-NMR (300MHz, DMSO^{d}) of undialyzed C6(0.13)-SNP(5) in the presence of a trace amount of TFA

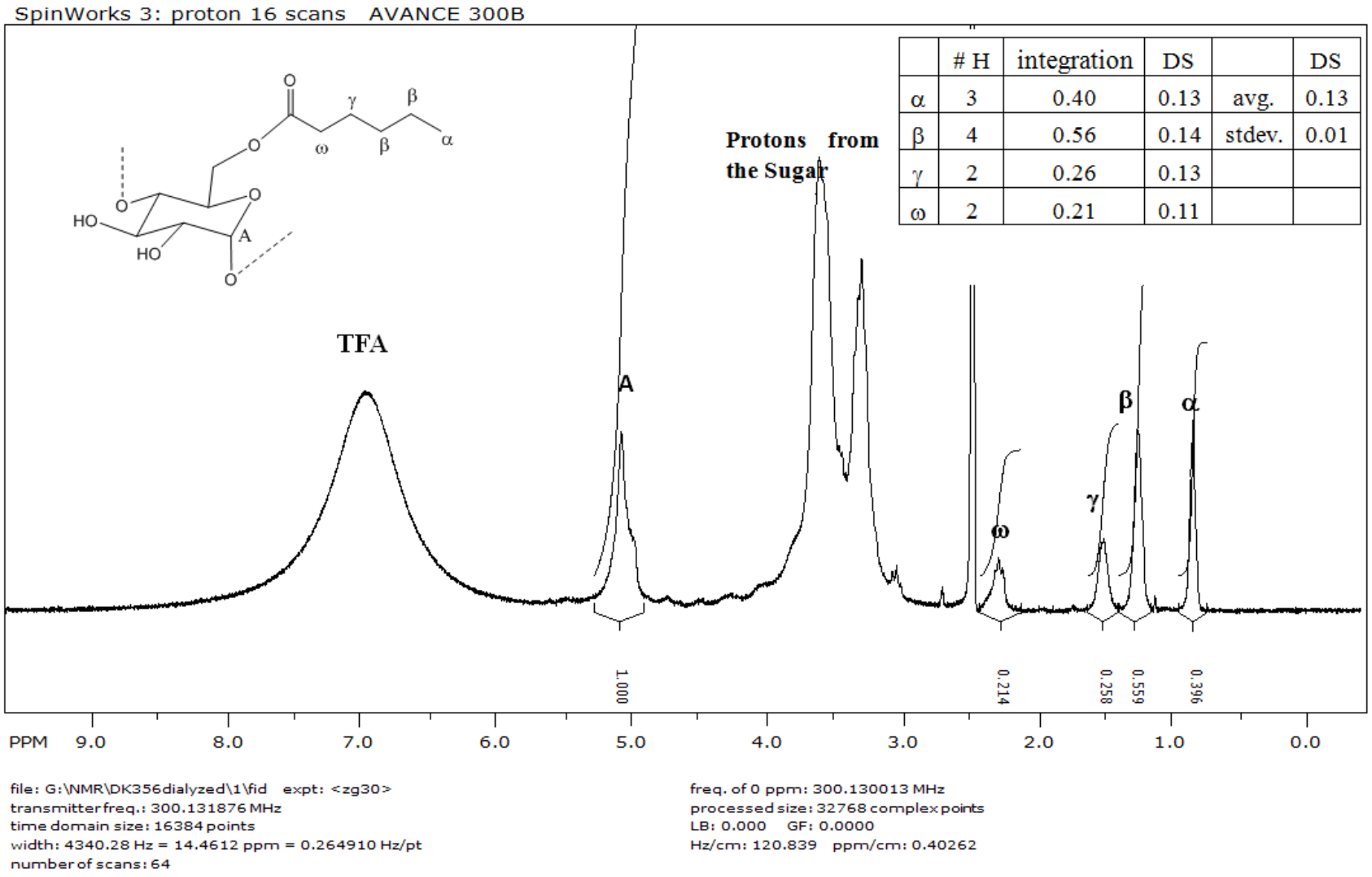

	# H	integration	DS		DS
α	3	0.40	0.13	avg.	0.13
β	4	0.56	0.14	stdev.	0.01
γ	2	0.26	0.13		
ω	2	0.21	0.11		

Figure A.5.2. ^{1}H-NMR (300MHz, DMSO^{d}) of dialyzed C6(0.13)-SNP(5) in the presence of a trace amount of TFA

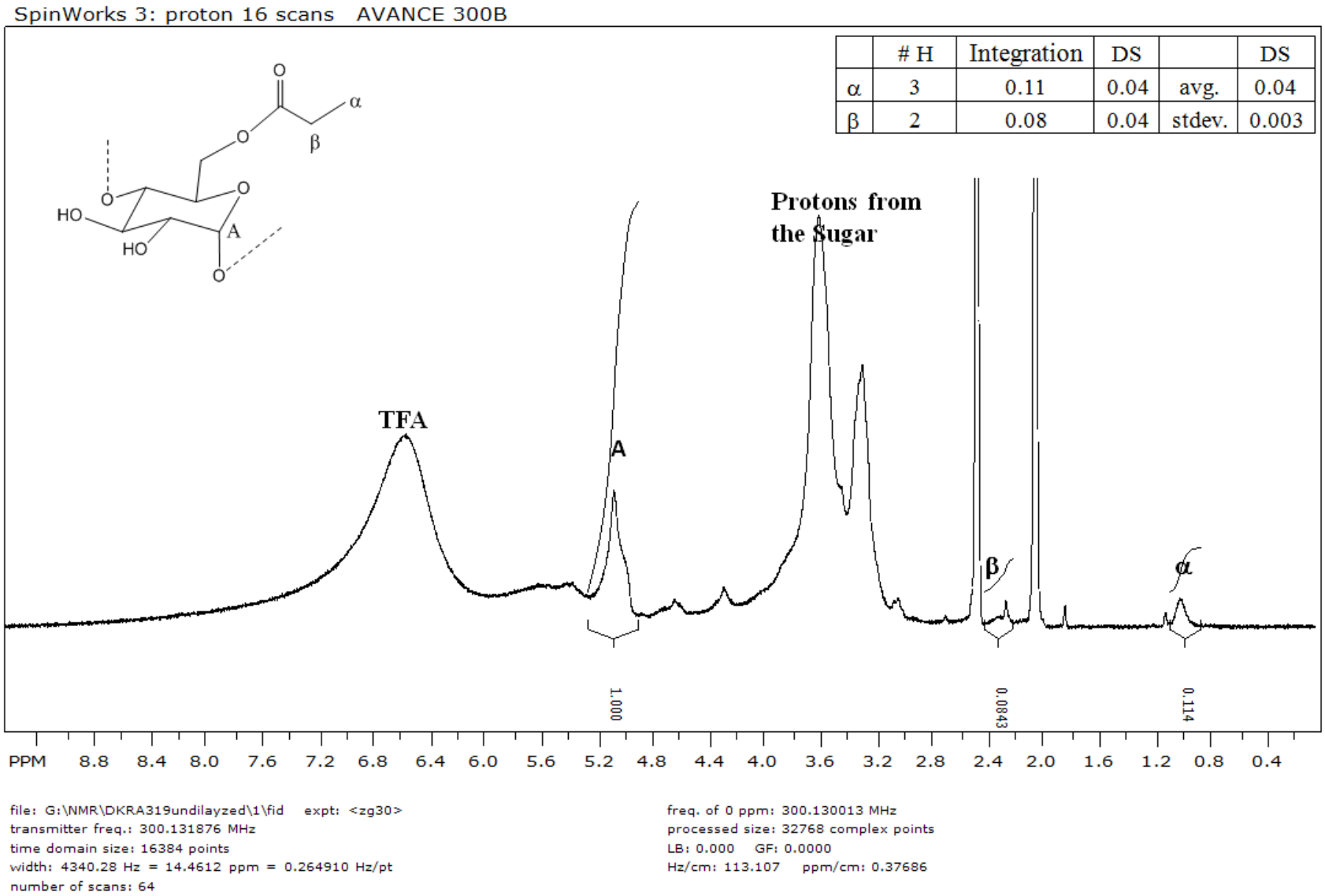

Figure A.6.1. ^{1}H-NMR (300MHz, DMSO^{d}) of undialyzed C3(0.03)-SNP(5) in the presence of a trace amount of TFA

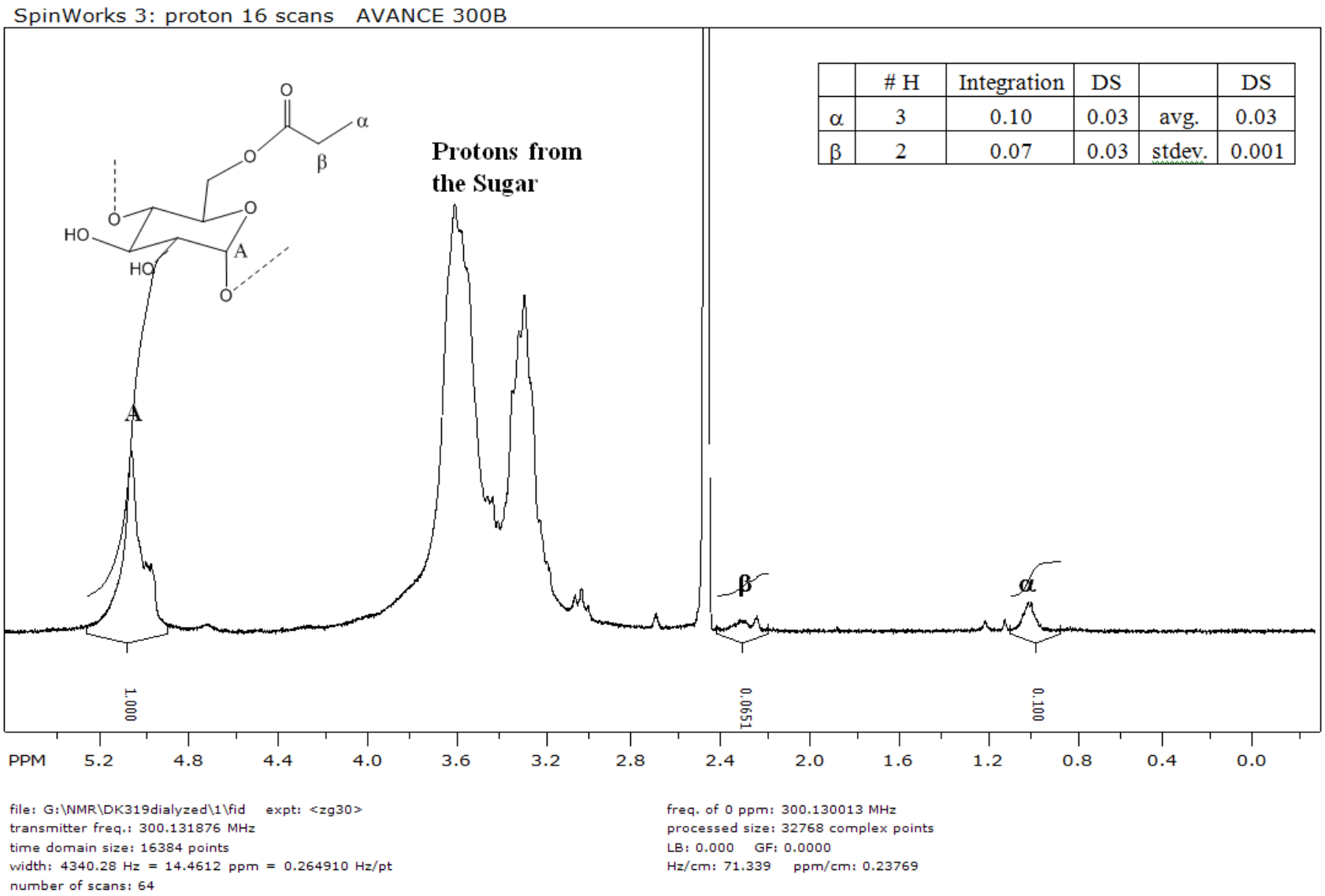

	# H	Integration	DS		DS
α	3	0.10	0.03	avg.	0.03
β	2	0.07	0.03	stdev.	0.001

Figure A.6.2. ^{1}H-NMR (300MHz, DMSO^{d}) of dialyzed C3(0.03)-SNP(5) in the presence of a trace amount of TFA

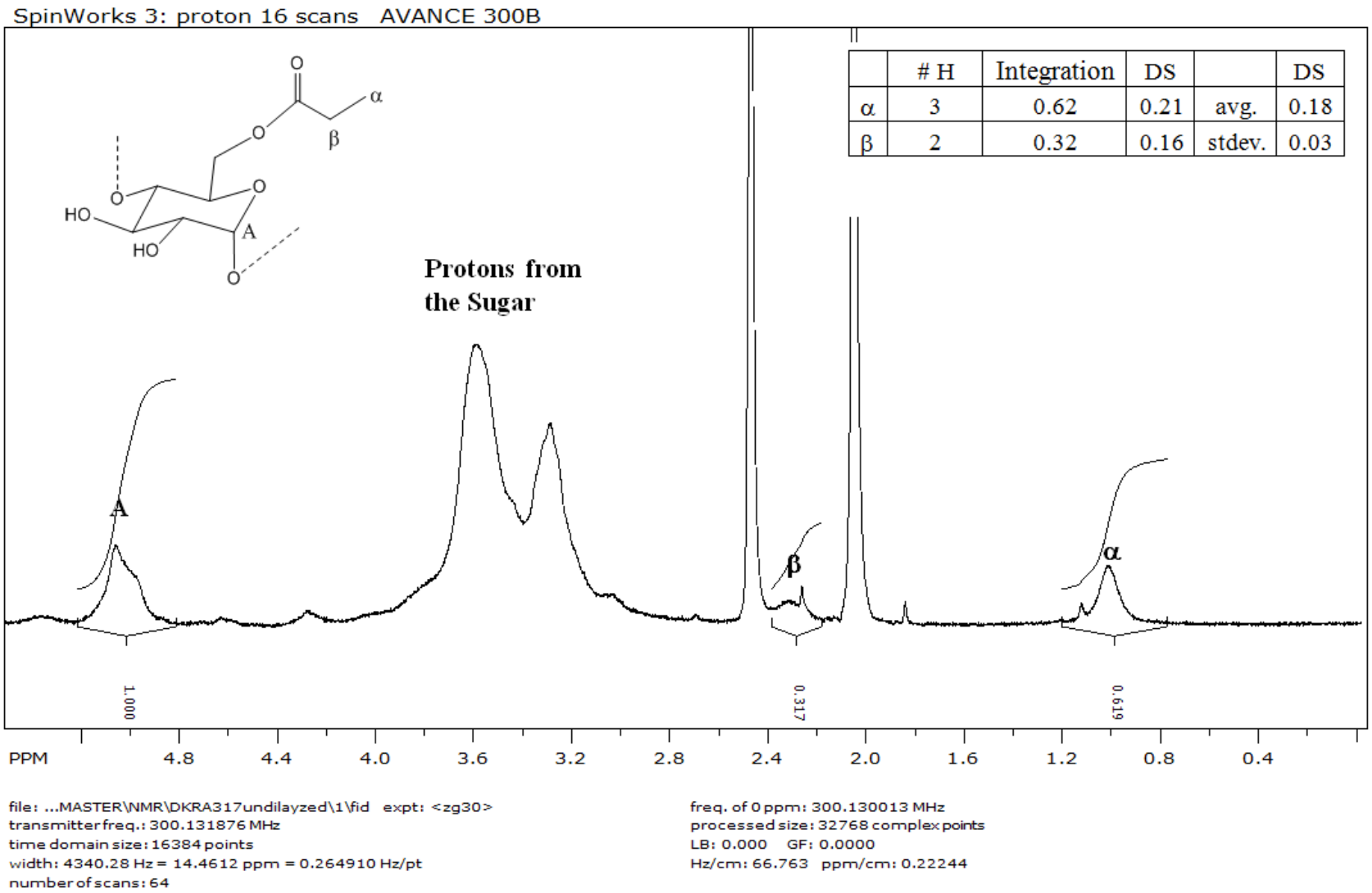

Figure A.7.1. ^{1}H-NMR (300MHz, DMSO^{d}) of undialyzed C3(0.13)-SNP(5) in the presence of a trace amount of TFA

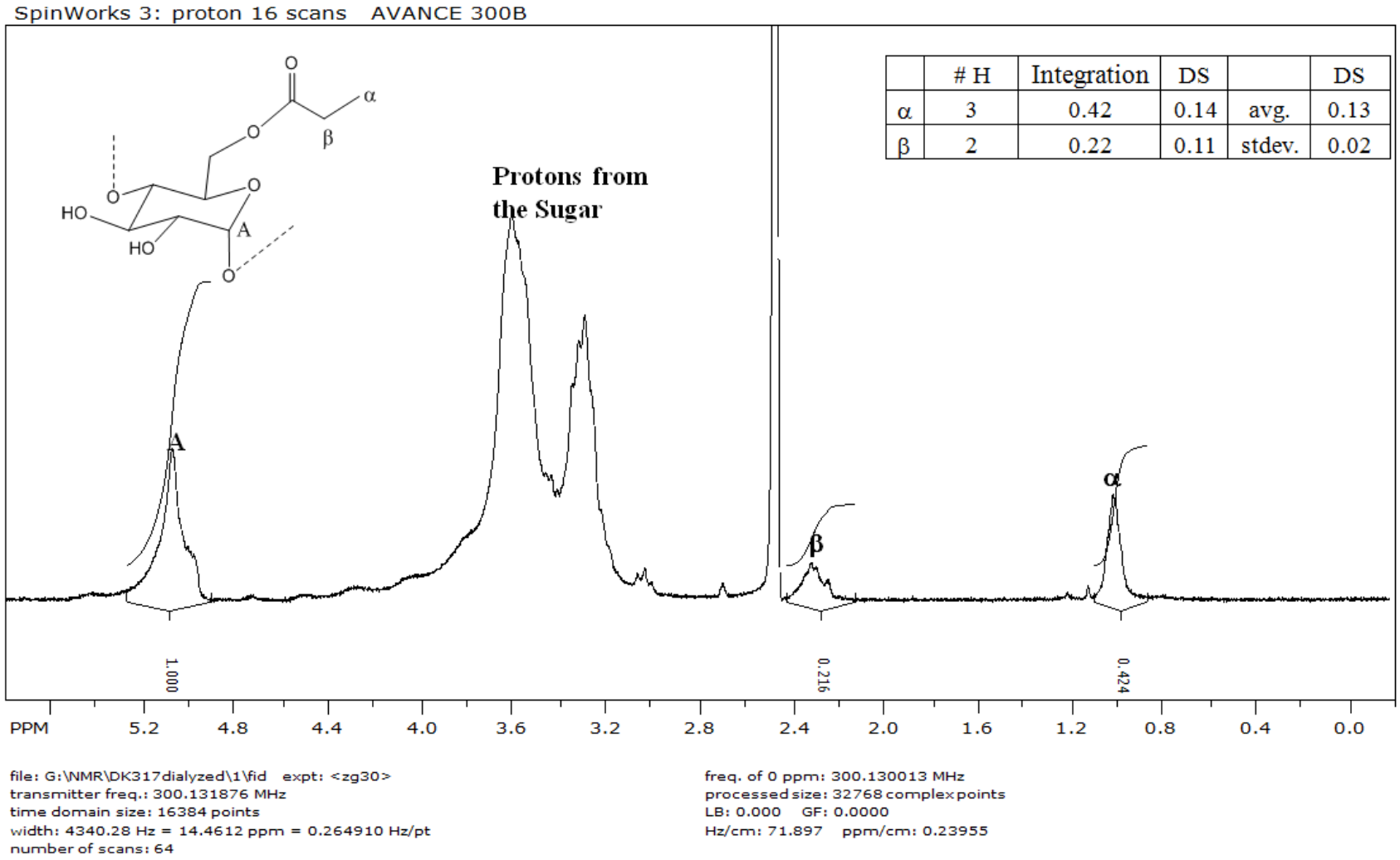

	# H	Integration	DS		DS
α	3	0.42	0.14	avg.	0.13
β	2	0.22	0.11	stdev.	0.02

Figure A.7.2. ^{1}H-NMR (300MHz, DMSO^{d}) of dialyzed C3(0.13)-SNP(5) in the presence of a trace amount of TFA

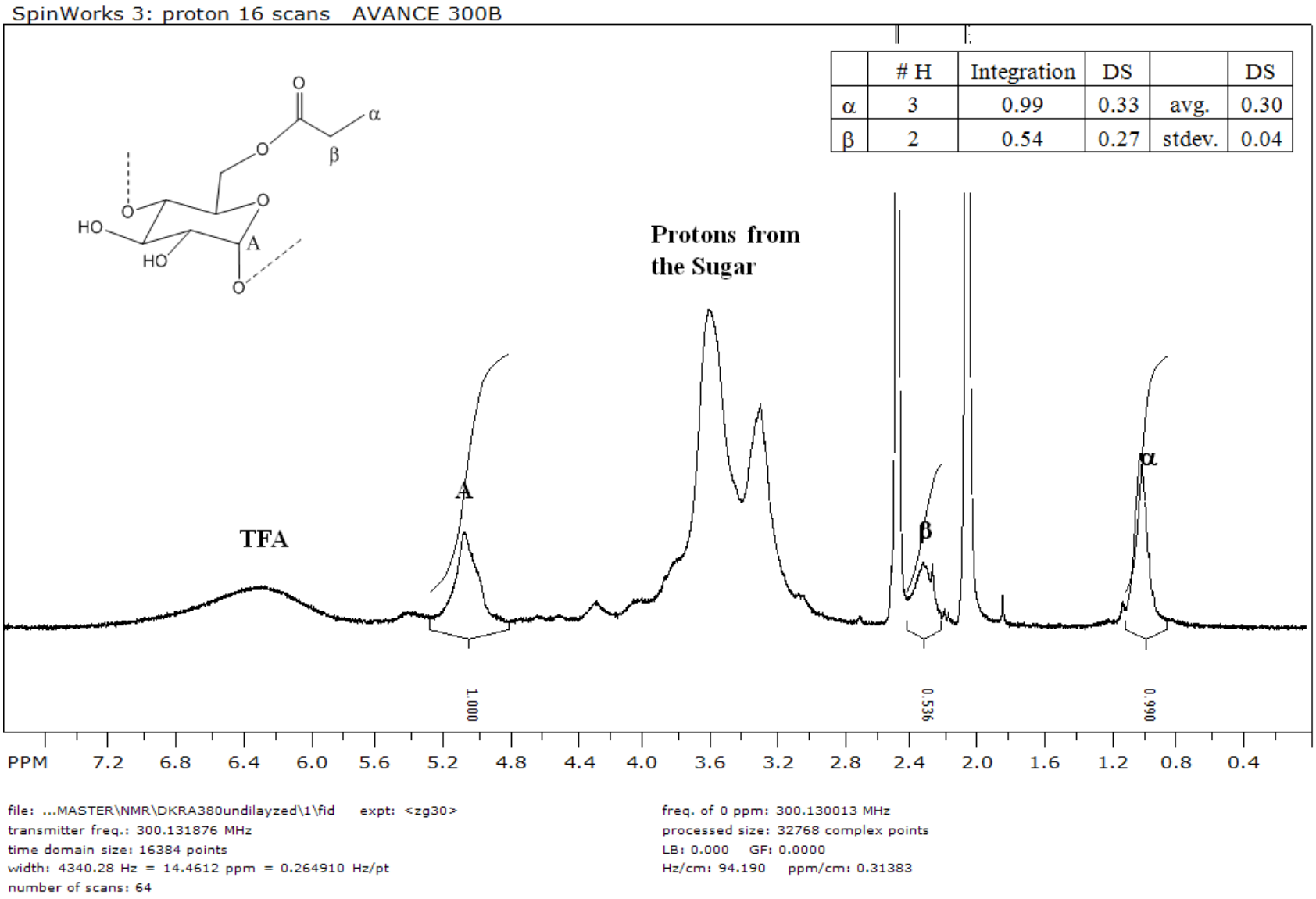

Figure A.8.1. ^{1}H-NMR (300MHz, DMSO^{d}) of undialyzed C3(0.20)-SNP(5) in the presence of a trace amount of TFA

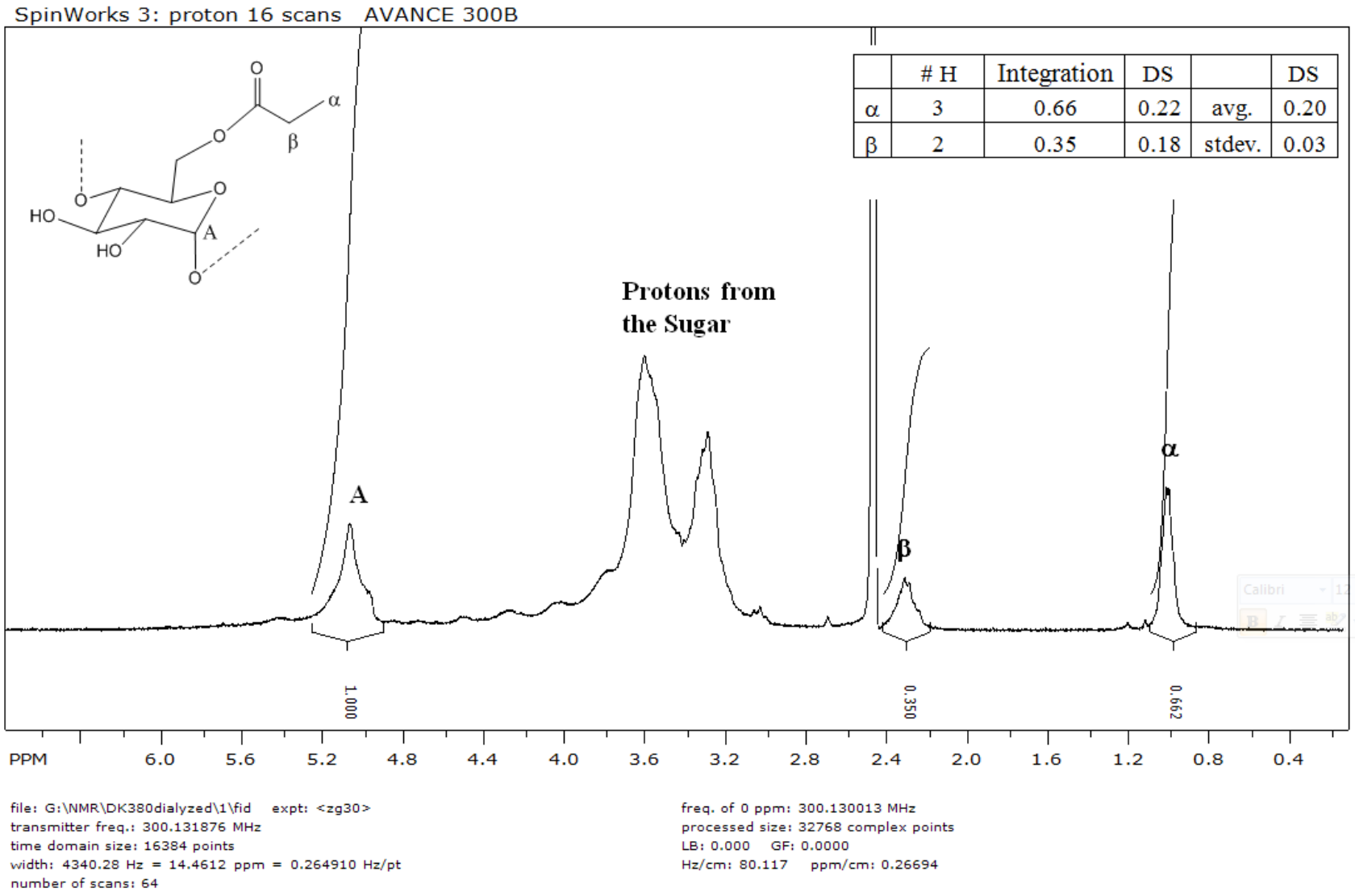

Figure A.8.2 ^{1}H-NMR (300MHz, DMSO^{d}) of dialyzed C3(0.20)-SNP(5) in the presence of a trace amount of TFA

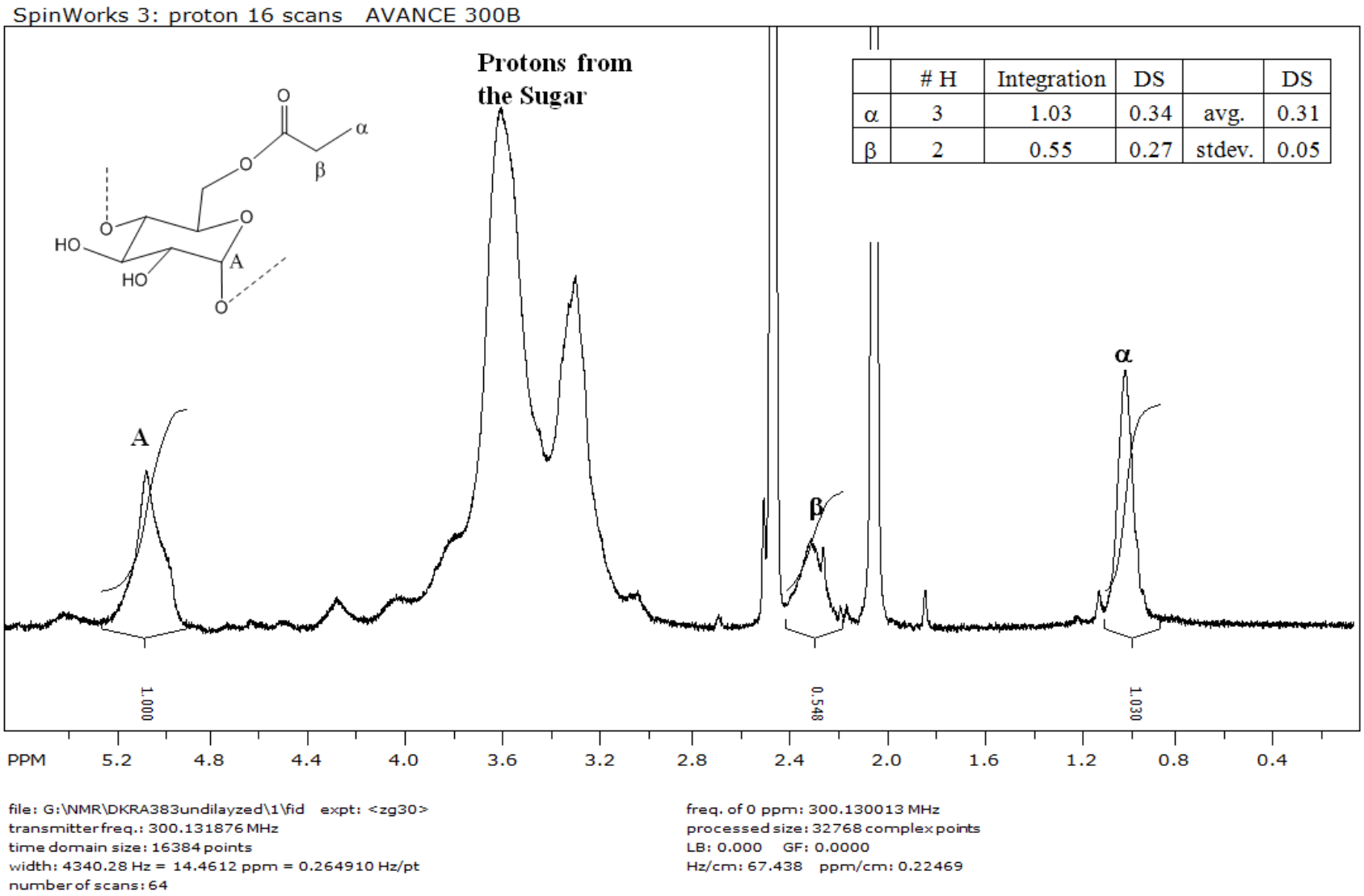

Figure A.9.1. ^{1}H-NMR (300MHz, DMSO^{d}) of undialyzed C3(0.25)-SNP(5) in the presence of a trace amount of TFA

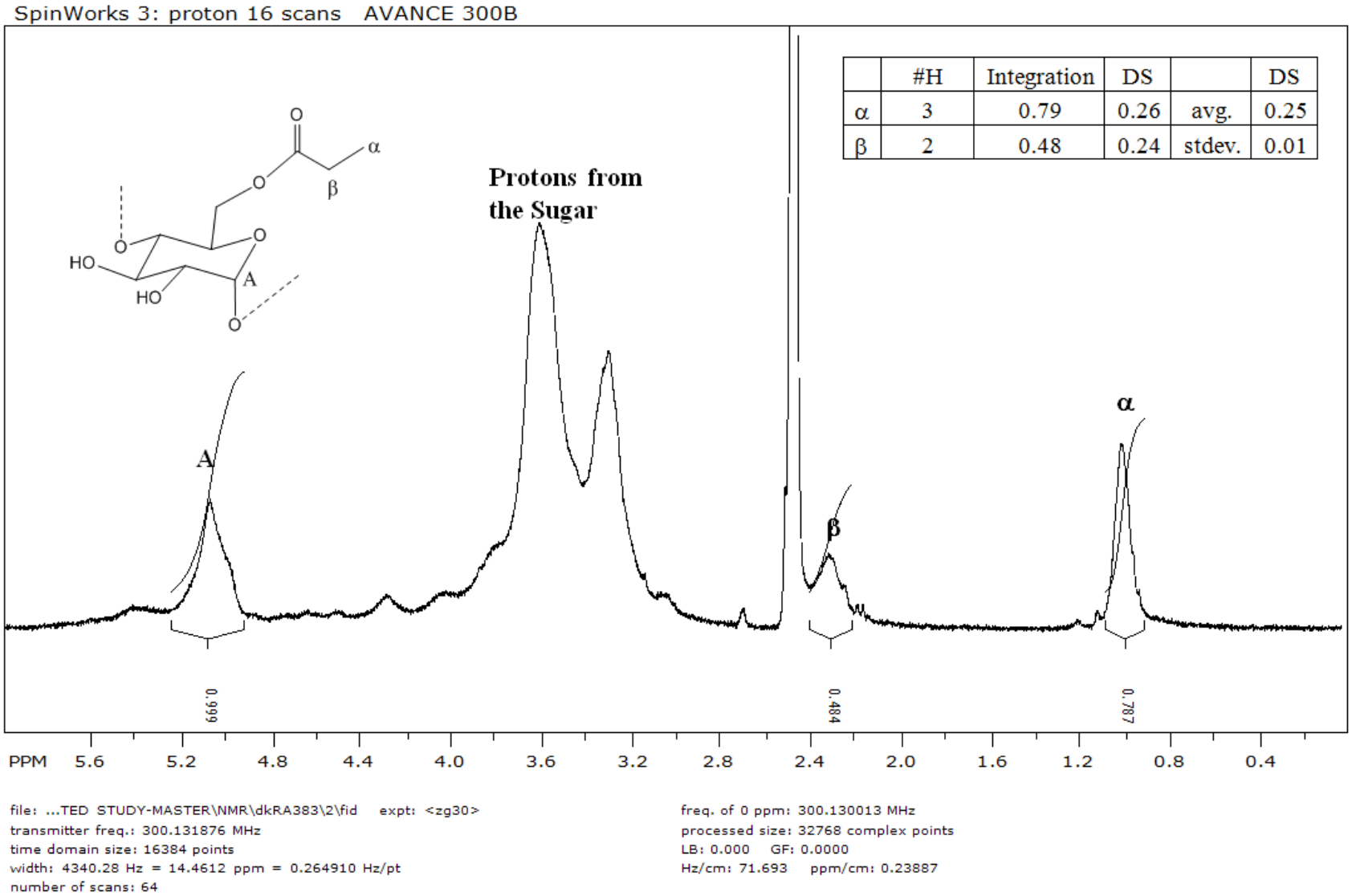

	#H	Integration	DS		DS
α	3	0.79	0.26	avg.	0.25
β	2	0.48	0.24	stdev.	0.01

Figure A.9.2. ^{1}H-NMR (300MHz, DMSO^{d}) of dialyzed C3(0.25)-SNP(5) in the presence of a trace amount of TFA

Determination of Equilibrium Constant K_B

Table B.1 Parameters retrieved from the analysis of the fluorescence spectra and decays with Equation 3.1 acquired with 0.5 μM pyrene in aqueous dispersions of SNP(A)

[SNP(A)], (g/L)	I_1	I_3	I_1/I_3	$\tau_{PySNP,}$ (ns)	α_{PySNP}	τ_{PyW} (ns)	α_{PyW}	τ_{SNP1} (ns)	α_{SNP1}	τ_{SNP2} ns	α_{SNP2}	f_{bound}	f_{free}	f_{bound}/f_{free}	f_{bound}/f_{free} (after Corr.)	χ^2
19.93				206	0.43	130	0.42	35	0.03	9.4	0.12	0.51	0.49	1.04	0.98	1.07
18.13				205	0.36	130	0.40	17.5	0.08	2.9	0.17	0.47	0.53	0.90	0.85	1.03
16.50				205	0.36	130	0.44	20.6	0.06	5.8	0.14	0.45	0.55	0.82	0.76	0.99
16.03	100	62	1.62	209	0.29	130	0.35	19.2	0.08	3.8	0.29	0.45	0.55	0.83	0.77	0.97
15.06				204	0.33	130	0.44	13.5	0.11	3.3	0.11	0.43	0.57	0.75	0.70	0.97
12.92	100	60	1.66	208	0.30	130	0.45	20.0	0.08	6.4	0.18	0.39	0.61	0.65	0.60	1.04
9.26	100	59	1.69	206	0.00	130	0.01	13.8	0.00			0.36	0.64	0.57	0.51	1.07
6.68	100	59	1.71	204	0.15	130	0.36	15.9	0.09			0.30	0.70	0.43	0.38	0.96
3.46	100	57	1.75	207	0.15	130	0.70	12.6	0.16			0.17	0.83	0.21	0.16	0.99
2.03	100	56	1.80	210	0.10	130	0.75	13.2	0.15			0.12	0.88	0.14	0.08	1.00
0.90	100	54	1.80	201	0.08	130	0.75	12.2	0.17			0.09	0.91	0.10	0.05	1.12
0.46	100	55	1.81	221	0.04	130	0.79	12.0	0.17			0.05	0.95	0.05	0.00	0.99

Table B.2. Parameters retrieved from the analysis of the fluorescence spectra and decays with Equation 3.1 acquired with 0.5 μM pyrene in aqueous dispersions of C6(0.06)-SNP(A)

[C6(0.05)-SNP(A)], (g/L)	I_1	I_3	I_1/I_3	τ_{PySNP} (ns)	α_{PySNP}	τ_{PyW} (ns)	α_{PyW}	τ_{SNP1} (ns)	α_{SNP1}	τ_{SNP2} (ns)	α_{SNP2}	f_{bound}	f_{free}	f_{bound}/f_{free}	f_{bound}/f_{free} (after Corr.)	χ^2
16.06				274	0.25	130	0.13	28.1	0.13	4.2	0.48	0.33	0.67	2.01	1.96	0.99
15.29				269	0.24	130	0.14	29.1	0.17	4.7	0.44	0.37	0.63	1.69	1.64	1.05
14.22	211106	143770	1.47	264	0.27	130	0.17	31.6	0.17	5.9	0.39	0.38	0.62	1.62	1.57	1.01
12.93				265	0.24	130	0.18	28.9	0.17	4.7	0.41	0.42	0.58	1.35	1.31	1.02
11.51				265	0.17	130	0.15	25.0	0.16	3.1	0.52	0.47	0.53	1.12	1.07	1.04
9.73	189120	124366	1.52	263	0.24	130	0.22	29.9	0.17	5.0	0.36	0.48	0.52	1.07	1.03	1.13
8.01				258	0.25	130	0.26	28.9	0.17	5.3	0.31	0.50	0.50	0.99	0.94	1.02
6.07	175050	115542	1.52	263	0.29	130	0.41	18.3	0.30			0.59	0.41	0.70	0.66	1.05
5.52				258	0.21	130	0.28	27.1	0.15	3.8	0.35	0.57	0.43	0.76	0.72	1.13
4.74				256	0.24	130	0.34	32.2	0.15	5.7	0.27	0.59	0.41	0.69	0.64	1.01
3.71	164956	104621	1.58	254	0.23	130	0.36	30.9	0.15	5.5	0.25	0.61	0.39	0.65	0.6	0.96
2.82				254	0.20	130	0.44	28.8	0.11	5.9	0.24	0.69	0.31	0.45	0.4	0.98
2.34	156652	96549	1.62	251	0.18	130	0.43	25.5	0.14	3.7	0.26	0.71	0.29	0.41	0.36	1.10
1.84	155294	98001	1.58	252	0.18	130	0.54	26.5	0.11	5.9	0.17	0.75	0.25	0.34	0.29	1.05
1.29	147875	88015	1.68	243	0.16	130	0.63	31.5	0.06	9.8	0.15	0.79	0.21	0.26	0.21	1.05
1.15				247	0.13	130	0.54	23.9	0.09	4.3	0.24	0.81	0.19	0.24	0.19	1.14
0.96				249	0.13	130	0.67	13.9	0.20			0.83	0.17	0.20	0.15	1.01
0.73	147289	84339	1.75	246	0.12	130	0.71	14.4	0.17			0.86	0.14	0.16	0.12	1.10
0.45	143754	82577	1.74	242	0.08	130	0.77	13.2	0.15			0.90	0.10	0.11	0.06	1.10
0.29	146037	82736	1.77	235	0.07	130	0.79	13.7	0.14			0.92	0.08	0.09	0.04	0.98
0.19				204	0.09	130	0.77	14.8	0.13			0.89	0.11	0.12	0.07	1.04

Table B.3. Parameters retrieved from the analysis of the fluorescence spectra and decays with Equation 3.1 acquired with 0.5 μM pyrene in aqueous dispersions of C6(0.08)-SNP(A)

[C6(0.08)-SNP(A)], (g/L)	I_1	I_3	I_1/I_3	τ_{PySNP} (ns)	α_{PySNP}	τ_{PyW} (ns)	α_{PyW}	τ_{SNP1} (ns)	α_{SNP1}	τ_{SNP2} (ns)	α_{SNP2}	f_{bound}	f_{free}	f_{bound}/f_{free}	f_{bound}/f_{free} (after Corr.)	χ^2
16.37	100	70	1.42	268	0.22	130	0.12	19.2	0.10	3.1	0.60	0.65	0.35	1.82	1.78	0.94
11.15	100	69	1.44	267	0.29	130	0.20	16.9	0.15	4.1	0.44	0.59	0.41	1.45	1.41	1.06
7.58	100	66	1.52	264	0.26	130	0.22	20.1	0.10	3.8	0.48	0.55	0.45	1.22	1.19	1.04
5.96	100	66	1.51	267	0.26	130	0.29	18.5	0.13	3.5	0.36	0.48	0.52	0.92	0.88	1.01
4.80	100	67	1.49	266	0.26	130	0.32	18.7	0.14	4.3	0.35	0.45	0.55	0.81	0.78	1.08
3.55	100	65	1.53	268	0.27	130	0.40	16.2	0.16	7.2	0.26	0.40	0.60	0.67	0.63	0.99
2.42	100	64	1.57	269	0.09	130	0.20	15.9	0.14	1.3	0.28	0.32	0.68	0.47	0.44	0.99
1.55	100	64	1.57	269	0.16	130	0.53	17.4	0.13	4.0	0.24	0.23	0.77	0.30	0.27	1.00
0.87	100	61	1.63	268	0.12	130	0.58	14.9	0.14	4.7	0.23	0.17	0.83	0.20	0.17	0.93
0.40	100	58	1.74	257	0.10	130	0.73	14.9	0.16	3.1	0.05	0.12	0.88	0.13	0.09	1.07
0.16	100	54	1.85	285	0.03	130	0.77	19.2	0.10	4.1	0.60	0.04	0.96	0.04	0.01	1.04

Table B.4. Parameters retrieved from the analysis of the fluorescence spectra and decays with Equation 3.1 acquired with 0.5 μM pyrene in aqueous dispersions of C6(0.09)-SNP(A)

[C6(0.09)-SNP(A)], (g/L)	τ_{PySNP} (ns)	α_{PySNP}	τ_{PyW} (ns)	α_{PyW}	τ_{SNP1} (ns)	α_{SNP}	τ_{SNP2} (ns)	α_{SNP}	f_{bound}	f_{free}	f_{bound}/f_{free}	f_{bound}/f_{free} (after Corr.)	χ^2
16.06	269	0.32	130	0.19	25.2	0.09	4.3	0.40	0.63	0.37	1.72	1.67	1.04
15.13	268	0.31	130	0.19	25.0	0.09	3.6	0.41	0.62	0.38	1.64	1.59	0.91
13.44	271	0.34	130	0.23	18.9	0.13	3.4	0.30	0.59	0.41	1.47	1.42	1.18
11.09	268	0.37	130	0.26	32.1	0.08	5.8	0.29	0.59	0.41	1.44	1.39	1.04
8.30	273	0.03	130	0.03	13.1	0.00	0.5	0.93	0.50	0.50	1.01	0.96	1.08
7.07	265	0.35	130	0.31	39.7	0.07	6.2	0.27	0.53	0.47	1.11	1.06	1.00
6.60	265	0.35	130	0.37	37.4	0.07	8.0	0.21	0.49	0.51	0.97	0.92	1.00
5.59	264	0.31	130	0.35	28.3	0.08	5.4	0.25	0.47	0.53	0.90	0.85	0.98
4.17	267	0.30	130	0.44	25.0	0.07	8.2	0.18	0.41	0.59	0.68	0.63	0.96
3.16	265	0.21	130	0.43	16.8	0.10	3.1	0.25	0.33	0.67	0.49	0.44	0.98
2.10	265	0.21	130	0.54	17.5	0.10	3.7	0.15	0.28	0.72	0.38	0.33	1.01
1.46	260	0.18	130	0.59	27.0	0.08	5.0	0.15	0.24	0.76	0.31	0.26	0.94
0.96	264	0.01	130	0.03	17.7	0.01	0.5	0.96	0.18	0.82	0.22	0.17	1.06
0.57	259	0.11	130	0.76	15.2	0.14	0.1	0.00	0.12	0.88	0.14	0.09	1.08
0.31	241	0.02	130	0.21	15.2	0.03	0.7	0.74	0.09	0.91	0.10	0.05	1.00
0.24	244	0.07	130	0.78	62.3	0.02	10.1	0.13	0.09	0.91	0.09	0.04	0.99
0.14	224	0.05	130	0.72	13.9	0.11	2.3	0.11	0.07	0.93	0.07	0.02	1.08
0.07	189	0.07	130	0.78	67.8	0.02	12.1	0.13	0.08	0.92	0.09	0.04	1.05

Table B.5. Parameters retrieved from the analysis of the fluorescence spectra and decays with Equation 3.1 acquired with 0.5 μM pyrene in aqueous dispersions of C6(0.11)-SNP(A)

[C6(0.11)-SNP(A)], (g/L)	I_1	I_3	I_1/I_3	τ_{PySNP} (ns)	α_{PySNP}	τ_{PyW} (ns)	α_{PyW}	τ_{SNP1} (ns)	α_{SNP1}	τ_{SNP2} (ns)	α_{SNP2}	f_{bound}	f_{free}	f_{bound}/f_{free}	f_{bound}/f_{free} (after Corr.)	χ^2
14.32	176132	125599	1.40	300	0.14	130	0.08	14.9	0.13	1.6	0.20	0.64	0.36	1.77	1.72	0.97
9.56	186974	131218	1.42	299	0.09	130	0.07	22.6	0.11	5.2	0.21	0.55	0.45	1.23	1.17	1.11
6.28	199124	134547	1.48	298	0.10	130	0.10	19.7	0.10	8.7	0.11	0.50	0.50	1.00	0.95	1.02
4.08	192294	128894	1.49	294	0.08	130	0.10	16.7	0.13	9.1	0.05	0.43	0.57	0.76	0.70	1.07
3.78	186916	122148	1.53	297	0.11	130	0.16	19.4	0.08	3.2	0.21	0.40	0.60	0.68	0.62	1.00
2.49	179080	114808	1.56	290	0.09	130	0.18	22.4	0.08	5.3	0.17	0.34	0.66	0.51	0.45	1.03
2.04	178529	112791	1.58	289	0.09	130	0.21	12.8	0.12	6.6	0.06	0.31	0.69	0.44	0.38	1.13
1.48	169133	105038	1.61	293	0.05	130	0.15	23.7	0.10	7.9	0.11	0.23	0.77	0.30	0.25	0.95
1.04	166406	101542	1.64	278	0.04	130	0.15	13.8	0.15			0.21	0.79	0.27	0.21	1.05
0.77	156271	93788	1.67	281	0.02	130	0.12	17.5	0.16			0.16	0.84	0.19	0.13	1.06
0.53	152308	88225	1.73	267	0.04	130	0.23	17.8	0.08	4.0	0.15	0.14	0.86	0.16	0.10	0.94
0.40	142885	85058	1.68	256	0.03	130	0.22	13.4	0.11	2.6	0.20	0.12	0.88	0.14	0.08	1.08
0.24	139856	82811	1.69	251	0.01	130	0.13	17.6	0.11	2.0	0.30	0.09	0.91	0.10	0.04	1.10
0.09	145298	81912	1.77	215	0.01	130	0.15	10.1	0.02	20.9	0.12	0.08	0.92	0.08	0.03	0.97
0.03	145201	83770	1.73	217	0.01	130	0.26	11.2	0.16			0.04	0.96	0.04	-0.02	1.06
0.02	147682	84008	1.76	184	0.02	130	0.26	11.2	0.05	12.4	0.07	0.07	0.93	0.07	0.01	0.96

Table B.6. Parameters retrieved from the analysis of the fluorescence spectra and decays with Equation 3.1 acquired with 0.5 μM pyrene in aqueous dispersions of C6(0.12)-SNP(A)

[C6(0.12)-SNP(A)], (g/L)	I_1	I_3	I_1/I_3	τ_{PySNP} (ns)	α_{PySNP}	τ_{PyW} (ns)	α_{PyW}	τ_{SNP1} (ns)	α_{SNP1}	τ_{SNP2} (ns)	α_{SNP2}	f_{bound}	f_{free}	f_{bound}/f_{free}	f_{bound}/f_{free} (after Corr.)	χ^2
15.32	100	71	1.41	282	0.40	130	0.14	27.0	0.08	5.5	0.38	0.74	0.26	2.82	2.70	1.03
14.52	100	71	1.42	286	0.01	130	0.01	12.3	0.01	0.6	0.98	0.69	0.31	2.28	2.16	0.98
13.23	100	71	1.41	284	0.35	130	0.15	20.2	0.12	3.5	0.37	0.71	0.29	2.39	2.27	0.98
11.27	100	70	1.43	285	0.40	130	0.20	20.8	0.10	4.5	0.30	0.67	0.33	1.99	1.87	1.05
9.92	100	70	1.42	284	0.01	130	0.01	13.6	0.01	0.6	0.97	0.64	0.36	1.80	1.68	1.00
8.63	100	68	1.47	284	0.38	130	0.22	21.9	0.10	3.7	0.29	0.63	0.37	1.73	1.61	1.05
6.73	100	69	1.45	284	0.28	130	0.18	17.6	0.11	1.9	0.44	0.61	0.39	1.53	1.41	1.03
6.12	100	69	1.45	283	0.20	130	0.14	17.4	0.07	1.6	0.58	0.58	0.42	1.40	1.28	0.98
5.05	100	67	1.49	281	0.39	130	0.28	27.6	0.08	5.2	0.25	0.58	0.42	1.36	1.24	0.96
4.34	100	69	1.46	284	0.34	130	0.30	18.9	0.11	3.2	0.25	0.54	0.46	1.16	1.04	0.97
3.62	100	68	1.47	284	0.36	130	0.37	33.9	0.06	7.5	0.21	0.49	0.51	0.96	0.84	1.05
2.40	100	67	1.50	288	0.22	130	0.34	17.9	0.08	2.1	0.37	0.39	0.61	0.63	0.51	1.06
1.99	100	66	1.52	279	0.21	130	0.32	16.1	0.11	1.4	0.36	0.39	0.61	0.64	0.52	1.08
1.57	100	64	1.56	283	0.01	130	0.03	17.7	0.01	0.6	0.95	0.33	0.67	0.49	0.37	1.03

Table B.7. Parameters retrieved from the analysis of the fluorescence spectra and decays with Equation 3.1 acquired with 0.5 μM pyrene in aqueous dispersions of C6(0.12)-SNP(A)

[C6(0.12)-SNP(A)], (g/L)	I_1	I_3	I_1/I_3	τ_{PySNP} (ns)	α_{PySNP}	τ_{PyW} (ns)	α_{PyW}	τ_{SNP1} (ns)	α_{SNP1}	τ_{SNP2} (ns)	α_{SNP2}	f_{bound}	f_{free}	f_{bound}/f_{free}	f_{bound}/f_{free} (after Corr.)	χ^2
14.09	100	69.8	1.43	291	0.27	130	0.10	21.8	0.06	1.6	0.57	0.72	0.28	2.60	2.55	1.01
13.51	100	70.4	1.42	291	0.55	130	0.22	22.0	0.09	8.5	0.14	0.71	0.29	2.47	2.42	1.03
12.74	100	70.4	1.42	290	0.02	130	0.01	17.5	0.52	0.5	0.97	0.71	0.29	2.46	2.41	1.06
11.62	100	69.7	1.43	291	0.30	130	0.13	16.8	0.09	1.7	0.47	0.69	0.31	2.27	2.22	1.14
10.34	100	68.8	1.45	288	0.04	130	0.02	13.1	0.01	0.5	0.93	0.67	0.33	2.03	1.98	0.97
8.96	100	69.8	1.43	286	0.53	130	0.24	27.5	0.06	9.8	0.16	0.68	0.32	2.17	2.12	1.05
7.56	100	67.7	1.48	286	0.45	130	0.21	28.1	0.07	4.7	0.26	0.68	0.32	2.11	2.06	1.03
6.13	100	67.6	1.48	287	0.01	130	0.01	15.5	0.00	0.5	0.97	0.62	0.38	1.62	1.57	1.04
5.81	100	67.9	1.47	286	0.42	130	0.28	19.9	0.10	4.5	0.21	0.60	0.40	1.51	1.46	0.97
5.09	100	68.4	1.46	286	0.43	130	0.30	20.5	0.08	5.2	0.19	0.59	0.41	1.43	1.38	0.99
4.24	100	67.4	1.48	284	0.45	130	0.33	20.2	0.13	4.7	0.09	0.58	0.42	1.35	1.30	0.99
3.32	100	67.1	1.49	285	0.40	130	0.37	15.0	0.14	5.0	0.09	0.52	0.48	1.08	1.03	1.06
2.61	100	66.3	1.51	286	0.28	130	0.31	13.2	0.13	1.7	0.27	0.48	0.52	0.91	0.86	1.09
1.93	100	65.4	1.53	280	0.35	130	0.44	15.4	0.14	5.7	0.07	0.44	0.56	0.78	0.73	0.92
1.43	100	64.5	1.55	280	0.35	130	0.47	37.6	0.01	12.8	0.17	0.42	0.58	0.74	0.69	1.06
1.11	100	61.6	1.62	278	0.27	130	0.55	28.4	0.06	6.7	0.12	0.32	0.68	0.48	0.43	1.14
0.76	100	60.4	1.65	278	0.24	130	0.61	28.8	0.03	10.3	0.13	0.28	0.72	0.40	0.35	1.02
0.48	100	59.5	1.68	275	0.02	130	0.08	14.9	0.01	0.5	0.88	0.20	0.80	0.24	0.19	1.08
0.15	100	57.2	1.75	261	0.09	130	0.77	19.7	0.08	8.1	0.06	0.10	0.90	0.11	0.06	1.08

Table B.8. Parameters retrieved from the analysis of the fluorescence spectra and decays with Equation 3.1 acquired with 0.5 μM pyrene in aqueous dispersions of C6(0.15)-SNP(A)

[C6(0.15)-SNP(A)], (g/L)	I_1	I_3	I_1/I_3	τ_{PySNP} (ns)	α_{PySNP}	τ_{PyW} (ns)	α_{PyW}	τ_{SNP1} (ns)	α_{SNP1}	τ_{SNP2} (ns)	α_{SNP2}	f_{bound}	f_{free}	f_{bound}/f_{free}	f_{bound}/f_{free} (after Corr.)	χ^2
13.61	100	75	1.33	307	0.41	130	0.10	15.4	0.11	2.6	0.38	0.80	0.20	3.90	3.85	1.06
12.98	100	76	1.32	309	0.46	130	0.12	19.3	0.08	3.8	0.34	0.79	0.21	3.75	3.69	1.02
12.02	100	76	1.32	307	0.46	130	0.11	18.4	0.10	3.7	0.33	0.80	0.20	3.98	3.92	1.11
10.70	100	76	1.32	309	0.42	130	0.12	16.5	0.08	3.1	0.38	0.77	0.23	3.39	3.33	1.10
8.91	100	75	1.33	308	0.48	130	0.14	18.1	0.09	3.8	0.28	0.77	0.23	3.33	3.27	1.06
7.28	100	75	1.34	307	0.34	130	0.11	15.9	0.08	2.0	0.47	0.76	0.24	3.09	3.04	1.00
5.89	100	74	1.35	308	0.01	130	0.00	13.7	0.00	0.4	0.99	0.71	0.29	2.49	2.43	1.01
5.57	100	74	1.36	308	0.57	130	0.23	13.7	0.19			0.71	0.29	2.46	2.40	1.00
4.66	100	74	1.34	308	0.08	130	0.04	12.9	0.03	0.7	0.85	0.70	0.30	2.37	2.31	1.02
3.60	100	73	1.36	308	0.53	130	0.29	13.2	0.18			0.65	0.35	1.83	1.77	1.06
3.22	100	72	1.39	309	0.41	130	0.25	17.8	0.09	3.3	0.24	0.62	0.38	1.64	1.58	0.99
2.52	100	73	1.37	308	0.48	130	0.32	11.0	0.19			0.60	0.40	1.48	1.42	1.06
2.08	100	74	1.36	305	0.35	130	0.27	27.2	0.07	3.5	0.30	0.57	0.43	1.31	1.26	0.94
1.64	100	70	1.43	304	0.42	130	0.42	13.4	0.16			0.50	0.50	1.02	0.96	1.05
1.18	100	70	1.42	305	0.35	130	0.46	26.6	0.05	6.8	0.15	0.43	0.57	0.76	0.70	1.07
0.77	100	67	1.50	305	0.29	130	0.56	14.1	0.15			0.35	0.65	0.53	0.47	1.00
0.56	100	65	1.55	303	0.02	130	0.04	13.8	0.01	0.6	0.93	0.28	0.72	0.39	0.34	1.05
0.41	100	63	1.58	302	0.20	130	0.67	13.1	0.13			0.23	0.77	0.29	0.23	1.01
0.24	100	61	1.65	300	0.12	130	0.62	18.0	0.09	3.7	0.17	0.17	0.83	0.20	0.14	1.07
0.11	100	58	1.71	295	0.09	130	0.77	14.7	0.14			0.11	0.89	0.12	0.06	1.02

Table B.9. Parameters retrieved from the analysis of the fluorescence spectra and decays with Equation 3.1 acquired with 0.5 μM pyrene in aqueous dispersions of C6(0.05)-SNP(F) (dialyzied before the modification).

[C6(0.05)-SNP(F)], (g/L)	I_1	I_3	I_1/I_3	τ_{PySNP} (ns)	α_{PySNP}	τ_{PyW} (ns)	α_{PyW}	τ_{SNP1} (ns)	α_{SNP1}	τ_{SNP2} (ns)	α_{SNP2}	f_{bound}	f_{free}	f_{bound}/f_{free}	f_{bound}/f_{free} (after Corr.)	χ^2
13.2	100	65	1.53	266	0.27	130	0.26	4.1	0.34	24.2	0.13	0.51	0.49	1.04	0.98	1.00
12.5	100	67	1.48	262	0.31	130	0.29	6.8	0.31	33.1	0.10	0.52	0.48	1.07	1.01	1.00
11.8	100	66	1.51	263	0.28	130	0.29	5.3	26.10	26.1	0.12	0.50	0.50	0.99	0.93	1.02
10.5	100	65	1.53	264	0.26	130	0.30	5.1	0.30	23.7	0.13	0.46	0.54	0.86	0.80	0.98
8.8	100	65	1.55	261	0.28	130	0.35	5.7	0.25	26.5	0.11	0.44	0.56	0.80	0.74	0.97
7.2	100	65	1.54	261	0.27	130	0.40	6.0	0.23	26.9	0.10	0.40	0.60	0.66	0.60	0.96
6.5	100	65	1.54	257	0.27	130	0.43	7.4	0.23	35.1	0.08	0.38	0.62	0.63	0.57	1.06
5.4				255	0.23	130	0.46	30.9	0.09	5.7	0.22	0.34	0.66	0.51	0.45	1.04
4.4	100	64	1.56	251	0.22	130	0.52	25.0	0.11	4.8	0.15	0.30	0.70	0.42	0.36	1.14
3.4	100	62	1.62	256	0.20	130	0.51	6.2	0.19	27.3	0.09	0.28	0.72	0.39	0.33	1.03
2.2	100	61	1.64	252	0.04	130	0.14	19.2	0.03			0.21	0.79	0.26	0.20	1.02
1.5	100	59	1.70	254	0.14	130	0.71	19.1	0.11	5.5	0.04	0.16	0.84	0.19	0.13	1.10
1.0	100	59	1.70	252	0.05	130	0.40	16.0	0.05	1.4	0.50	0.12	0.88	0.13	0.07	1.10
0.7	100	57	1.76	240	0.10	130	0.76	22.7	0.14			0.12	0.88	0.13	0.07	1.01
0.4	100	58	1.73	233	0.08	130	0.83	17.9	0.09			0.08	0.92	0.09	0.03	0.99
0.2	100	56	1.78	239	0.04	130	0.88	16.1	0.08			0.05	0.95	0.05	-0.01	0.98
0.0	100	56	1.78	219	0.03	130	0.95	28.0	0.02			0.03	0.97	0.03	-0.03	1.00

Table B.10. Parameters Retrieved from the Analysis of the Fluorescence spectra and Decays with Equation 3.1 Acquired with 0.5 μM pyrene in Aqueous Dispersions of C6(0.06)-SNP(F) (dialyzied after the modification)

[C6(0.06) -SNP(F)], (g/L)	I_1	I_3	I_1/I_3	τ_{PySNP} (ns)	α_{PySNP}	τ_{PyW} (ns)	α_{PyW}	τ_{SNP1} (ns)	α_{SNP1}	τ_{SNP2} (ns)	α_{SNP2}	f_{bound}	f_{free}	f_{bound}/f_{free}	f_{bound}/f_{free} (after Corr.)	χ^2
15.28	100	69	1.45	247	0.07	130	0.06	15.6	0.10	3.3	0.77	0.56	0.44	1.25	1.21	1.06
12.03	100	67	1.49	247	0.09	130	0.08	16.4	0.11	3.6	0.72	0.84	0.16	1.12	1.08	0.98
7.43	100	65	1.53	250	0.10	130	0.13	15.4	0.14	3.4	0.63	0.77	0.23	0.80	0.76	1.14
5.77	100	64	1.55	245	0.11	130	0.15	15.5	0.12	3.3	0.62	0.74	0.26	0.70	0.66	1.01
4.09	100	64	1.57	243	0.13	130	0.22	17.8	0.13	4.1	0.53	0.65	0.35	0.59	0.55	1.03
2.69	100	61	1.65	246	0.11	130	0.30	15.7	0.13	3.5	0.45	0.58	0.42	0.37	0.33	1.13
1.04	100	58	1.72	240	0.11	130	0.57	9.5	0.57			0.57	0.43	0.20	0.16	1.05
0.50	100	57	1.74	246	0.07	130	0.66	10.5	0.26			0.26	0.74	0.11	0.07	1.10
0.27	100	57	1.74	230	0.05	130	0.74	11.8	0.21			0.21	0.79	0.07	0.03	0.96

Table B.11. Parameters retrieved from the analysis of the fluorescence spectra and decays with Equation 3.1 acquired with 0.5 μM pyrene in aqueous dispersions of C6(0.08)-SNP(F) (dialyzied before the modification)

[C6(0.08)- SNP(F)], (g/L)	I_1	I_3	I_1/I_3	τ_{PySNP} (ns)	α_{PySNP}	τ_{PyW} (ns)	α_{PyW}	τ_{SNP1} (ns)	α_{SNP1}	τ_{SNP2} (ns)	α_{SNP2}	f_{bound}	f_{free}	f_{bound}/f_{free}	f_{bound}/f_{free} (after Corr.)	χ^2
13.77	100	69	1.44	272	0.18	130	0.15	24.2	0.11	4.4	0.56	0.55	0.45	1.23	1.20	0.99
12.51				270	0.20	130	0.16	23.1	0.11	4.3	0.53	0.56	0.44	1.25	1.22	0.99
10.51	100	68	1.47	268	0.21	130	0.19	21.3	0.11	3.4	0.49	0.52	0.48	1.09	1.05	1.14
8.70	100	69	1.46	266	0.27	130	0.29	26.0	0.10	5.0	0.35	0.48	0.52	0.93	0.90	1.01
6.23	100	67	1.49	264	0.29	130	0.37	41.3	0.08	6.9	0.26	0.44	0.56	0.80	0.77	1.04
4.67	100	65	1.53	265	0.23	130	0.40	21.3	0.11	3.5	0.25	0.37	0.63	0.58	0.55	1.12
3.45	100	65	1.53	259	0.23	130	0.47	29.3	0.09	5.4	0.22	0.33	0.67	0.49	0.45	0.22
2.61	100	63	1.59	266	0.16	130	0.39	21.6	0.10	2.6	0.35	0.29	0.71	0.42	0.38	1.06
1.77	100	62	1.62	260	0.17	130	0.58	30.2	0.09	5.7	0.16	0.23	0.77	0.30	0.27	1.04
1.38	100	62	1.61	267	0.14	130	0.62	19.8	0.11	4.3	0.13	0.18	0.82	0.22	0.19	1.03
0.99				265	0.12	130	0.72	16.6	0.16			0.14	0.86	0.16	0.13	1.05
0.77	100	60	1.66	264	0.10	130	0.74	18.0	0.16			0.12	0.88	0.13	0.10	1.02
0.51	100	60	1.65	248	0.09	130	0.78	19.2	0.13			0.10	0.90	0.12	0.08	1.03
0.32	100	61	1.65	251	0.06	130	0.82	22.3	0.12			0.07	0.93	0.07	0.04	1.09
0.29	100	59	1.70	253	0.04	130	0.86	21.5	0.11			0.04	0.96	0.04	0.01	1.07
0.06	100	60	1.66	255	0.02	130	0.88	21.3	0.10			0.02	0.98	0.02	-0.01	1.19

Table B.12. Parameters retrieved from the analysis of the fluorescence spectra and decays with Equation 3.1 acquired with 0.5 μM pyrene in aqueous dispersions of C6(0.10)-SNP(F) (dialyzied before the modification)

[C6(0.10) SNP(F)], (g/L)	I_1	I_3	I_1/I_3	τ_{PySNP} (ns)	α_{PySNP}	τ_{PyW} (ns)	α_{PyW}	τ_{SNP1} (ns)	α_{SNP1}	τ_{SNP2} (ns)	α_{SNP2}	f_{bound}	f_{free}	f_{bound}/f_{free}	f_{bound}/f_{free} (after Corr.)	χ^2
21.82	175	122	1.43	285	0.17	130	0.07	18.1	0.07	4.5	0.70	0.72	0.28	2.51	2.46	1.08
21.43	170	121	1.41	284	0.26	130	0.11	20.5	0.07	6.6	0.56	0.70	0.30	2.38	2.33	1.07
20.66	176	125	1.41	283	0.15	130	0.06	22.6	0.04	4.8	0.75	0.70	0.30	2.38	2.33	1.03
19.97	177	124	1.43	284	0.13	130	0.05	22.0	0.04	4.3	0.77	0.71	0.29	2.44	2.39	1.06
18.94	181	128	1.41	281	0.20	130	0.08	17.2	0.08	4.8	0.64	0.70	0.30	2.36	2.31	0.96
17.38	192	136	1.41	283	0.06	130	0.03	15.8	0.03	2.5	0.88	0.67	0.33	2.07	2.02	1.01
15.28	189	134	1.42	282	0.33	130	0.18	17.8	0.11	6.7	0.38	0.66	0.34	1.91	1.86	1.07
13.27	203	141	1.44	282	0.35	130	0.19	24.7	0.08	6.2	0.38	0.65	0.35	1.88	1.83	1.03
11.42	268	185	1.45	282	0.17	130	0.10	13.4	0.11	3.4	0.61	0.63	0.37	1.67	1.62	1.13
10.87	260	180	1.45	282	0.29	130	0.18	17.0	0.10	4.9	0.43	0.61	0.39	1.57	1.52	0.96
9.71	289	195	1.48	280	0.08	130	0.05	19.4	0.03	2.5	0.85	0.61	0.39	1.59	1.54	1.07
7.68	373	258	1.45	278	0.33	130	0.23	21.8	0.09	4.6	0.35	0.59	0.41	1.43	1.38	1.00
6.81	377	260	1.45	277	0.31	130	0.25	21.2	0.07	4.7	0.36	0.55	0.45	1.24	1.19	1.05
5.48	447	301	1.49	275	0.32	130	0.31	20.8	0.09	4.8	0.28	0.51	0.49	1.04	0.99	1.03
4.09	572	383	1.49	276	0.29	130	0.34	17.8	0.11	3.3	0.26	0.46	0.54	0.86	0.81	1.02
3.25	639	422	1.52	276	0.25	130	0.35	16.9	0.09	2.7	0.30	0.41	0.59	0.71	0.66	1.07
2.29	838	529	1.58	276	0.24	130	0.46	22.5	0.07	3.9	0.23	0.35	0.65	0.53	0.48	1.08
1.35	1069	655	1.63	271	0.18	130	0.62	27.6	0.06	5.0	0.14	0.23	0.77	0.29	0.24	1.07
0.70	1732	1045	1.66	270	0.04	130	0.18	19.3	0.02			0.19	0.81	0.23	0.18	1.06
0.30	3656	2069	1.77	263	0.09	130	0.84	18.9	0.07			0.09	0.91	0.10	0.05	1.10
0.13	5135	2811	1.83	249	0.06	130	0.87	16.3	0.07			0.06	0.94	0.07	0.02	1.13
0.05	6520	3551	1.84	219	0.06	130	0.88	30.7	0.06			0.06	0.94	0.06	0.01	1.17

Table B.13. Parameters retrieved from the analysis of the fluorescence spectra and decays with Equation 3.1 acquired with 0.5 μM pyrene in aqueous dispersions of C6(0.12)-SNP(F) (dialyzied after the modification)

[C6(0.12) SNP(F)], (g/L)	I_1	I_3	I_1/I_3	τ_{PySNP} (ns)	α_{PySNP}	τ_{PyW} (ns)	α_{PyW}	τ_{SNP1} (ns)	α_{SNP1}	τ_{SNP2} (ns)	α_{SNP2}	f_{bound}	f_{free}	f_{bound}/f_{free}	f_{bound}/f_{free} (after Corr.)	χ^2
17.25	100	74	1.35	269	0.10	130	0.06	23.5	0.13	4.3	0.69	0.68	0.32	2.15	2.14	1.09
14.40	100	73	1.38	270	0.11	130	0.07	22.0	0.13	4.3	0.68	0.65	0.35	1.86	1.84	1.00
12.41	100	70	1.42	269	0.11	130	0.08	23.0	0.13	4.3	0.66	0.63	0.37	1.71	1.70	1.05
11.08				267	0.12	130	0.08	21.5	0.13	4.3	0.65	0.61	0.39	1.59	1.58	0.98
10.13	100	71	1.41	266	0.13	130	0.10	22.9	0.12	4.3	0.66	0.60	0.40	1.47	1.46	1.05
7.85	100	71	1.4	263	0.15	130	0.12	22.0	0.13	4.3	0.60	0.55	0.45	1.23	1.21	1.05
6.15	100	69	1.45	265	0.14	130	0.15	25.9	0.12	4.3	0.58	0.50	0.50	1.01	1.00	0.98
4.23	100	68	1.46	265	0.17	130	0.23	25.9	0.12	4.3	0.52	0.44	0.56	0.77	0.76	0.96
2.18	100	66	1.52	260	0.15	130	0.34	26.0	0.13	4.3	0.40	0.30	0.70	0.43	0.41	0.93
1.23	100	63	1.59	259	0.11	130	0.41	25.7	0.13	4.3	0.31	0.20	0.80	0.26	0.24	0.95
0.48	100	60	1.68	241	0.09	130	0.59	27.1	0.12	4.3	0.26	0.10	0.90	0.11	0.10	1.00
0.19	100	59	1.69	258	0.04	130	0.71	28.0	0.12	4.3	0.21	0.05	0.95	0.05	0.03	0.90
0.04	100	58	1.73	257	0.02	130	0.75	25.1	0.14	4.3	0.13	0.02	0.98	0.02	0.00	0.91

Table B.14. Parameters retrieved from the analysis of the fluorescence spectra and decays with Equation 3.1 acquired with 0.5 μM pyrene in aqueous dispersions of C6(0.12)-SNP(F) (dialyzied before the modification)

[C6(0.12) SNP(F)], (g/L)	I_1	I_3	I_1/I_3	τ_{PySNP} (ns)	α_{PySNP}	τ_{PyW} (ns)	α_{PyW}	τ_{SNP1} (ns)	α_{SNP1}	τ_{SNP2} (ns)	α_{SNP2}	f_{bound}	f_{free}	f_{bound}/f_{free}	f_{bound}/f_{free} (after Corr.)	χ^2
19.12	214	156	1.37	296	0.23	130	0.08	14.1	0.10	3.4	0.59	0.75	0.25	2.94	2.91	1.05
17.84	212	156	1.36	296	0.22	130	0.08	13.1	0.10	3.1	0.60	0.74	0.26	2.79	2.76	1.10
16.36	221	161	1.38	296	0.28	130	0.10	18.0	0.09	3.8	0.53	0.74	0.26	2.86	2.83	1.06
13.68	242	177	1.37	301	0.17	130	0.08	9.9	0.11	1.9	0.63	0.67	0.33	2.05	2.01	1.09
10.43	300	217	1.38	297	0.28	130	0.14	13.3	0.10	3.2	0.47	0.67	0.33	2.01	1.97	0.99
9.50	311	223	1.39	297	0.26	130	0.14	13.5	0.10	2.6	0.50	0.64	0.36	1.79	1.75	0.99
7.62	374	270	1.38	295	0.30	130	0.18	13.0	0.12	3.0	0.40	0.63	0.37	1.69	1.65	1.04
5.76	430	300	1.43	295	0.37	130	0.29	22.4	0.07	4.9	0.27	0.56	0.44	1.28	1.25	1.02
4.29	501	354	1.41	293	0.36	130	0.26	16.6	0.09	4.5	0.29	0.58	0.42	1.40	1.36	1.04
2.86	668	466	1.43	295	0.26	130	0.27	17.7	0.07	2.6	0.40	0.50	0.50	0.98	0.94	1.00
2.06	755	516	1.46	292	0.31	130	0.37	13.1	0.13	2.5	0.19	0.45	0.55	0.83	0.79	1.14
1.33	1046	681	1.53	290	0.29	130	0.55	28.2	0.06	6.6	0.11	0.34	0.66	0.52	0.49	1.03
0.99	1336	845	1.58	292	0.21	130	0.57	16.4	0.08	2.9	0.14	0.27	0.73	0.37	0.33	1.05
0.64	1749	1083	1.62	289	0.18	130	0.72	15.5	0.10			0.20	0.80	0.25	0.21	0.92
0.37	2776	1601	1.73	282	0.13	130	0.79	18.6	0.08			0.14	0.86	0.16	0.13	1.05
0.18	3951	2263	1.75	264	0.09	130	0.83	17.3	0.08			0.10	0.90	0.11	0.08	1.04
0.06	5746	3264	1.76	243	0.06	130	0.87	20.4	0.07			0.07	0.93	0.07	0.04	1.23
0.01	8045	4443	1.81	245	0.03	130	0.90	13.9	0.07			0.03	0.97	0.03	0.00	0.98

Table B.15. Parameters retrieved from the analysis of the fluorescence spectra and decays with Equation 3.1 acquired with 0.5 μM pyrene in aqueous dispersions of C6(0.13)-SNP(F) (dialyzied after the modification)

[C6(0.13) SNP(F)], (g/L)	I_1	I_3	I_1/I_3	τ_{PySNP} (ns)	α_{PySNP}	τ_{PyW} (ns)	α_{PyW}	τ_{SNP1} (ns)	α_{SNP1}	τ_{SNP2} (ns)	α_{SNP2}	f_{bound}	f_{free}	f_{bound}/f_{free}	f_{bound}/f_{free} (after Corr.)	χ^2
17.80	100	76	1.31	285	0.04	130	0.02	11.7	0.12	3.1	0.81	0.63	0.37	1.69	1.65	1.10
10.92	100	73	1.36	283	0.07	130	0.04	14.2	0.10	3.4	0.79	0.61	0.39	1.59	1.55	1.12
7.97	100	72	1.39	279	0.08	130	0.06	15.7	0.10	3.5	0.76	0.60	0.40	1.49	1.44	1.07
5.94	100	71	1.41	280	0.10	130	0.08	15.3	0.11	3.6	0.72	0.55	0.45	1.23	1.19	1.10
3.96	100	69	1.45	277	0.10	130	0.09	14.1	0.13	3.2	0.68	0.51	0.49	1.06	1.02	1.02
2.27	100	67	1.49	275	0.14	130	0.21	20.8	0.09	4.6	0.56	0.39	0.61	0.64	0.60	1.03
1.29	100	64	1.57	276	0.11	130	0.28	13.8	0.14	3.3	0.47	0.28	0.72	0.39	0.35	1.10
0.64	100	60	1.66	271	0.09	130	0.41	18.1	0.14	3.5	0.36	0.18	0.82	0.23	0.19	1.07
0.33	100	58	1.72	272	0.08	130	0.66	11.3	0.27			0.10	0.90	0.12	0.08	1.09
0.13	100	57	1.76	263	0.04	130	0.76	14.8	0.20			0.05	0.95	0.06	0.02	1.13

Table B.16. Parameters retrieved from the analysis of the fluorescence spectra and decays with Equation 3.1 acquired with 0.5 μM pyrene in aqueous dispersions of C3(0.03)-SNP(F) (dialyzied after the modification)

[C3(0.05)- SNP(F)], (g/L)	I_1	I_3	I_1/I_3	τ_{PySNP} (ns)	α_{PySNP}	τ_{PyW} (ns)	α_{PyW}	τ_{SNP1} (ns)	α_{SNP1}	τ_{SNP2} (ns)	α_{SNP2}	f_{bound}	f_{free}	f_{bound}/f_{free}	f_{bound}/f_{free} (after Corr.)	χ^2
17.11	100	66.0	1.51	196	0.07	130	0.07	17.0	0.07	4.6	0.79	0.53	0.47	1.15	1.14	1.06
11.26	100	60.8	1.64	197	0.07	130	0.10	13.9	0.11	3.7	0.72	0.40	0.60	0.66	0.65	1.09
8.25	100	60.8	1.65	194	0.09	130	0.16	16.6	0.09	4.8	0.67	0.37	0.63	0.59	0.58	1.01
6.39	100	59.8	1.67	195	0.09	130	0.19	14.9	0.11	4.4	0.61	0.31	0.69	0.46	0.45	1.10
4.51	100	59.8	1.67	188	0.09	130	0.22	17.9	0.11	4.3	0.58	0.29	0.71	0.41	0.40	1.02
2.68	100	60.4	1.66	195	0.06	130	0.27	13.9	0.13	3.8	0.54	0.19	0.81	0.23	0.22	0.97
1.26	100	58.7	1.70	192	0.06	130	0.43	13.1	0.19	3.8	0.32	0.12	0.88	0.13	0.12	1.10
0.41	100	56.4	1.77	197	0.04	130	0.66	35.4	0.04	9.5	0.26	0.05	0.95	0.05	0.04	1.10
0.17	100	58.1	1.72	261	0.01	130	0.75	12.6	0.24			0.01	0.99	0.01	0.00	0.93

Table B.17. Parameters retrieved from the analysis of the fluorescence spectra and decays with Equation 3.1 acquired with 0.5 μM pyrene in aqueous dispersions of C3(0.13)-SNP(F) (dialyzied after the modification)

[C3(0.15)- SNP(F)], (g/L)	I_1	I_3	I_1/I_3	τ_{PySNP} (ns)	α_{PySNP}	τ_{PyW} (ns)	α_{PyW}	τ_{SNP1} (ns)	α_{SNP1}	τ_{SNP2} (ns)	α_{SNP2}	f_{bound}	f_{free}	f_{bound}/f_{free}	f_{bound}/f_{free} (after Corr.)	χ^2
19.41				215	0.14	130	0.10	19.6	0.11	4.0	0.65	0.60	0.40	1.51	1.51	1.01
16.73				214	0.13	130	0.10	21.4	0.08	4.3	0.68	0.57	0.43	1.32	1.32	1.16
14.17				211	0.13	130	0.11	18.7	0.09	3.7	0.61	0.54	0.46	1.19	1.19	1.20
11.64	73400	47114	1.56	208	0.14	130	0.11	20.4	0.09	3.6	0.66	0.55	0.45	1.21	1.20	1.03
9.23	114032	72121	1.58	204	0.16	130	0.15	20.4	0.10	3.9	0.58	0.52	0.48	1.11	1.10	0.97
6.99				203	0.16	130	0.18	18.2	0.11	3.6	0.54	0.47	0.53	0.89	0.88	1.12
6.21	140815	88083	1.60	203	0.17	130	0.22	20.7	0.10	4.1	0.51	0.44	0.56	0.78	0.78	1.05
5.62				197	0.17	130	0.19	23.8	0.08	3.9	0.56	0.48	0.52	0.78	0.78	1.04
4.96	159687	98537	1.62	200	0.16	130	0.23	22.3	0.09	3.8	0.52	0.42	0.58	0.72	0.72	0.95
4.13				205	0.15	130	0.30	18.9	0.10	3.8	0.44	0.34	0.66	0.51	0.51	1.07
3.49				203	0.14	130	0.31	16.6	0.12	3.5	0.44	0.32	0.68	0.46	0.46	1.13
3.05	183723	109755	1.67	201	0.16	130	0.38	16.1	0.12	4.7	0.34	0.30	0.70	0.43	0.43	1.00
2.51	189016	112870	1.67	193	0.17	130	0.40	20.8	0.09	4.6	0.34	0.29	0.71	0.42	0.42	1.07
2.02				194	0.15	130	0.43	18.3	0.12	3.9	0.30	0.26	0.74	0.35	0.35	1.08
1.69	200895	117396	1.71	199	0.12	130	0.50	25.6	0.06	4.9	0.32	0.19	0.81	0.24	0.24	0.98
1.49				190	0.12	130	0.42	17.7	0.08	2.8	0.38	0.22	0.78	0.28	0.28	0.91
1.21				193	0.11	130	0.51	17.1	0.11	3.2	0.27	0.18	0.82	0.22	0.22	0.96
0.99				197	0.09	130	0.48	14.2	0.10	2.9	0.33	0.16	0.84	0.20	0.19	1.01
0.72				216	0.07	130	0.74	10.8	0.19			0.08	0.92	0.09	0.09	1.06
0.36				214	0.04	130	0.78	8.8	0.18			0.05	0.95	0.06	0.05	1.06

Table B.18. Parameters retrieved from the analysis of the fluorescence spectra and decays with Equation 3.1 acquired with 0.5 μM pyrene in aqueous dispersions of C3(0.20)-SNP(F) (dialyzied after the modification)

[C3(0.20)- SNP(F)], (g/L)	I_1	I_3	I_1/I_3	τ_{PySNP} (ns)	α_{PySNP}	τ_{PyW} (ns)	α_{PyW}	τ_{SNP1} (ns)	α_{SNP1}	τ_{SNP2} (ns)	α_{SNP2}	f_{bound}	f_{free}	f_{bound}/f_{free}	f_{bound}/f_{free} (after Corr.)	χ^2
17.02				222	0.11	130	0.04	15.1	0.08	4.0	0.77	0.72	0.28	2.56	2.52	1.17
14.10	29490	19278	1.53	216	0.12	130	0.05	16.7	0.09	4.0	0.75	0.72	0.28	2.59	2.55	1.01
10.49	33616	21217	1.58	221	0.10	130	0.07	13.5	0.11	3.4	0.72	0.60	0.40	1.51	1.47	0.92
7.73				214	0.14	130	0.10	16.7	0.10	3.9	0.66	0.57	0.43	1.34	1.30	1.04
6.36	33748	21161	1.59	220	0.13	130	0.13	14.1	0.14	3.4	0.61	0.49	0.51	0.96	0.92	1.00
4.34	34365	21094	1.63	210	0.14	130	0.23	15.7	0.12	3.7	0.51	0.37	0.63	0.60	0.56	1.03
2.06	32830	19959	1.64	210	0.13	130	0.32	18.1	0.10	3.9	0.45	0.29	0.71	0.40	0.36	1.07
1.29	31293	17791	1.76	213	0.11	130	0.42	20.4	0.08	4.6	0.39	0.21	0.79	0.27	0.23	0.99
0.65	31525	18037	1.75	200	0.11	130	0.57	19.7	0.08	5.6	0.25	0.16	0.84	0.19	0.15	0.95
0.31	33553	19210	1.75	221	0.05	130	0.67	17.1	0.10	4.4	0.18	0.07	0.93	0.07	0.03	1.16

C. Determination of Biomolecular quenching constant k_q

Table C.1. Parameters retrieved from the analysis of the fluorescence decays with Equation 4.1 acquired with 0.5 μM pyrene in water at different concentration nitromethane

[Nitromethane] (M)	τ_{PyW} (ns)	χ^2
0.0000	131	0.95
0.0006	86	1.11
0.0012	65	1.10
0.0015	55	1.12
0.0021	46	1.04
0.0027	38	1.15
0.0032	34	0.95
0.0043	28.2	1.02
0.0052	23.7	1.02
0.0067	20.5	1.06
0.0085	17.0	1.15

Table C.2. Parameters retrieved from the analysis of the fluorescence decays with Equation 2.1 acquired with 0.5 μM pyrene in 2.4 g/L aqueous dispersion of SNP(A) at different concentration nitromethane.($\alpha_{PySNP\text{-}P}/\alpha_{PySNP}$= 0.36, $f_{SNP}(t)=0.02e^{-(t/27.2ns)}+0.80\ e^{-(t/1.2ns)}+0.18e^{-(t/3.2ns)}$)

[Nitromethane] (M)	τ_{PyW} (ns)	α_{PyW}	$\tau_{PySNP\text{-}P}$ (ns)	$a_{PySNP\text{-}P}$	τ_{PySNP} (ns)	a_{PySNP}	χ^2
0.0000	130	0.540	221	0.290			1.02
0.0004	99	0.529	221	0.066	165	0.182	0.94
0.0015	57	0.580	221	0.072	137	0.195	1.14
0.0021	46	0.598	221	0.074	114	0.201	1.18
0.0030	36	0.587	221	0.073	99	0.192	1.11
0.0040	28.9	0.615	221	0.076	83	0.208	1.11
0.0056	22.2	0.642	221	0.080	69	0.218	1.02
0.0077	16.9	0.639	221	0.079	59	0.215	1.17

Table C.3. Parameters retrieved from the analysis of the fluorescence decays with Equation 2.1 acquired with 0.5 μM pyrene in 16.0 g/L aqueous dispersion of SNP(A) at different concentration nitromethane ($\alpha_{PySNP\text{-}P}/\alpha_{PySNP}$= 0.36, $f_{SNP}(t)=0.02e^{-(t/27.2ns)}+0.80\ e^{-(t/1.2ns)}+0.18e^{-(t/3.2ns)}$)

[Nitromethane] (M)	τ_{PyW} (ns)	α_{PyW}	$\tau_{PySNP\text{-}P}$ (ns)	$a_{PySNP\text{-}P}$	τ_{PySNP} (ns)	a_{PySNP}	χ^2
0.0000	130		218				
0.0005	90	0.155	218	0.050	176	0.208	1.15
0.0017	54	0.042	218	0.061	92	0.255	1.20
0.0022	45	0.106	218	0.053	89	0.219	1.20
0.0027	39	0.189	218	0.068	86	0.281	1.10
0.0038	31	0.258	218	0.061	78	0.253	1.14
0.0048	25.56	0.280	218	0.052	67	0.216	1.20
0.0069	19.03	0.343	218	0.054	57	0.224	1.04
0.0086	15.59	0.344	218	0.050	50	0.206	1.04

Table C.4. Parameters retrieved from the analysis of the fluorescence decays with Equation 2.1 acquired with 0.5 μM pyrene in 15.1 g/L aqueous dispersion of SNP(B) at different concentration nitromethane ($\alpha_{PySNP\text{-}P}/\alpha_{PySNP}$= 0.02, $f_{SNP}(t)=0.06e^{-(t/10.2ns)}+0.34e^{-(t/3.8ns)}+0.60^{-(t/1.3ns)}$)

[Nitromethane] (M)	τ_{PyW} (ns)	α_{PyW}	$\tau_{PySNP\text{-}P}$ (ns)	$a_{PySNP\text{-}P}$	τ_{PySNP} (ns)	a_{PySNP}	χ^2
0.0000	130		199				1.03
0.0002	115	0.030	199	0.0004	181	0.020	1.14
0.0004	101	0.031	199	0.0004	171	0.187	1.19
0.0005	92	0.031	199	0.0004	162	0.017	1.50
0.0007	83	0.031	199	0.0004	149	0.019	1.21
0.0014	61	0.033	199	0.0005	123	0.023	1.12
0.0016	55	0.030	199	0.0005	114	0.025	1.14
0.0021	48	0.033	199	0.0005	105	0.024	1.12
0.0024	42	0.036	199	0.0005	98	0.024	1.13
0.0032	35	0.036	199	0.0006	85	0.026	1.09
0.0039	30	0.038	199	0.0006	77	0.027	1.14
0.0046	26.7	0.048	199	0.0007	73	0.035	1.19
0.0052	24.2	0.048	199	0.0007	69	0.034	1.05

Table C.5. Parameters retrieved from the analysis of the fluorescence decays with Equation 2.1 acquired with 0.5 μM pyrene in 16.1 g/L aqueous dispersion of SNP(C) at different concentration nitromethan**e** ($\alpha_{PySNP\text{-}P}/\alpha_{PySNP}$= 0.03, $f_{SNP}(t)=0.10e^{-(t/9.4\ ns)}+0.41e^{-(t/3.5\ ns)}+0.50^{-(t/1.2\ ns)}$)

[Nitromethane] (M)	τ_{PyW} (ns)	α_{PyW}	$\tau_{PySNP\text{-}P}$ (ns)	$a_{PySNP\text{-}P}$	τ_{PySNP} (ns)	a_{PySNP}	χ^2
0.0000	133						1.05
0.0005	91	0.059	197	0.001	155	0.030	1.11
0.0010	71	0.042	197	0.001	131	0.041	1.17
0.0018	52	0.044	197	0.001	107	0.027	1.08
0.0022	45	0.036	197	0.001	100	0.034	0.94
0.0028	39	0.036	197	0.001	88	0.033	1.18
0.0032	35	0.045	197	0.001	82	0.037	1.12
0.0041	29.0	0.034	197	0.001	70	0.035	0.99
0.0051	24.5	0.030	197	0.001	61	0.034	1.19
0.0068	19.2	0.076	197	0.001	57	0.050	1.08
0.0083	16.1	0.037	197	0.001	46	0.416	1.12

Table C.6. Parameters retrieved from the analysis of the fluorescence decays with Equation 2.1 acquired with 0.5 μM pyrene in 16.0 g/L aqueous dispersion of SNP(D) at different concentration nitromethane ($\alpha_{PySNP\text{-}P}/\alpha_{PySNP}$= 0.03, $f_{SNP}(t)=0.01e^{-(t/23.8ns)}+0.30e^{-(t/5.0ns)}+0.69^{-(t/1.7ns)}$)

[Nitromethane] (M)	τ_{PyW} (ns)	α_{PyW}	$\tau_{PySNP\text{-}P}$ (ns)	$a_{PySNP\text{-}P}$	τ_{PySNP} (ns)	a_{PySNP}	χ^2
0.0000	133						1.18
0.0006	86	0.033	190	0.002	152	0.085	1.17
0.0013	61	0.055	190	0.002	117	0.066	1.16
0.0019	49	0.068	190	0.001	104	0.055	1.04
0.0026	41	0.073	190	0.001	92	0.049	1.16
0.0031	36	0.078	190	0.001	86	0.053	1.04
0.0037	31	0.076	190	0.001	80	0.052	1.06
0.0048	25.5	0.080	190	0.002	71	0.060	1.18
0.0064	20.2	0.084	190	0.001	59	0.048	1.16
0.0079	16.8	0.089	190	0.001	52	0.055	1.14

Table C.7. Parameters retrieved from the analysis of the fluorescence decays with Equation 2.1 acquired with 0.5 μM pyrene in 16.0 g/L aqueous dispersion of SNP(E) at different concentration nitromethane ($\alpha_{PySNP\text{-}P}/\alpha_{PySNP}$= 0.04, $f_{SNP}(t)=0.07e^{-(t/9.23\ ns)}+0.33e^{-(t/4.1\ ns)}+0.61^{-(t/1.8ns)}$)

[Nitromethane] (M)	τ_{PyW} (ns)	α_{PyW}	$\tau_{PySNP\text{-}P}$ (ns)	$a_{PySNP\text{-}P}$	τ_{PySNP} (ns)	a_{PySNP}	χ^2
0.0000	130		191				1.07
0.0006	89	0.090	191	0.003	147	0.086	1.04
0.0011	67	0.080	191	0.003	123	0.094	1.06
0.0017	54	0.104	191	0.003	107	0.070	1.19
0.0021	47	0.090	191	0.003	97	0.075	1.20
0.0027	40	0.102	191	0.002	88	0.066	1.67
0.0033	34	0.109	191	0.002	81	0.067	1.09
0.0044	27.6	0.098	191	0.003	70	0.080	0.93
0.0059	21.5	0.107	191	0.003	60	0.076	1.20
0.0073	18.0	0.108	191	0.003	54	0.075	1.11
0.0093	14.6	0.132	191	0.003	49	0.077	1.19

Table C.8. Parameters retrieved from the analysis of the fluorescence decays with Equation 2.1 acquired with 0.5 μM pyrene in 15.3 g/L aqueous dispersion of SNP(F) at different concentration nitromethane ($\alpha_{PySNP-P}/\alpha_{PySNP}$= 0.03, $f_{SNP}(t)=0.06e^{-(t/13.3\ ns)}+0.37e^{-(t/3.3\ ns)}+0.57^{-(t/1.3ns)}$)

[Nitromethane] (M)	τ_{PyW} (ns)	α_{PyW}	$\tau_{PySNP-P}$ (ns)	$a_{PySNP-P}$	τ_{PySNP} (ns)	a_{PySNP}	χ^2
0.0000	130		187				1.04
0.0006	88	0.042	187	0.003	157	0.124	1.10
0.0012	64	0.068	187	0.003	122	0.095	1.07
0.0024	43	0.060	187	0.002	95	0.079	0.98
0.0030	37	0.064	187	0.002	84	0.067	1.10
0.0034	33	0.063	187	0.002	77	0.068	1.10
0.0045	26.8	0.068	187	0.002	66	0.060	1.10
0.0055	22.9	0.059	187	0.002	60	0.061	1.20
0.0075	17.6	0.060	187	0.002	52	0.062	1.17

Table C.9. Parameters retrieved from the analysis of the fluorescence decays with Equation 2.1 acquired with 0.5 μM pyrene in 2.3 g/L aqueous dispersion of C6(0.05)-SNP(A) at different concentration nitromethane ($\alpha_{PySNP\text{-}P}/\alpha_{PySNP}$= 0.09, $f_{SNP}(t)=0.31e^{-(t/28.7\ ns)}+0.69e^{-(t/5.9\ ns)}$)

[Nitromethane] (M)	τ_{PyW} (ns)	α_{PyW}	$\tau_{PySNP\text{-}P}$ (ns)	$a_{PySNP\text{-}P}$	$\tau_{1PySNP*}$ (ns)	$a_{1PySNP*}$	$\tau_{2PySNP*}$ (ns)	$\alpha_{2PySNP*}$	χ^2
0.0000	130	0.629	259	0.034					1.09
0.0004	99	0.644	259	0.021			230	0.134	1.00
0.0007	82	0.657	259	0.023			210	0.141	1.07
0.0016	54	0.592	259	0.032	107	0.138	214	0.060	1.03
0.0019	49	0.595	259	0.032	102	0.145	217	0.054	1.02
0.0022	45	0.594	259	0.032	93	0.139	199	0.059	1.04
0.0024	42	0.542	259	0.029	93	0.129	197	0.052	0.99
0.0029	36	0.580	259	0.031	90	0.155	204	0.038	0.99
0.0035	32	0.517	259	0.028	78	0.112	163	0.061	0.98
0.0042	28.1	0.583	259	0.031	69	0.126	152	0.068	1.06
0.0054	22.7	0.554	259	0.030	70	0.140	171	0.044	1.15
0.0069	18.5	0.662	259	0.035	36	0.087	96	0.133	1.01
0.0086	15.2	0.681	259	0.036	31	0.095	89	0.132	1.09

*Parameters representing $f_{PySNP}(t)$ in Equation 2.1.

Table C.10. Parameters retrieved from the analysis of the fluorescence decays with Equation 2.1 acquired with 0.5 μM pyrene in 2.3 g/L aqueous dispersion of C6(0.08)-SNP(A) at different concentration nitromethane ($\alpha_{PySNP\text{-}P}/\alpha_{PySNP}$= 0.17, $f_{SNP}(t)=0.33e^{-(t/15.5\ ns)}+0.67e^{-(t/2.1\ ns)}$)

[Nitromethane] (M)	τ_{PyW} (ns)	α_{PyW}	$\tau_{PySNP\text{-}P}$ (ns)	$a_{PySNP\text{-}P}$	τ_{PySNP} (ns)	a_{PySNP}	χ^2
0.0000	130	0.171	267	0.053			1.13
0.0004	98	0.189	267	0.008	239	0.049	1.04
0.0007	83	0.233	267	0.011	219	0.067	1.09
0.0010	69	0.178	267	0.008	211	0.045	0.98
0.0013	61	0.180	267	0.008	194	0.047	0.99
0.0016	54	0.228	267	0.010	185	0.058	1.11
0.0019	49	0.212	267	0.011	171	0.062	1.18
0.0021	45	0.279	267	0.013	158	0.079	0.98
0.0027	39	0.273	267	0.014	146	0.080	1.08
0.0032	34	0.229	267	0.012	134	0.069	1.01
0.0040	29.1	0.344	267	0.017	123	0.101	1.12
0.0049	24.6	0.539	267	0.028	108	0.162	1.05

Table C.11. Parameters retrieved from the analysis of the fluorescence decays with Equation 2.1 acquired with 0.5 μM pyrene in 2.4 g/L aqueous dispersion of C6(0.09)-SNP(A) at different concentration nitromethane ($\alpha_{PySNP\text{-}P}/\alpha_{PySNP}$= 0.07, $f_{SNP}(t)=0.29e^{-(t/16.8\ ns)}+0.71e^{-(t/\ 3.2\ ns)}$)

[Nitromethane] (M)	τ_{PyW} (ns)	α_{PyW}	$\tau_{PySNP\text{-}P}$ (ns)	$a_{PySNP\text{-}P}$	$\tau_{1PySNP*}$ (ns)	$a_{1PySNP*}$	$\tau_{2PySNP*}$ (ns)	$\alpha_{2PySNP*}$	χ^2
0.0000	130	0.550	265	0.021					1.05
0.0004	96	0.587	265	0.016			236	0.230	0.97
0.0008	77	0.608	265	0.015			224	0.209	1.09
0.0015	56	0.572	265	0.022	118	0.20	239	0.123	0.95
0.0019	50	0.551	265	0.021	113	0.20	232	0.109	1.02
0.0026	40	0.570	265	0.022	106	0.22	226	0.098	1.12
0.0032	34	0.555	265	0.022	89	0.19	197	0.116	1.11
0.0038	30	0.590	265	0.023	80	0.20	187	0.128	1.08
0.0047	25.5	0.541	265	0.021	70	0.17	163	0.135	1.03
0.0059	21.1	0.627	265	0.024	53	0.19	144	0.162	1.08
0.0074	17.3	0.551	265	0.021	53	0.16	136	0.142	1.15

*Parameters representing $f_{PySNP}(t)$ in Equation 2.1.

Table C.12. Parameters retrieved from the analysis of the fluorescence decays with Equation 2.1 acquired with 0.5 μM pyrene in 12.6 g/L aqueous dispersion of C6(0.09)-SNP(A) at different concentration nitromethane ($\alpha_{PySNP\text{-}P}/\alpha_{PySNP}$= 0.09, $f_{SNP}(t)=0.29e^{-(t/16.8\ ns)}+0.71e^{-(t/\ 3.2\ ns)}$)

[Nitromethane] (M)	τ_{PyW} (ns)	α_{PyW}	$\tau_{PySNP\text{-}P}$ (ns)	$a_{PySNP\text{-}P}$	$\tau_{1PySNP*}$ (ns)	$a_{1PySNP*}$	$\tau_{2PySNP*}$ (ns)	$\alpha_{2PySNP*}$	χ^2
0.0000	130	0.334	277	0.530					1.03
0.0004	98	0.318	277	0.037			252	0.408	0.95
0.0007	80	0.334	277	0.035			234	0.388	1.09
0.0011	68	0.345	277	0.037			220	0.415	1.10
0.0027	39	0.331	277	0.055	122	0.358	231	0.255	1.07
0.0035	32	0.331	277	0.055	105	0.348	207	0.266	0.98
0.0042	27.8	0.323	277	0.054	97	0.350	190	0.249	0.12
0.0049	24.5	0.331	277	0.055	85	0.359	176	0.254	1.00
0.0060	20.8	0.324	277	0.054	75	0.335	155	0.264	1.13
0.0078	16.6	0.324	277	0.054	60	0.292	129	0.308	0.96
0.0092	14.4	0.310	277	0.052	60	0.313	125	0.261	0.90

*Parameters representing $f_{PySNP}(t)$ in Equation 2.1.

Table C.13. Parameters retrieved from the analysis of the fluorescence decays with Equation 2.1 acquired with 0.5 μM pyrene in 2.2 g/L aqueous dispersion of C6(0.11)-SNP(A) at different concentration nitromethane ($\alpha_{PySNP\text{-}P}/\alpha_{PySNP}$= 0.04, $f_{SNP}(t)=0.67e^{-(t/12.8\ ns)}+0.33e^{-(t/\ 6.6\ ns)}$)

[Nitromethane] (M)	τ_{PyW} (ns)	α_{PyW}	$\tau_{PySNP\text{-}P}$ (ns)	$a_{PySNP\text{-}P}$	$\tau_{1PySNP*}$ (ns)	$a_{1PySNP*}$	$\tau_{2PySNP*}$ (ns)	$\alpha_{2PySNP*}$	χ^2
0.0000	130	0.204	279	0.005					1.01
0.0003	102	0.665	279	0.011			259	0.263	1.02
0.0006	83	0.622	279	0.011			242	0.267	1.06
0.0009	71	0.637	279	0.010			229	0.262	1.04
0.0015	56	0.343	279	0.008	90	0.056	217	0.134	0.99
0.0021	45	0.354	279	0.008	96	0.069	207	0.127	1.10
0.0024	42	0.372	279	0.008	91	0.072	200	0.135	1.08
0.0030	36	0.332	279	0.007	103	0.093	204	0.092	1.07
0.0037	31	0.391	279	0.009	93	0.113	191	0.103	1.05
0.0049	24.8	0.391	279	0.009	78	0.106	170	0.111	0.96
0.0061	20.6	0.420	279	0.009	74	0.125	158	0.109	0.99
0.0077	16.9	0.427	279	0.009	72	0.141	150	0.096	1.10
0.0095	13.9	0.473	279	0.011	61	0.151	136	0.114	1.18

*Parameters representing $f_{PySNP}(t)$ in Equation 2.1.

Table C.14. Parameters retrieved from the analysis of the fluorescence decays with Equation 2.1 acquired with 0.5 μM pyrene in 13.0 g/L aqueous dispersion of C6(0.11)-SNP(A) at different concentration nitromethane ($\alpha_{PySNP\text{-}P}/\alpha_{PySNP}$= 0.04, $f_{SNP}(t)=0.67e^{-(t/12.8\ ns)}+0.33e^{-(t/\ 6.6\ ns)}$)

[Nitromethane] (M)	τ_{PyW} (ns)	α_{PyW}	$\tau_{PySNP\text{-}P}$ (ns)	$a_{PySNP\text{-}P}$	$\tau_{1PySNP*}$ (ns)	$a_{1PySNP*}$	$\tau_{2PySNP*}$ (ns)	$\alpha_{2PySNP*}$	χ^2
0.000	130	0.319	285	0.413					1.01
0.001	77	0.379	285	0.019			242	0.484	1.11
0.003	33	0.177	285	0.011	113	0.175	210	0.120	1.04
0.005	24.8	0.196	285	0.012	95	0.192	183	0.135	1.00
0.006	19.9	0.187	285	0.012	80	0.180	163	0.132	1.05
0.008	16.2	0.193	285	0.012	67	0.183	144	0.139	1.05
0.010	13.4	0.195	285	0.012	59	0.183	131	0.142	1.16

*Parameters representing $f_{PySNP}(t)$ in Equation 2.1.

Table C.15. Parameters retrieved from the analysis of the fluorescence decays with Equation 2.1 acquired with 0.5 μM pyrene in 2.3 g/L aqueous dispersion of C6(0.12)-SNP(A) at different concentration nitromethane ($\alpha_{PySNP\text{-}P}/\alpha_{PySNP}$= 0.37, $f_{SNP}(t)=0.18e^{-(t/18.0\ ns)}+0.82e^{-(t/\ 2.1\ ns)}$)

[Nitromethane] (M)	τ_{PyW} (ns)	α_{PyW}	$\tau_{PySNP\text{-}P}$ (ns)	$a_{PySNP\text{-}P}$	$\tau_{1PySNP*}$ (ns)	$a_{1PySNP*}$	$\tau_{2PySNP*}$ (ns)	$\alpha_{2PySNP*}$	χ^2
0.0000	130	0.445	288	0.290					0.95
0.0003	102	0.566	288	0.093			273	0.253	1.05
0.0006	86	0.578	288	0.096			254	0.260	1.06
0.0011	65	0.591	288	0.096			231	0.258	1.06
0.0014	58	0.595	288	0.096			219	0.258	1.16
0.0019	49	0.574	288	0.100			194	0.271	1.17
0.0024	42	0.570	288	0.094			180	0.264	1.19
0.0029	37	0.558	288	0.094	155	0.22	257	0.036	1.09
0.0050	24.4	0.616	288	0.104	118	0.21	165	0.070	1.17

*Parameters representing $f_{PySNP}(t)$ in Equation 2.1.

Table C.16. Parameters retrieved from the analysis of the fluorescence decays with Equation 2.1 acquired with 0.5 μM pyrene in 2.2 g/L aqueous dispersion of C6(0.12)-SNP(A) at different concentration nitromethane ($\alpha_{PySNP\text{-}P}/\alpha_{PySNP}$= 0.15, $f_{SNP}(t)=0.33e^{-(t/13.2\ ns)}+0.37e^{-(t/\ 1.7\ ns)}$)

[Nitromethane] (M)	τ_{PyW} (ns)	α_{PyW}	$\tau_{PySNP\text{-}P}$ (ns)	$a_{PySNP\text{-}P}$	$\tau_{1PySNP*}$ (ns)	$a_{1PySNP*}$	$\tau_{2PySNP*}$ (ns)	$\alpha_{2PySNP*}$	χ^2
0.0000	130	0.495	286	0.230					0.95
0.0003	102	0.533	286	0.049			252	0.323	1.09
0.0006	84	0.583	286	0.038			249	0.256	1.14
0.0009	72	0.607	286	0.036			232	0.237	1.07
0.0017	52	0.395	286	0.033	133	0.121	246	0.098	1.05
0.0022	44	0.421	286	0.035	119	0.127	232	0.106	1.03
0.0030	36	0.327	286	0.027	112	0.098	214	0.084	1.00
0.0043	27.2	0.391	286	0.033	92	0.121	188	0.096	1.08
0.0056	22.0	0.607	286	0.051	75	0.188	173	0.149	1.07
0.0071	18.1	0.610	286	0.051	56	0.167	144	0.172	1.03
0.0086	15.2	0.610	286	0.051	53	0.183	138	0.156	1.11

*Parameters representing $f_{PySNP}(t)$ in Equation 2.1.

Table C.17. Parameters retrieved from the analysis of the fluorescence decays with Equation 2.1 acquired with 0.5 μM pyrene in 12.7 g/L aqueous dispersion of C6(0.12)-SNP(A) at different concentration nitromethane ($\alpha_{PySNP\text{-}P}/\alpha_{PySNP}$= 0.04, $f_{SNP}(t)=0.67e^{-(t/12.8\ ns)}+0.33e^{-(t/\ 6.6\ ns)}$)

[Nitromethane] (M)	τ_{PyW} (ns)	α_{PyW}	$\tau_{PySNP\text{-}P}$ (ns)	$a_{PySNP\text{-}P}$	$\tau_{1PySNP*}$ (ns)	$a_{1PySNP*}$	$\tau_{2PySNP*}$ (ns)	$\alpha_{2PySNP*}$	χ^2
0.0000	130	0.200	294	0.310					0.95
0.0003	102	0.269	294	0.020			277	0.493	1.10
0.0006	83	0.292	294	0.020			259	0.509	1.05
0.0024	42	0.163	294	0.016	140	0.220	241	0.187	1.05
0.0032	34	0.187	294	0.019	118	0.231	218	0.237	1.03
0.0045	26.4	0.171	294	0.017	113	0.249	212	0.180	1.00
0.0060	20.8	0.179	294	0.018	93	0.253	186	0.193	1.08
0.0073	17.6	0.177	294	0.018	80	0.225	171	0.217	1.07
0.0084	15.6	0.155	294	0.016	80	0.207	163	0.180	1.03

*Parameters representing $f_{PySNP}(t)$ in Equation 2.1.

Table C.18. Parameters retrieved from the analysis of the fluorescence decays with Equation 2.1 acquired with 0.5 μM pyrene in 2.2 g/L aqueous dispersion of C6(0.15)-SNP(A) at different concentration nitromethane ($\alpha_{PySNP\text{-}P}/\alpha_{PySNP}$= 0.04, $f_{SNP}(t)=0.19e^{-(t/27.2\ ns)}+0.81e^{-(t/\ 3.5\ ns)}$)

[Nitromethane] (M)	τ_{PyW} (ns)	α_{PyW}	$\tau_{PySNP\text{-}P}$ (ns)	$a_{PySNP\text{-}P}$	$\tau_{1PySNP*}$ (ns)	$a_{1PySNP*}$	$\tau_{2PySNP*}$ (ns)	$\alpha_{2PySNP*}$	χ^2
0.0000	130	0.478	312	0.019			312	0.435	1.07
0.0003	101	0.476	312	0.017			296	0.427	1.01
0.0006	85	0.486	312	0.017			283	0.437	1.03
0.0009	72	0.490	312	0.017			270	0.413	1.05
0.0013	61	0.371	312	0.015	156	0.113	280	0.257	0.98
0.0016	54	0.382	312	0.015	149	0.138	277	0.244	1.04
0.0019	49	0.395	312	0.016	124	0.120	258	0.275	0.97
0.0024	41	0.375	312	0.015	128	0.131	249	0.244	1.03
0.0035	32	0.358	312	0.014	119	0.153	230	0.206	1.11
0.0046	26.0	0.417	312	0.017	101	0.159	214	0.258	0.97
0.0061	20.5	0.418	312	0.017	84	0.155	190	0.263	1.01
0.0081	16.2	0.444	312	0.018	77	0.179	173	0.265	0.99
0.0098	13.6	0.462	312	0.018	66	0.180	158	0.282	1.20

*Parameters representing $f_{PySNP}(t)$ in Equation 2.1.

Table C.19. Parameters retrieved from the analysis of the fluorescence decays with Equation 2.1 acquired with 0.5 μM pyrene in 12.2 g/L aqueous dispersion of C6(0.15)-SNP(A) at different concentration nitromethane ($\alpha_{PySNP\text{-}P}/\alpha_{PySNP}$= 0.02, $f_{SNP}(t)=0.19e^{-(t/27.2\ ns)}+0.81e^{-(t/\ 3.5\ ns)}$)

[Nitromethane] (M)	τ_{PyW} (ns)	α_{PyW}	$\tau_{PySNP\text{-}P}$ (ns)	$a_{PySNP\text{-}P}$	$\tau_{1PySNP*}$ (ns)	$a_{1PySNP*}$	$\tau_{2PySNP*}$ (ns)	$\alpha_{2PySNP*}$	χ^2
0.0000	130	0.208	315	0.487					0.97
0.0004	99	0.254	315	0.012			296	0.619	1.10
0.0008	76	0.254	315	0.012			275	0.614	1.15
0.0012	63	0.310	315	0.013			268	0.650	1.17
0.0019	49	0.185	315	0.011	169	0.199	277	0.330	1.07
0.0025	41	0.193	315	0.011	149	0.193	260	0.359	1.02
0.0037	31	0.205	315	0.012	133	0.232	240	0.353	0.98
0.0047	25.6	0.191	315	0.011	117	0.217	225	0.328	1.04
0.0062	20.3	0.189	315	0.011	109	0.248	212	0.292	1.06
0.0077	16.8	0.202	315	0.012	91	0.233	191	0.344	1.03
0.0092	14.3	0.209	315	0.012	81	0.242	178	0.355	1.08

*Parameters representing $f_{PySNP}(t)$ in Equation 2.1.

Table C.20. Parameters retrieved from the analysis of the fluorescence decays with Equation 2.1 acquired with 0.5 μM pyrene in 2.3 g/L aqueous dispersion of C6(0.05)-SNP(F) (dialyzied before the modification) at different concentration nitromethane ($\alpha_{PySNP\text{-}P}/\alpha_{PySNP}$= 0.03, $f_{SNP}(t)=0.73e^{-(t/19.1\ ns)}+0.27e^{-(t/\ 5.5\ ns)}$)

[Nitromethane] (M)	τ_{PyW} (ns)	α_{PyW}	$\tau_{PySNP\text{-}P}$ (ns)	$a_{PySNP\text{-}P}$	$\tau_{1PySNP*}$ (ns)	$a_{1PySNP*}$	$\tau_{2PySNP*}$ (ns)	$\alpha_{2PySNP*}$	χ^2
0.0000	130	0.426	263	0.006					1.04
0.0006	83	0.589	263	0.006			226	0.195	1.10
0.0019	49	0.412	263	0.006	99	0.098	206	0.108	1.08
0.0024	42	0.482	263	0.007	105	0.135	206	0.106	1.02
0.0036	31	0.418	263	0.006	92	0.129	185	0.080	1.05
0.0048	25.1	0.455	263	0.007	75	0.123	160	0.105	1.11
0.0058	21.3	0.420	263	0.006	74	0.122	153	0.088	1.13

*Parameters representing $f_{PySNP}(t)$ in Equation 2.1.

Table C.21. Parameters retrieved from the analysis of the fluorescence decays with Equation 2.1 acquired with 0.5 μM pyrene in 2.2 g/L aqueous dispersion of C6 (0.06)-SNP(F) (dialyzied after the modification) at different concentration nitromethane ($\alpha_{PySNP\text{-}P}/\alpha_{PySNP}$= 0.03, $f_{SNP}(t)=0.22e^{-(t/15.7\ ns)}+0.78e^{-(t/\ 3.5\ ns)}$)

[Nitromethane] (M)	τ_{PyW} (ns)	α_{PyW}	$\tau_{PySNP\text{-}P}$ (ns)	$a_{PySNP\text{-}P}$	$\tau_{1PySNP*}$ (ns)	$a_{1PySNP*}$	$\tau_{2PySNP*}$ (ns)	$\alpha_{2PySNP*}$	χ^2
0	130	0.015	249	0.0175					1.10
0.0006	87	0.140	249	0.0048			206	0.160	1.16
0.0013	62	0.027	249	0.0013	133	0.030	226	0.013	1.03
0.0019	49	0.036	249	0.0018	111	0.038	200	0.019	1.17
0.0030	36	0.040	249	0.0020	95	0.044	179	0.018	1.04
0.0046	25.8	0.047	249	0.0023	75	0.053	147	0.022	1.05
0.0060	20.8	0.057	249	0.0028	72	0.063	144	0.027	1.05
0.0074	17.5	0.071	249	0.0035	59	0.071	124	0.041	1.01
0.0088	14.9	0.078	249	0.0038	50	0.073	112	0.050	1.18

*Parameters representing $f_{PySNP}(t)$ in Equation 2.1.

Table C.22. Parameters retrieved from the analysis of the fluorescence decays with Equation 2.1 acquired with 0.5 μM pyrene in 2.3 g/L aqueous dispersion of C6(0.08)-SNP(F) (dialyzied before the modification) at different concentration nitromethane ($\alpha_{PySNP\text{-}P}/\alpha_{PySNP}$= 0.01, $f_{SNP}(t)=0.36e^{-(t/30.2\ ns)}+0.64e^{-(t/\ 5.7\ ns)}$)

[Nitromethane] (M)	τ_{PyW} (ns)	α_{PyW}	$\tau_{PySNP\text{-}P}$ (ns)	$a_{PySNP\text{-}P}$	$\tau_{1PySNP*}$ (ns)	$a_{1PySNP*}$	$\tau_{2PySNP*}$ (ns)	$\alpha_{2PySNP*}$	χ^2
0.0000	130	0.608	271	0.0023					0.99
0.0006	85	0.571	271	0.0024			237	0.237	1.20
0.0012	64	0.752	271	0.0024			211	0.242	1.18
0.0017	52	0.710	271	0.0020			192	0.240	1.10
0.0023	43	0.647	271	0.0020	135	0.161	226	0.087	1.00
0.0029	37	0.684	271	0.0021	128	0.181	224	0.082	1.12
0.0039	29.3	0.712	271	0.0022	104	0.174	185	0.100	1.07
0.0049	24.5	0.708	271	0.0022	96	0.183	187	0.089	1.01
0.0059	21.2	0.714	271	0.0022	90	0.187	189	0.088	1.97
0.0073	17.7	0.721	271	0.0022	67	0.157	149	0.120	1.13
0.0092	14.3	0.721	271	0.0022	60	0.171	139	0.106	0.97

*Parameters representing $f_{PySNP}(t)$ in Equation 2.1.

Table C.23. Parameters retrieved from the analysis of the fluorescence decays with Equation 2.1 acquired with 0.5 μM pyrene in 2.0 g/L aqueous dispersion of C6(0.10)-SNP(F) (dialyzied before the modification) at different concentration nitromethane ($\alpha_{PySNP\text{-}P}/\alpha_{PySNP}$= 0.06, $f_{SNP}(t)=0.23e^{-(t/22.5\ ns)}+0.77e^{-(t/3.9\ ns)}$)

[Nitromethane] (M)	τ_{PyW} (ns)	α_{PyW}	$\tau_{PySNP\text{-}P}$ (ns)	$a_{PySNP\text{-}P}$	$\tau_{1PySNP*}$ (ns)	$a_{1PySNP*}$	$\tau_{2PySNP*}$ (ns)	$\alpha_{2PySNP*}$	χ^2
0.0000	130	0.556	270	0.253					0.94
0.0003	102	0.592	270	0.013	252	0.216			1.05
0.0006	84	0.566	270	0.012	233	0.207			1.02
0.0009	71	0.583	270	0.014	213	0.240			1.22
0.0013	62	0.538	270	0.015	218	0.160	131	0.084	0.98
0.0018	51	0.485	270	0.013	211	0.106	141	0.115	0.99
0.0023	43	0.499	270	0.014	231	0.049	143	0.178	1.09
0.0028	37	0.517	270	0.014	217	0.058	131	0.177	0.98
0.0036	31	0.490	270	0.013	177	0.084	114	0.139	1.17
0.0043	27.2	0.498	270	0.014	157	0.113	100	0.113	1.16
0.0050	24.3	0.441	270	0.012	162	0.048	109	0.152	1.15
0.0056	22.2	0.478	270	0.013	138	0.126	86	0.091	1.20
0.0066	19.2	0.444	270	0.012	134	0.083	94	0.119	1.10

*Parameters representing $f_{PySNP}(t)$ in Equation 2.1.

.

Table C.24. Parameters retrieved from the analysis of the fluorescence decays with Equation 2.1 acquired with 0.5 μM pyrene in 2.5 g/L aqueous dispersion of C6(0.12)-SNP(F) (dialyzied before the modification) at different concentration nitromethane ($\alpha_{PySNP\text{-}P}/\alpha_{PySNP}$= 0.03, $f_{SNP}(t)=0.76e^{-(t/26.0\ ns)}+0.24e^{-(t/4.3\ ns)}$)

[Nitromethane] (M)	τ_{PyW} (ns)	α_{PyW}	$\tau_{PySNP\text{-}P}$ (ns)	$a_{PySNP\text{-}P}$	$\tau_{1PySNP*}$ (ns)	$a_{1PySNP*}$	$\tau_{2PySNP*}$ (ns)	$\alpha_{2PySNP*}$	χ^2
0.0000	130	0.470	294	0.371					1.05
0.0005	89	0.492	294	0.010			265	0.334	1.14
0.0010	71	0.528	294	0.010			246	0.341	1.20
0.0017	52	0.414	294	0.011	135	0.162	252	0.214	1.05
0.0022	44	0.403	294	0.011	128	0.170	242	0.196	1.09
0.0031	35	0.401	294	0.011	110	0.160	217	0.205	1.02
0.0040	29.2	0.384	294	0.010	104	0.152	200	0.198	1.10
0.0047	25.4	0.393	294	0.011	102	0.180	193	0.178	1.09
0.0059	21.1	0.357	294	0.010	95	0.162	172	0.163	1.08
0.0069	18.4	0.380	294	0.010	77	0.139	158	0.207	1.07
0.0082	16.0	0.363	294	0.010	78	0.150	152	0.180	0.90

*Parameters representing $f_{PySNP}(t)$ in Equation 2.1.

Table C.25. Parameters retrieved from the analysis of the fluorescence decays with Equation 2.1 acquired with 0.5 μM pyrene in 2.2 g/L aqueous dispersion of C6(0.12)-SNP(F) (dialyzied after the modification) at different concentration nitromethane ($\alpha_{PySNP-P}/\alpha_{PySNP}$= 0.02, $f_{SNP}(t)=0.41e^{-(t/13.1\ ns)}+0.59e^{-(t/2.5\ ns)}$) .

[Nitromethane] (M)	τ_{PyW} (ns)	α_{PyW}	$\tau_{PySNP-P}$ (ns)	$a_{PySNP-P}$	$\tau_{1PySNP*}$ (ns)	$a_{1PySNP*}$	$\tau_{2PySNP*}$ (ns)	$\alpha_{2PySNP*}$	χ^2
0.0000	130	0.040	279	0.081					1.16
0.0005	93	0.128	279	0.005			250	0.231	1.15
0.0009	73	0.162	279	0.005			235	0.269	1.06
0.0035	32	0.102	279	0.002	134	0.117	243	0.038	0.93
0.0041	28.1	0.098	279	0.002	122	0.110	227	0.038	1.03
0.0052	23.3	0.099	279	0.002	95	0.101	183	0.049	1.03
0.0067	19.1	0.106	279	0.003	80	0.102	166	0.058	1.01
0.0082	15.9	0.108	279	0.003	73	0.106	158	0.058	1.19
0.0101	13.2	0.115	279	0.003	59	0.104	136	0.070	1.13

*Parameters representing $f_{PySNP}(t)$ in Equation 2.1.

Table C.26. Parameters retrieved from the analysis of the fluorescence decays with Equation 2.1 acquired with 0.5 μM pyrene in 2.2 g/L aqueous dispersion of C6 (0.13)-SNP(F) (dialyzied after the modification) at different concentration nitromethane ($\alpha_{PySNP\text{-}P}/\alpha_{PySNP}$= 0.04, $f_{SNP}(t)=0.14e^{-(t/20.8\ ns)}+0.86e^{-(t/4.6\ ns)}$)

[Nitromethane] (M)	τ_{PyW} (ns)	α_{PyW}	$\tau_{PySNP\text{-}P}$ (ns)	$a_{PySNP\text{-}P}$	$\tau_{1PySNP*}$ (ns)	$a_{1PySNP*}$	$\tau_{2PySNP*}$ (ns)	$\alpha_{2PySNP*}$	χ^2
0.0000	130	0.028	281	0.070					1.10
0.0004	97	0.151	281	0.010			251	0.239	1.12
0.0008	75	0.200	281	0.012			232	0.289	1.17
0.0025	41	0.063	281	0.005	152	0.091	259	0.030	1.11
0.0032	34	0.058	281	0.004	122	0.076	215	0.036	0.98
0.0039	29.5	0.075	281	0.006	122	0.099	224	0.045	1.01
0.0049	24.5	0.076	281	0.006	107	0.096	205	0.051	0.94
0.0060	20.9	0.082	281	0.006	88	0.092	178	0.066	1.00
0.0072	17.9	0.093	281	0.007	74	0.094	159	0.086	1.03
0.0086	15.2	0.083	281	0.006	63	0.083	146	0.077	1.06
0.0098	13.6	0.094	281	0.007	56	0.089	135	0.092	1.03

*Parameters representing $f_{PySNP}(t)$ in Equation 2.1.

Table C.27. Parameters retrieved from the analysis of the fluorescence decays with Equation 2.1 acquired with 0.5 μM pyrene in 2.1 g/L aqueous dispersion of C3 (0.03)-SNP(F) (dialyzied after the modification) at different concentration nitromethane ($\alpha_{PySNP\text{-}P}/\alpha_{PySNP}$= 0.12, $f_{SNP}(t)=0.17e^{-(t/13.9\ ns)}+0.83e^{-(t/3.8\ ns)}$) .

[Nitromethane] (M)	τ_{PyW} (ns)	α_{PyW}	$\tau_{PySNP\text{-}P}$ (ns)	$a_{PySNP\text{-}P}$	τ_{PySNP} (ns)	a_{PySNP}	χ^2
0.0000	130	0.035	201	0.042			1.10
0.0006	88	0.037	201	0.005	163	0.042	1.19
0.0011	66	0.041	201	0.005	136	0.044	1.10
0.0017	53	0.042	201	0.006	116	0.048	1.03
0.0023	44	0.041	201	0.006	103	0.046	1.19
0.0033	34	0.040	201	0.006	88	0.046	1.16
0.0044	27.0	0.042	201	0.006	77	0.047	1.04
0.0063	20.1	0.050	201	0.005	65	0.045	0.99

Table C.28. Parameters retrieved from the analysis of the fluorescence decays with Equation 2.1 acquired with 0.5 μM pyrene in 2.0 g/L aqueous dispersion of C3 (0.13)-SNP(F) (dialyzied after the modification) at different concentration nitromethane ($\alpha_{PySNP\text{-}P}/\alpha_{PySNP}$= 0.07, $f_{SNP}(t)=0.21e^{-(t/20.8\ ns)}+0.79e^{-(t/4.6\ ns)}$)

[Nitromethane] (M)	τ_{PyW} (ns)	α_{PyW}	$\tau_{PySNP\text{-}P}$ (ns)	$a_{PySNP\text{-}P}$	τ_{PySNP} (ns)	a_{PySNP}	χ^2
0.0000	130	0.027	220	0.042			1.01
0.0007	82	0.030	220	0.003	172	0.040	1.10
0.0013	61	0.031	220	0.003	151	0.045	1.17
0.0019	49	0.033	220	0.003	125	0.042	1.14
0.0030	36	0.037	220	0.003	106	0.045	1.11
0.0043	27.6	0.063	220	0.004	94	0.054	1.14
0.0053	23.0	0.066	220	0.004	84	0.052	1.02
0.0068	18.7	0.067	220	0.004	72	0.051	1.07

Table C.29. Parameters retrieved from the analysis of the fluorescence decays with Equation 2.1 acquired with 0.5 μM pyrene in 2.0 g/L aqueous dispersion of C3 (0.20)-SNP(F) (dialyzied after the modification) at different concentration nitromethane ($\alpha_{PySNP-P}/\alpha_{PySNP}$= 0.06, $f_{SNP}(t)=0.19e^{-(t/18.1\ ns)}+0.81e^{-(t/3.9\ ns)}$)

[Nitromethane] (M)	τ_{PyW} (ns)	α_{PyW}	$\tau_{PySNP-P}$ (ns)	$a_{PySNP-P}$	τ_{PySNP} (ns)	a_{PySNP}	χ^2
0.0000	130	0.028	223	0.045			1.13
0.0007	79	0.026	223	0.004	184	0.059	1.06
0.0015	56	0.032	223	0.003	144	0.045	1.06
0.0022	44	0.036	223	0.003	126	0.052	0.96
0.0028	37	0.036	223	0.003	112	0.053	1.09
0.0042	27.8	0.059	223	0.004	96	0.066	1.03
0.0054	22.6	0.055	223	0.004	86	0.065	1.15
0.0073	17.6	0.060	223	0.004	71	0.065	1.20

Table C.30. Parameters retrieved from the analysis of the fluorescence decays with Equation 2.1 acquired with 0.5 μM pyrene in 2.0 g/L aqueous dispersion of C3 (0.25)-SNP(F) (dialyzied after the modification) at different concentration nitromethane ($\alpha_{PySNP-P}/\alpha_{PySNP}$= 0.03, $f_{SNP}(t)=0.22e^{-(t/20.4\ ns)}+0.78e^{-(t/34.6\ ns)}$)

[Nitromethane] (M)	τ_{PyW} (ns)	α_{PyW}	$\tau_{PySNP-P}$ (ns)	$a_{PySNP-P}$	τ_{PySNP} (ns)	a_{PySNP}	χ^2
0	130	0.040	220	0.057			1.07
0.0007	82	0.050	220	0.003	185	0.100	1.08
0.0014	58	0.080	220	0.003	143	0.090	1.09
0.0021	45	0.070	220	0.003	126	0.110	1.08
0.0035	32	0.100	220	0.003	98	0.110	1.05
0.0049	24.7	0.120	220	0.004	83	0.130	1.07
0.0061	20.4	0.120	220	0.004	72	0.130	1.18
0.0073	17.7	0.230	220	0.004	66	0.130	1.08
0.0087	15.1	0.130	220	0.004	60	0.130	1.19